Flexural-Torsional Coupled Vibration of Rotating Beams Using Orthogonal Polynomials

Yong Y. Kim

Thesis submitted to the Faculty of the
Virginia Polytechnic Institute and State University
in partial fulfillment of the requirements for the degree of

Master of Science
in
Aerospace Engineering

Rakesh K. Kapania, Chair
Eric R. Johnson
Efstratios Nikolaidis

May 1, 2000
Blacksburg, Virginia

Keywords: Natural Frequency, Rotating Blade, Rayleigh-Ritz Method, Orthogonal Polynomials, Flexural-Torsional coupled vibration.

Flexural-Torsional Coupled Vibration of Rotating Beams using Orthogonal Polynomials

Yong Y. Kim

(ABSTRACT)

Dynamic behavior of flexural-torsional coupled vibration of rotating beams using the Rayleigh-Ritz method with orthogonal polynomials as basis functions is studied. The present work starts from a review of the development and analysis of four basic types of beam theories: the Euler-Bernoulli, Rayleigh, Shear and Timoshenko and goes over to a study of flexural-torsional coupled vibration analysis using basic beam theories. In obtaining natural frequencies, orthogonal polynomials used in the Rayleigh-Ritz method are studied as an efficient way of getting results. The study is also performed for both non-rotating and rotating beams.

Performance of various orthogonal polynomials is compared to each other in terms of their efficiency and accuracy in determining the required natural frequencies. Orthogonal polynomials and functions studied in the present work are : Legendre, Chebyshev, integrated Legendre, modified Duncan polynomials, the eigenfunctions of a pinned-free uniform beam, and the special trigonometric functions used in conjunction with Hermite cubics. A total of 5 cases of beam boundary conditions and loading are studied for their natural frequencies. Studied cases are non-rotating and rotating Timoshenko beams, bending-torsion coupled beam with free-free boundary conditions, a cantilever beam, and a rotating cantilever beam. The obtained natural frequencies and mode shapes are compared to those available in various references and results for coupled flexural-torsional vibrations are compared to both previously available references and with those obtained using NASTRAN finite element package.

Among all the examined orthogonal functions, Legendre and Chebyshev orthogonal polynomials are the most efficient in overall CPU time, mainly because of ease in performing the integration required for determining the stiffness and mass matrices. Beam charac-

teristic orthogonal polynomials give most accurate results but with a higher computation time. The eigenfunctions and the special trigonometric functions with Hermite cubics do not give, despite using a considerably more CPU time, results which are any better than the simpler Legendre or Chebyshev orthogonal polynomials. Overall, for the first few modes, the orthogonal functions give very close approximation for each mode. These orthogonal functions, however, show limitations in finding every mode in the flexural-torsional coupled vibration.

Acknowledgments

I want to first express my deep appreciation to Dr. Rakesh K. Kapania, for his graceful support and valuable and patient advices throughout this program, and to my parents for supporting me always in every way with their love. I also would like to thank Dr. Eric R. Johnson and Dr. Efstratios Nikolaidis for serving as committee members. I also want to thank many colleagues for the good company and inspiration. I would also like to acknowledge financial assistance of National Science Foundation for JAVA applet development that helped me to finish this program.

Contents

List of Figures

List of Tables

Chapter 1

Introduction

Flexural-torsional coupled vibration of a rotating structure can occur in many engineering applications such as turbomachinery blades, slewing robot arms, aircraft propellers, helicopter rotors, and spinning spacecraft. To design these components, the dynamic characteristic, especially near resonant condition, need to be well examined to assure a safe operation. Among the dynamic characteristics of these structures, determining the natural frequencies and associated mode shapes are of fundamental importance in the study of resonant responses, aeroelasticity, and for forced vibration analysis. An accurate prediction of the forced response is usually very difficult because of the uncertainty of the excitation. Moreover, under the resonance conditions, what limits the vibration amplitude is the amount of damping available. In most cases, the damping is almost entirely aerodynamic and its assessment is just as uncertain as the excitation. Thus, classic design practice for such structures has been mainly to rely on the knowledge of the natural frequencies to avoid anticipated resonances.

Flexural-torsional coupled vibration occurs when the centroid and the shear center of the cross section of the beam do not coincide. This lack of coincidence between the centroid and the shear center occurs when the beam has less than two axis of symmetry or has anisotropy in the material. This makes the torsional axis different from the elastic axis and thus causes torsional vibration when flexural vibration occur. When the beam is isotropic

and the cross-section of it has two axes of symmetry, centroid and shear center coincides and flexural vibrations and torsional vibration become independent. The flexural-torsional coupled vibration can be analyzed by combining one of the beam theories for bending with a torsional theory and a consideration of the various warping effects. The simplest model for the analysis of coupled bending and torsional vibration is combining the classical Bernoulli-Euler theory for bending and St. Venant theory for torsion [1]. Inclusion of a warping effect, Bishop and Miao[2], results in a better approximation, especially for higher modes. Also, for non slender beams, applying the Timoshenko Beam theory instead of the Bernoulli-Euler theory along with the inclusion of a warping effect can improve the accuracy for higher modes [3].

Centrifugal force on rotating structure affects dynamic characteristic of the structure by inducing additional stiffness. In high rotational speed, centrifugal forces of considerable magnitude results in an additional stiffening of the beam, thus increasing the natural frequencies of the structure. There are two more forces induced by inertia force when rotation occurs. They are the Coriolis force and the gyroscopic force [4]. However, the effect of these two forces on the dynamic characteristic is insignificant compared to the effect induced by the centrifugal force. The numerical results on the rectangular cantilever plates show that the Coriolis force has an insignificant effect upon the natural frequencies if the angular speed is less than the first natural frequency of the configuration [5]. Current work only focus on the effect of centrifugal force.

Since the flexural-torsional coupled vibration of rotating structures can be studied by being modeled as beams, the dynamic characteristic of beams need to be examined as well. Beams are structural elements that can be studied as one dimensional elements. In reality, all structures are three dimensional bodies and every point in such a body, if not restrained, can displace along three mutually perpendicular directions. Therefore, the key in a beam modeling is implementing various three dimensional properties into one dimensional beam element. Pochhammer and Chree [6] investigated an exact formulation of the beam problem in terms of general elasticity equations. However, it is not practical to solve the full prob-

lem. Getting approximate solutions for transverse displacement is usually sufficient in most applications In the early study of beams, bending was identified as a single most important factor in a transversely vibrating beam. This is the Euler-Bernoulli beam theory [7] and is the most commonly used one because it is simple and provides reasonable engineering approximations for many problems. However, for the natural frequencies of higher modes, this approximation cannot give good estimation of the higher mode natural frequencies and the natural frequencies of non-slender beams, in which case shear effects can't be ignored. To overcome these limitations, various effects have been included by successive researchers working on the analysis of beams. Rayleigh [8] included rotation effects. The shear model includes shear deformation. In Timoshenko's beam theory [9] [10], both the rotation and the shear effects are included giving better approximations for higher-mode responses and non-slender beams. Although several beam theories have been developed after Timoshenko's beam theory, the Euler-Bernoulli and Timoshenko beam theories are still widely used. The development and analysis of four types of beam theories, the Euler-Bernoulli, Rayleigh, Shear, and Timoshenko beam theories, are reviewed and studied in the present work.

When obtaining the natural frequencies and the mode shapes, the Rayleigh-Ritz method is a good candidate both because of its simplicity and its ability to give good results with relatively less efforts. The Rayleigh-Ritz method is a very powerful technique that can be used to predict the natural frequencies and mode shapes of vibrating structures with less calculation time and effort. The method requires a linear combination of assumed deflection shapes of structures in free harmonic vibration that satisfies at least the geometrical or kinematical boundary conditions of the vibrating structure. Results from the Rayleigh-Ritz method depend directly on how closely the assumed shape functions resemble the actual mode shapes. When an assumed shape function contributes to several modes, or when some modes are not represented in the assumed shape functions, then it is difficult to draw definite conclusions from the Rayleigh-Ritz results. It is very important that the assumed shape functions form a complete set so as to represent all the modes of the structure, and they satisfy at least the geometrical boundary conditions. This study presents some insight into

the nature of the natural frequency values, as obtained by the Rayleigh-Ritz method and their dependence on the nature of the assumed shape functions.

The choice of the admissible functions is very important to simplify the calculations and to guarantee convergence to the actual solution. As basis functions for the Rayleigh-Ritz method, orthogonal polynomials enable the computation of higher natural frequencies of any order to be accomplished without facing any numerical difficulties arising from the ill-conditioning of the matrices like the ones one encounters when using simple polynomials as the basis functions [11]. Main objective of the present work is to study the development and analysis of the flexural-torsional vibration of beams and discover the effect of using orthogonal functions in obtaining natural frequencies of structures experiencing flexural-torsional coupled vibration. Six sets of orthogonal functions are examined and compared to each other in terms of performance when used as basis functions. The partial differential equation of motion for each model is solved as a reference to a method using approximating functions. To find most appropriate approximating orthogonal function to be used in Ritz method, 7 types of orthogonal functions are examined and compared for their use as basis functions. These functions are

1. Legendre.
2. Chebyshev.
3. Integrated Legendre.
4. Modified Duncan polynomials.
5. Kwak's new admissible function for a slewing beam.
6. The special trigonometric functions used in conjunction with Hermite cubics.
7. Beam characteristic orthogonal polynomials

In the present work, above orthogonal polynomials are used in the analysis of non-rotating and rotating uncoupled Timoshenko beam for verification purpose and then applied

to find the natural frequencies of the coupled flexural-torsional vibration of rotating and non-rotating beams. The results are compared to those given in the references and in the case of coupled flexural-torsional vibrations of Euler-Bernoulli beam are also compared to references and results obtained using the NASTRAN finite element package.

Chapter 2

Literature Review

2.1 Basic Beam Theories

A beam theory formulates the problem of the transversely vibrating beams in terms of the partial differential equation of motion, an external forcing function, boundary conditions and initial conditions. The earliest theory for studying beam behavior is the Euler-Bernoulli beam theory which concentrate only on bending effect as the most important factor for a transversely vibrating beam. Jacob Bernoulli first discovered that the curvature of an elastic beam at any point is proportional to the bending moment at that point and Daniel Bernoulli formulated the differential equation of motion of a vibrating beam. Leonhard Euler [7] accepted Jacob Bernoulli's theory in his investigation of the shape of elastic beams under various loading conditions and made many advances in the analysis of elastic curves. Because of its simplicity and capability of providing reasonable engineering approximations for many problems, this Euler-Bernoulli beam theory is most commonly used. However, the Euler-Bernoulli model slightly overestimate the natural frequencies. For the natural frequencies of higher modes, this problem is exacerbated. Also, the prediction gets worse for non-slender beams.

The Rayleigh beam theory [8] provides a slight improvement on the Euler-Bernoulli theory by including the effect of rotations of the cross-section. It partially corrects the overestimation of natural frequencies in the Euler-Bernoulli model. However, the natural frequencies are still overestimated with this method especially in the case of non-slender beams because shear effect is not considered in this method. The shear model adds shear distortion to the Euler-Bernoulli model. By adding shear distortion to the Euler-Bernoulli beam, the estimate of the natural frequencies improves considerably.

The Timoshenko beam theory [9][10] gives a significant improvement for non-slender beams and for high-frequency responses when shear or rotary effects are not negligible. This theory adds the effect of shear and rotation to the Euler-Bernoulli beam.

There have been several other works which have formulated frequency equations and the mode shape for various boundary conditions using Timoshenko's work. Kruszewski [12] obtained the first antisymmetric and symmetric modes of a free-free beam. Traill-Nash and Collar [13] gave a reasonably complete theoretical treatment as well as experimental results for the case of the uniform Euler-Bernoulli, shear, and Timoshenko beams. Huang [14] obtained the frequency equations and expressions for the mode shapes for all six end conditions.

Kruszewski, Trail-Nash and Collar, and Huang only gave expressions for the natural frequencies and mode shapes. They did not solve for the complete response of the beam due to initial conditions and external forces. To do so, using the modal super position method, knowledge of the orthogonality conditions among the eigenfunctions is required. The orthogonality conditions for the Timoshenko beam were independently obtained by Dolph [15] and Herrmann [16]. Dolph solved the initial and boundary-value problem for a hinged-hinged beam with no external forces. The methods used to solve for the forced initial boundary-value problem and for the problem with time-dependent boundary conditions are briefly mentioned in his paper.

A refined engineering beam theory which contains two shear coefficients was de-

rived based on the asymptotic expansion approach applied to the equations of linear three-dimensional elasticity theory by Fan and Widera [18]. The advantage of the new engineering beam theory over the Timoshenko beam theory is that the axial tension can be determined directly.

A crucial parameter in Timoshenko beam theory is the shape factor. The parameter arises because the shear is not constant over the cross-section. The shape factor is a function of Poisson's ratio, the frequency of vibrations, and the shape of the cross-section. Typically, the functional dependence on frequency is ignored. Calculating a function of the shape of the cross-section and Poisson's ratio was suggested by Davies [17] and others.

Despite current efforts, the Euler-Bernoulli and Timoshenko beam theories are still widely used because of their relatively reliable results in most practices.

2.2 Rotating Beams

There have been a number of studies on rotating beams. Boyce and Handelman [19] studied the vibrations of rotating cantilever beams by the Southwell principle and the Rayleigh-Ritz method. Carnegie [20] derived energy expressions for a rotating beam undergoing transverse vibrations and obtained the natural frequency of vibration using the Rayleigh's method. In this work, the characteristic differential equations of motion for the rotating system were obtained from the energy expressions using variational calculus. Schilhansl [21], Rubinstein and Stadter [22], and Pnuelli [23] investigated the vibrations of rotating cantilever beams. They found that the rotation increase the natural frequencies of flexural vibration above those for the non-rotating beam. Lo *et al.* [24] and Boyce *et al.* [25] used the perturbation technique. Kumar [26] used the Myklestad method. Stafford and Giurgiutiu [27] and McDaniel and Murthy [28] used the transfer matrix approach. Subrahmanyam *et al.* [29] used the Reissner method to obtain the natural frequencies of rotating blades of asymmetric aerofoil cross section with allowance for shear deflection and rotary inertia

and showed that the method gives results which are superior to those obtained by using the potential energy expression in the Ritz method. Bhat [30] studied natural frequencies and mode shapes of a rotating uniform cantilever beam with a tip mass by using beam characteristic orthogonal polynomials in the Rayleigh-Ritz method using the Gram-Schmidt process [43]. Bazoune and Khulief [33] developed a finite beam element for vibration analysis of a rotating tapered beam including shear deformations and rotary inertia. Yokoyama [34] analyzed the in-plane and out-of-plane free vibrations of a rotating Timoshenko beam by means of a finite element technique. In this work, the beam was discretized into a number of simple elements with four degrees of freedom each. The governing equations for the free vibrations of the rotating beam are derived from Hamilton's principle. The effects of hub radius, setting angle, shear deformation and rotary inertia are incorporated into a finite element model for determining the bending frequencies of the rotating beam.

2.3 Flexural-torsional coupled beam

Dokumaci [1] presented an exact determination of coupled bending and torsional vibration characteristics of uniform beams having single cross-sectional symmetry. In his study, the simplest continuous mathematical model for the analysis of coupled bending and torsion vibrations is obtained by combining the Euler-Bernoulli theory for bending and St. Venant theory for torsion. Dokumaci showed that the exact solutions can be expressed in real form in a way customary for the more elementary free vibration problems of uniform beams and explained the effect of coupling between bending and torsional vibrations on the natural frequencies and modes. Also, he showed that the roots of the characteristic equation of the governing differential equations of motions can be separated to obtain real exact solutions. The effect of shear center offset on natural frequencies and modes were studied as well. Bishop *et al.* [2] started from Dokumaci's theory that the Euler-Bernoulli theory of beam flexure may be combined with the Saint-Venant theory of torsion to describe the coupled antisymmetric free vibration of uniform beams having a plane of symmetry and extended this

theory to allow for warping of the beam cross-section. He found that inclusion of warping effect could make a large difference to results for thin-walled beam of open section. Bercin and Tanaka [3] studied coupled flexural-torsional vibrations of Timoshenko beams taking into account the warping stiffness using Bishop's technique [2] which was extended from Dokumaci's. They demonstrated the method in numerical results and showed that the effect of including warping increase the natural frequencies and Timoshenko effects decrease the natural frequencies. Banerjee and Fisher [36] studied coupled bending-torsional vibration in axially loaded condition in the method of dynamic stiffness matrix. Adam [37] analyzed coupled bending and torsional vibrations of beams under forced vibration. Adam solved the governing coupled set of partial differential equations by separating the dynamic response in a quasistatic and in a complementary dynamic response and getting the generalized decoupled single-degree-of-freedom oscillators by means of Duhamel's convolution integral.

2.4 Orthogonal Polynomials

The subject of orthogonal polynomials can be traced back to Legendre's work on planetary motion. There was important applications to physics and to probability and statistics and other branches of mathematics in that era. In recent years, the availability of the computers has enabled a higher activity in approximation theory and numerical analysis. These activities have raised interest in using the orthogonal polynomials for obtaining approximate results.

Karunamoorthy *et al.* [38] developed a complete set of orthogonal polynomials by applying Gram-Schmidt orthogonalization process to the Duncan trinomials and binomials. Duncan polynomials can be used as basis functions for elastic bending and torsion but these are not orthogonal and may lead to a poor numerical conditioning. Karunamoorthy's new polynomials for hingeless and articulated rotors are orthogonal and satisfy both geometric and natural boundary conditions at both the tip and the root of a rotating beam. Bardell *et*

al. [39] used ascending hierarchy of special trigonometric functions, used in conjunction with Hermite cubics as assumed displacement functions in the h-p version of the finite element method. Bardell *et al.* used the same set of assumed displacement functions to represent the motions in all coordinate directions. This ascending hierarchy of special trigonometric functions, used in conjunction with Hermite cubics, furnished a robust complete set of admissible displacement functions. Amabili and Garziera [41] built a technique for the systematic choice of admissible functions, which are the eigenfunctions of the closest, simple problem extracted from the one considered. Ruta [42] dealt with the problem of the linear vibration of a beam with variable strength and geometric parameters, resting on a two-parameter, heterogeneous elastic foundation. It was assumed that the variable parameters of the bar, such as flexural and axial rigidity and density, the variable parameters of the foundation and the load was represented by a series expansion in relation to Chebyshev polynomials of first kind and the longitudinal and transverse vibration of the bar were analyzed. Bhat [30] developed beam characteristic orthogonal polynomials using Gram-Schmidt process to be used as basis functions in the Rayleigh-Ritz analysis. These orthogonal polynomials satisfy the geometrical boundary conditions of the beam and are generated by Gram-Schmidt process [43].

Chapter 3

Basic Beam Theories

Since the study of the coupled flexural-torsional vibration start from the basic beam theories, it is important to review and study the derivation of the various basic beam theories prior to the study of coupled flexural-torsional vibration of beams. Here, basic beam theories of Euler-Bernoulli, Rayleigh, shear and Timoshenko beam theories are reviewed from their derivation. The assumptions made by all models are as follows.

1. One dimension (the axial direction) is considerably larger than the other two.
2. The material is linear elastic (Hookean).
3. The Poisson effect is neglected.
4. The cross-sectional area is symmetric so that the neutral and centroidal axes coincide.
5. The angle of rotation is small so that the small angle assumption can be used.

3.1 The Euler-Bernoulli Beam Theory

The simplest beam theory is the Euler-Bernoulli Beam theory which rely on bending effect only. The Euler-Bernoulli beam theory does not consider the rotatory inertia and the shear effects. The strain energy of a uniform beam due to bending is

$$PE = \frac{1}{2}\int_0^L EI\left(\frac{\partial^2 v(x,\,t)}{\partial x^2}\right)^2 \mathrm{d}x \tag{3.1}$$

where E is the modulus of elasticity, I the area moment of inertia of the cross-section about the neutral axis, $v(x,t)$ the transverse deflection at the axial location x and time t, and L the length of the beam. The kinetic energy is

$$KE = \frac{1}{2}\int_0^L \rho A\left(\frac{\partial v(x,\,t)}{\partial t}\right)^2 \mathrm{d}x \tag{3.2}$$

where ρ is the density of the beam and A, the cross-sectional area. The Lagrangian is given by

$$\begin{aligned}\mathbf{L} &= KE - PE \\ &= \int_0^L \left[\frac{\rho A}{2}\left(\frac{\partial v(x,\,t)}{\partial t}\right)^2 - \frac{EI}{2}\left(\frac{\partial^2 v(x,\,t)}{\partial x^2}\right)^2\right]\mathrm{d}x\end{aligned} \tag{3.3}$$

The Hamilton's principle states that the path of admissible configurations that satisfies Newton's law at each instant during the interval is the path that yields a stationary value of the time integral of the Lagrangian during the interval [32]. Therefore, Hamilton's principle requires that

$$\delta\int_{t1}^{t2}\int_0^L \left[\frac{\rho A}{2}\left(\frac{\partial v(x,\,t)}{\partial t}\right)^2 - \frac{EI}{2}\left(\frac{\partial^2 v(x,\,t)}{\partial x^2}\right)^2\right]\mathrm{d}x\,\mathrm{d}t = 0 \tag{3.4}$$

Using integration by parts, we get

$$\begin{aligned}-\int_{t1}^{t2}\int_0^L \left(\rho A\frac{\partial^2 v}{\partial t^2} + EI\frac{\partial^4 v}{\partial x^4}\right)\delta v\,\mathrm{d}x\,\mathrm{d}t + \int_0^L \rho A\frac{\partial v}{\partial t}\delta v\,dx\Big|_{t1}^{t2} \\ - \int_{t1}^{t2} EI\frac{\partial^2 v}{\partial x^2}\delta\frac{\partial v}{\partial x}\,dt\Big|_0^L + \int_{t1}^{t2} EI\frac{\partial^3 v}{\partial x^3}\delta v\,dt\Big|_0^L &= 0\end{aligned} \tag{3.5}$$

The governing differential equation and boundary conditions are derived from the above equation. The differential equation for Euler-Bernoulli beam is

$$\rho A \frac{\partial^2 v(x,\,t)}{\partial t^2} + EI \frac{\partial^4 v(x,\,t)}{\partial x^4} = 0. \tag{3.6}$$

Since δv is zero at time t_1 and time t_2, the boundary conditions are

$$\frac{\partial^2 v}{\partial x^2}\,\delta\left(\frac{\partial v}{\partial x}\right)\Bigg|_0^L = 0, \qquad \frac{\partial^3 v}{\partial x^3}\,\delta v\Bigg|_0^L = 0 \tag{3.7}$$

To see the physical meanings of the boundary conditions, v is the displacement, $\frac{\partial v}{\partial x}$ is the dimensionless slope, $\frac{\partial^2 v}{\partial x^2}$ is the dimensionless moment, $\frac{\partial^3}{\partial x^3}$ is the dimensionless shear. Althogh expression on variations, $\delta v = 0$ and $\delta\left(\frac{\partial v}{\partial x}\right) = 0$, means that only the variation of the displacement or the slope is zero, because base excited or end forcing problems are not considered in current study, they means that the displacement or the slope is zero here. Therefore, in satisfying the boundary conditions, four combinations of end boundary conditions are possible as:

$$\begin{aligned}
&\frac{\partial^2 v}{\partial x^2} = 0\ , \quad \frac{\partial^3 v}{\partial x^3} = 0 && \text{free end}\\
&\frac{\partial v}{\partial x} = 0\ , \quad v = 0 && \text{clamped end}\\
&\frac{\partial^2 v}{\partial x^2} = 0\ , \quad v = 0 && \text{hinged end}\\
&\frac{\partial v}{\partial x} = 0\ , \quad \frac{\partial^3 v}{\partial x^3} = 0 && \text{sliding end}
\end{aligned} \tag{3.8}$$

3.2 The Rayleigh Beam Model

The Rayleigh beam adds the rotary inertia effects to the Euler-Bernoulli beam. The Kinetic energy due to the rotary inertia is

$$KE_{rot} = \frac{1}{2}\int_0^L \rho I \left(\frac{\partial^2 v(x,\,t)}{\partial t \partial x}\right)^2 \mathrm{d}x \tag{3.9}$$

Therefore, the Lagrangian becomes the addition of the rotating effect to the Lagrangian of Euler-Bernoulli beam and to be

$$\mathbf{L} = \frac{1}{2}\int_0^L \left[\rho A \left(\frac{\partial v(x,\,t)}{\partial t}\right)^2 + \rho I \left(\frac{\partial^2 v(x,\,t)}{\partial t \partial x}\right)^2 - EI \left(\frac{\partial^2 v(x,\,t)}{\partial x^2}\right)^2\right] \tag{3.10}$$

Applying Hamilton's principle to the Lagrangian, we obtain the equation of motion as:

$$\rho A\frac{\partial^2 v(x,\,t)}{\partial t^2}+EI\frac{\partial^4 v(x,\,t)}{\partial x^4}-\rho I\frac{\partial^4 v(x,\,t)}{\partial x^2\partial t^2}=0 \tag{3.11}$$

The boundary conditions in this case are

$$\frac{\partial^2 v}{\partial x^2}\delta\left(\frac{\partial v}{\partial x}\right)\Bigg|_0^L=0,\qquad\left(\frac{\partial^3 v}{\partial x^3}-\rho I\frac{\partial^3 v}{\partial x\partial t^2}\right)\delta v\Bigg|_0^L=0 \tag{3.12}$$

The physical meanings of the boundary conditions are that v is the displacement, $\frac{\partial v}{\partial x}$ is the dimensionless slope, $\frac{\partial^2 v}{\partial x^2}$ is the dimensionless moment, $\frac{\partial^3 v}{\partial x^3}-\rho I\frac{\partial^3 v}{\partial x\partial t^2}$ is the dimensionless shear. The end conditions from the four combinations of boundary conditions are

$$\begin{aligned}
&\frac{\partial^2 v}{\partial x^2}=0\,,\quad &&\frac{\partial^3 v}{\partial x^3}-\rho I\frac{\partial^3 v}{\partial x\partial t^2}=0 &&\text{free end}\\
&\frac{\partial v}{\partial x}=0\,, &&v=0 &&\text{clamped end}\\
&\frac{\partial^2 v}{\partial x^2}=0\,, &&v=0 &&\text{hinged end}\\
&\frac{\partial v}{\partial x}=0\,,\quad &&\frac{\partial^3 v}{\partial x^3}-\rho I\frac{\partial^3 v}{\partial x\partial t^2}=0 &&\text{sliding end}
\end{aligned} \tag{3.13}$$

3.3 The Shear Beam Model

The Shear Beam Model adds the effect of shear distortion to the Euler-Bernoulli model. The total rotation is the sum of the rotation of the cross-section due to the bending moment, s, and the angle of distortion due to shear, α, and is approximated by the first derivative of the deflection.

$$s(x,\,t)+\alpha(x,\,t)=\frac{\partial v(x,\,t)}{\partial z} \tag{3.14}$$

Therefore, the strain energy resulting in bending becomes:

$$PE_{bending}=\frac{1}{2}\int_0^L\left(EI\frac{\partial s(x,\,t)}{\partial x}\right)^2\,\mathrm{d}x \tag{3.15}$$

and the strain energy resulting from shear becomes:

$$PE_{shear}=\frac{1}{2}\int_0^L\kappa GA\left(\frac{\partial v(x,t)}{\partial x}-s(x,t)\right)^2\,\mathrm{d}x \tag{3.16}$$

where κ is the shear factor.

The Lagrangian of the shear beam model is

$$\mathbf{L} = \frac{1}{2}\int_0^L \left[\rho A\left(\frac{\partial v(x,t)}{\partial t}\right)^2 - EI\left(\frac{\partial s(x,t)}{\partial x}\right)^2 - \kappa GA\left(\frac{\partial v(x,t)}{\partial x} - s(x,t)\right)^2\right] dx. \tag{3.17}$$

Equations of motion are obtained by Hamilton's principle as:

$$\rho A\frac{\partial^2 v(x,t)}{\partial t^2} - \kappa GA\left(\frac{\partial^2 v}{\partial x^2} - \frac{\partial s(x,t)}{\partial x}\right) = 0 \tag{3.18}$$

$$EI\frac{\partial^2 s(x,t)}{\partial x^2} + \kappa GA\left(\frac{\partial v}{\partial x} - s(x,t)\right) = 0 \tag{3.19}$$

The boundary conditions become:

$$\frac{\partial s}{\partial x}\,\delta s\Big|_0^L = 0, \quad \kappa GA\left(\frac{\partial v}{\partial x} - s\right)\delta v\Big|_0^L = 0 \tag{3.20}$$

The physical meanings are that v is the displacement and s is the rotation angle, $\frac{\partial s}{\partial x}$ is the dimensionless moment, and $\kappa GA\left(\frac{\partial v}{\partial x} - s\right)$ is the dimensionless shear. The end conditions from the four possible combinations of boundary conditions are

$$\begin{aligned}
\frac{\partial s}{\partial x} &= 0\,, \quad \kappa GA\left(\frac{\partial v}{\partial x} - s\right) = 0 && \text{free end}\\
s &= 0\,, \quad v = 0 && \text{clamped end}\\
\frac{\partial s}{\partial x} &= 0\,, \quad v = 0 && \text{hinged end}\\
s &= 0\,, \quad \kappa GA\left(\frac{\partial v}{\partial x} - s\right) = 0 && \text{sliding end}
\end{aligned} \tag{3.21}$$

3.4 The Timoshenko Beam Model

Timoshenko beam model includes shear deformation and rotatory inertia along with bending displacement. The strain energy includes shear bending effect.

$$PE = \frac{1}{2}\int_0^L \left[EI\left(\frac{\partial s(x,t)}{\partial x}\right)^2 + kGA\left(\frac{\partial v(x,\,t)}{\partial x} - s(x,\,t)\right)^2\right] \mathrm{d}x \tag{3.22}$$

The kinetic energy includes rotatory inertia and bending motion.

$$KE = \frac{1}{2}\int_0^L \left[\rho A\left(\frac{\partial v(x,t)}{\partial t}\right)^2 + \rho I\left(\frac{\partial s(x,\,t)}{\partial t}\right)^2\right] \mathrm{d}x \tag{3.23}$$

The Lagrangian for the Timoshenko beam becomes:

$$\begin{aligned}\mathbf{L} &= \frac{1}{2}\int_0^L \left[\rho A\left(\frac{\partial v(x,t)}{\partial t}\right)^2 + \rho I\left(\frac{\partial s(x,\,t)}{\partial t}\right)^2 - EI\left(\frac{\partial s(x,t)}{\partial x}\right)^2\right. \\ &\quad \left. -kGA\left(\frac{\partial v(x,\,t)}{\partial x} - s(x,\,t)\right)^2\right] \mathrm{d}x \end{aligned} \tag{3.24}$$

The equations of motions obtained using the Hamilton's principle are:

$$\begin{aligned}\rho A\frac{\partial^2 v(x,t)}{\partial t^2} - kGA\left(\frac{\partial^2 v(x,\,t)}{\partial x^2} - \frac{\partial s(x,t)}{\partial x}\right) &= 0 \\ \rho I\frac{\partial^2 s(x,t)}{\partial t^2} - EI\frac{\partial^2 s(x,t)}{\partial x^2} - kGA\left(\frac{\partial v(x,t)}{\partial x} - s(x,t)\right) &= 0 \end{aligned} \tag{3.25}$$

The boundary conditions from the equations of motions are

$$\frac{\partial s}{\partial x}\delta s\Big|_0^L = 0, \quad kGA\left(\frac{\partial v}{\partial x} - s\right)\delta v\Big|_0^L = 0. \tag{3.26}$$

These boundary conditions are same as those for the shear beam model.

3.5 The Rotating Timoshenko Beam

When a beam rotates, the induced centrifugal force adds stiffness to the beam. Designating centrifugal force in axial direction as F_{cent}, the potential energy becomes:

$$PE = \frac{1}{2}\int_0^L \left[EI\left(\frac{\partial s(x,t)}{\partial x}\right)^2 + kGA\left(\frac{\partial v(x,\,t)}{\partial x} - s(x,\,t)\right)^2 + F_{cent}\left(\frac{\partial v(x,t)}{\partial x}\right)^2\right] \mathrm{d}x \tag{3.27}$$

Lagrangian in this case is

$$\begin{aligned}\mathrm{L} &= \frac{1}{2}\int_0^L \left[\rho A\left(\frac{\partial v(x,t)}{\partial t}\right)^2 + \rho I\left(\frac{\partial s(x,\,t)}{\partial t}\right)^2 - EI\left(\frac{\partial s(x,t)}{\partial x}\right)^2\right. \\ &\quad \left. -kGA\left(\frac{\partial v(x,\,t)}{\partial x} - s(x,\,t)\right)^2 - F_{cent}\left(\frac{\partial v(x,t)}{\partial x}\right)^2\right] \mathrm{d}x \end{aligned} \tag{3.28}$$

Applying Hamilton's principle, the equations of motion of this case with added stiffness due to the centrifugal force become:

$$-\frac{\partial}{\partial x}\left\{\kappa GA\left(\frac{\partial v}{\partial x}+s\right)\right\}+\rho A\frac{\partial^2 v}{\partial t^2}-\frac{\partial}{\partial x}\left(F_{cent}\frac{\partial v}{\partial x}\right) = 0 \quad (3.29)$$

$$\kappa GA\left(\frac{\partial v}{\partial x}+s\right)-\frac{\partial}{\partial x}\left\{EI\left(\frac{\partial v}{\partial x}\right)\right\}+\rho I\frac{\partial^2 s}{\partial t^2} = 0 \quad (3.30)$$

Assuming the solution of the above differential equations to be in the form of

$$v(x,t) = V(x)e^{-i\omega t} \quad (3.31)$$

$$s(x,t) = S(x)e^{-i\omega t}, \quad (3.32)$$

where ω denotes the frequency of natural flexural-torsional coupled motion, and $V(x)$ and $S(x)$ denotes mode shapes, and that the beam is uniform in the axial direction, (3.29) and (3.30) can be expressed as:

$$e^{-i\omega t}\left\{\kappa GA\left(\frac{\mathrm{d}^2V}{\mathrm{d}x^2}+\frac{\mathrm{d}S}{\mathrm{d}x}\right)+F_{cent}\frac{\mathrm{d}^2V}{\mathrm{d}x^2}-\omega^2\rho AV\right\} = 0 \quad (3.33)$$

$$e^{-i\omega t}\left\{\kappa GAw_2\left(\frac{\mathrm{d}V}{\mathrm{d}x}+S\right)+EI\frac{\mathrm{d}S}{\mathrm{d}x}-\omega^2\rho IS\right\} = 0 \quad (3.34)$$

Omitting $e^{-i\omega t}$ and integrating above differential equation after multiplying weight function w_1 and w_2, we obtain the weak forms to be

$$\int_0^L\left\{\kappa GA\frac{\mathrm{d}w_1}{\mathrm{d}x}\left(\frac{\mathrm{d}V}{\mathrm{d}x}+S\right)+F_{cent}\frac{\mathrm{d}w_1}{\mathrm{d}x}\frac{\mathrm{d}V}{\mathrm{d}x}-\omega^2\rho Aw_1V\right\}\mathrm{d}x - \left[w_1\kappa GA\left(\frac{\mathrm{d}V}{\mathrm{d}x}+S\right)\right]_0^L-\left[w_1F_{cent}\frac{\mathrm{d}V}{\mathrm{d}x}\right]_0^L = 0 \quad (3.35)$$

$$\int_0^L\left\{\kappa GAw_2\left(\frac{\mathrm{d}V}{\mathrm{d}x}+S\right)+EI\frac{\mathrm{d}w_2}{\mathrm{d}x}\frac{\mathrm{d}S}{\mathrm{d}x}-\omega^2\rho Iw_2S\right\}\mathrm{d}x-\left[w_2EI\frac{\mathrm{d}S}{\mathrm{d}x}\right]_0^L = 0 \quad (3.36)$$

The essential and natural boundary conditions expressed in Equation (3.21) eliminate boundary terms in the weak forms. Amplitudes V and S can be expressed using the approximating functions as:

$$V = \sum_{j=1}^{m} v_j\Psi_j^{(1)} \quad (3.37)$$

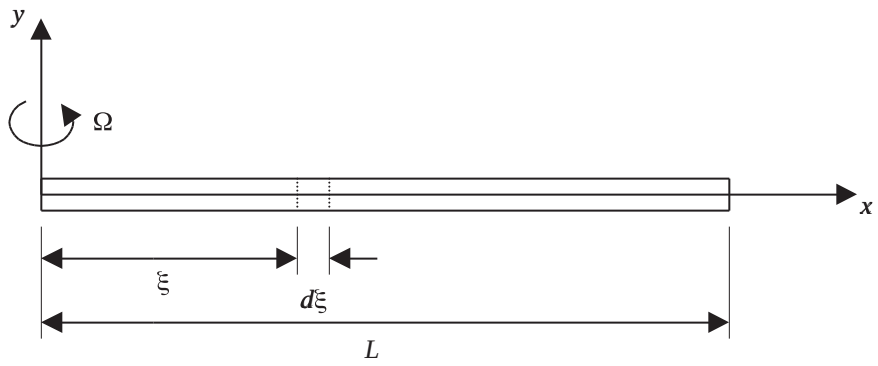

Figure 3.1: Centrifugal force

$$S = \sum_{j=1}^{n} s_j \Psi_j^{(2)} \tag{3.38}$$

where Ψ_0, Ψ_1, Ψ_2, ... are approximating functions that fulfill the essential boundary conditions and v_j and s_j are the undetermined parameters. The centrifugal force shown, acting on a differential element, in Figure 3.1 can be expressed for the axial location as:

$$F_{cent}(x) = \Omega^2 \int_x^L \rho A \xi \, \mathrm{d}\xi \tag{3.39}$$

where Ω is rotating speed. Substituting approximating functions with v and j in the weak (3.35) and (3.36) result in mass and stiffness matrix as:

$$\begin{bmatrix} [K^{11}] & [K^{12}] \\ [K^{12}] & [K^{22}] \end{bmatrix} \begin{Bmatrix} \{A\} \\ \{B\} \end{Bmatrix} - \lambda \begin{bmatrix} [M^{11}] & [0] \\ [0] & [M^{22}] \end{bmatrix} \begin{Bmatrix} \{A\} \\ \{B\} \end{Bmatrix} = \begin{Bmatrix} \{0\} \\ \{0\} \end{Bmatrix} \tag{3.40}$$

$$K_{ij}^{11} = \int_0^L \kappa G A \frac{\mathrm{d}\Psi_i^{(1)}}{\mathrm{d}x} \frac{\mathrm{d}\Psi_j^{(1)}}{\mathrm{d}x} \, \mathrm{d}x + \int_0^L F_z \frac{\mathrm{d}\Psi_i^{(1)}}{\mathrm{d}x} \frac{\mathrm{d}\Psi_j^{(1)}}{\mathrm{d}x} \, \mathrm{d}x + \int_0^L F_{cent}(x) \Psi_i^{(1)} \Psi_j^{(1)} \, \mathrm{d}x \tag{3.41}$$

$$K_{ij}^{12} = \int_0^L \kappa GA \frac{\mathrm{d}\Psi_i^{(1)}}{\mathrm{d}x} \Psi_j^{(2)} \, \mathrm{d}x \tag{3.42}$$

$$K_{ij}^{22} = \int_0^L \left(EI \frac{\mathrm{d}\Psi_i^{(2)}}{\mathrm{d}x} \frac{\mathrm{d}\Psi_j^{(2)}}{\mathrm{d}x} + \kappa GA \Psi_i^{(2)} \Psi_j^{(2)} \right) \, \mathrm{d}x \tag{3.43}$$

$$M_{ij}^{11} = \int_0^L \rho A \Psi_i^{(1)} \Psi_j^{(1)} \, \mathrm{d}x \tag{3.44}$$

$$M_{ij}^{22} = \int_0^L \rho I \Psi_i^{(2)} \Psi_j^{(2)} \, \mathrm{d}x \tag{3.45}$$

where $\lambda = \omega^2$.

Chapter 4

Bending-Torsion Coupled Beams

4.1 Equations of Motion and Boundary Conditions

A beam that displays flexural-torsional vibration is shown in Figure 4.1. The equations of motion of a uniform beam executing coupled free bending and torsional vibration with warping are obtained from [2]. The equations of motion for coupled bending and torsional vibration of an Euler-Bernoulli beam are

$$EI\frac{\partial^4 v}{\partial x^4} + m\frac{\partial^2 (v + e\theta)}{\partial t^2} = 0 \tag{4.1}$$

$$EI_w\frac{\partial^4 \theta}{\partial x^4} - GJ\frac{\partial^2 \theta}{\partial x^2} + m\frac{\partial^2 [(e^2 + r^2)\theta + ev]}{\partial t^2} = 0. \tag{4.2}$$

Here, t denotes time, x is the distance along the elastic axis of the beam and v is the bending displacement of the shear center in the direction of the y axis, the beam cross-section being assumed symmetrical about the plane O_{xz}. The quantity θ is the torsional rotation, e the position of the section centroid C relative to the shear center S, m is the mass per unit length and r the polar radius of gyration of the cross-section about the centroid. The flexural rigidity in the O_{yx} plane is EI, while EI_w is the torsional rigidity associated with warping and GJ is the Saint-Venant torsional rigidity.

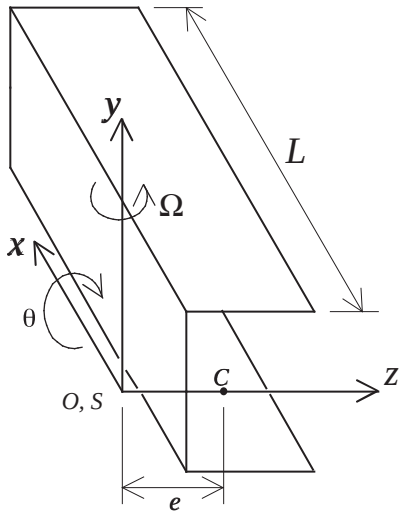

Figure 4.1: Uniform Channel Beam

The boundary conditions are : at a clamped end ($x = 0$),

$$v = 0 = \frac{\partial v}{\partial x} \quad \text{and} \quad \theta = 0 = \frac{\partial \theta}{\partial x} \tag{4.3}$$

at a free end ($x = L$),

$$\frac{\partial^2 v}{\partial x^2} = 0, \quad \frac{\partial^3 v}{\partial x^3} = 0, \quad \frac{\partial^2 \theta}{\partial x^2} = 0, \quad \text{and} \quad -EI_w \frac{\partial^3 \theta}{\partial z^3} + GJ \frac{\partial \theta}{\partial x} = 0. \tag{4.4}$$

When the rotation occurs in the structure the centrifugal force of $m\Omega^2 \int_x^L \xi \, d\xi$ (m is the mass over unit length and Ω is the rotating speed)is applied in axial direction. The effect of this axial force in the equation of motion is obtained from [36]. Therefore, the equations of motions (4.1) and (4.2) become

$$\begin{aligned} EI\frac{\partial^4 v}{\partial x^4} - m\Omega^2 \int_x^L \zeta \, d\zeta \, \frac{\partial^2 v}{\partial x^2} + m\Omega^2 e \int_x^L \zeta \, d\zeta \, \frac{\partial^2 \theta}{\partial x^2} + m\frac{\partial^2 v}{\partial t^2} - me\frac{\partial^2 \theta}{\partial t^2} &= 0 \\ m\Omega^2 e \int_x^L \zeta \, d\zeta \, \frac{\partial^2 v}{\partial x^2} + EI_w \frac{\partial^4 \theta}{\partial x^4} - GJ\frac{\partial^2 \theta}{\partial x^2} - m\Omega^2(e^2 + r^2) \int_x^L \zeta \, d\zeta \, \frac{\partial^2 \theta}{\partial x^2} & \end{aligned} \tag{4.5}$$

$$-me\frac{\partial^2 v}{\partial t^2} + m(e^2 + r^2)\frac{\partial^2 \theta}{\partial t^2} = 0 \qquad (4.6)$$

4.2 Derivation of Mass and Stiffness Matrix

We assume the solution of the differential equations (4.5) and (4.6) to be in the form of

$$v(x,\, t) = V(x)e^{-i\omega t} \qquad (4.7)$$

$$\theta(x,\, t) = \Theta(x)e^{-i\omega t} \qquad (4.8)$$

where ω denotes the frequency of natural flexural-torsional coupled motion, and $V(x)$ and $\theta(x)$ denotes mode shapes during the vibration. Substitution of (4.7) and (4.8) into (4.5) and (4.6) gives

$$\left[EI\frac{\mathrm{d}^4 V}{\mathrm{d}x^4} - m\Omega^2 \int_x^L \zeta\, d\zeta \left(\frac{\mathrm{d}^2 V}{\mathrm{d}x^2} - e\frac{\mathrm{d}^2 \Theta}{\mathrm{d}x^2}\right) - \omega^2(mV - me\Theta)\right] e^{-i\omega t} = 0 \qquad (4.9)$$

$$\left[m\Omega^2 \int_x^L \zeta\, d\zeta \left\{e\frac{\mathrm{d}^2 V}{\mathrm{d}x^2} - (e^2 + r^2)\frac{\mathrm{d}^2 \Theta}{\mathrm{d}x^2}\right\} + EI_w\frac{\mathrm{d}^4 \Theta}{\mathrm{d}x^4} - GJ\frac{\mathrm{d}^2 \Theta}{\mathrm{d}x^2} - \omega^2\left\{m(e^2 + r^2)\Theta - meV\right\}\right] e^{-i\omega t} = 0 \qquad (4.10)$$

The weak forms are derived by multiplying Equation (4.9) with a weight function w_1 and Equation (4.10) with a weight function w_2 and integrating the resulting equations over the beam length. Replace ω^2 by λ and the weak forms become:

$$\int_0^L w_1 \left\{EI\frac{\mathrm{d}^4 V}{\mathrm{d}x^4} - m\Omega^2 \int_x^L \zeta\, d\zeta \left(\frac{\mathrm{d}^2 V}{\mathrm{d}x^2} - e\frac{\mathrm{d}^2 \Theta}{\mathrm{d}x^2}\right) - \lambda(mV - me\Theta)\right\} \mathrm{d}x = 0 \qquad (4.11)$$

$$\int_0^L w_2 \left\{m\Omega^2 \int_x^L \zeta\, d\zeta \left\{e\frac{\mathrm{d}^2 V}{\mathrm{d}x^2} - (e^2 + r^2)\frac{\mathrm{d}^2 \Theta}{\mathrm{d}x^2}\right\} + EI_w\frac{\mathrm{d}^4 \Theta}{\mathrm{d}x^4} - GJ\frac{\mathrm{d}^2 \Theta}{\mathrm{d}x^2} - \lambda\left\{m(e^2 + r^2)\Theta - meV\right\}\right\} \mathrm{d}x = 0 \qquad (4.12)$$

Using integration by parts, the order of differentiation of the weight function and the dependent variable is distributed evenly.

$$\int_0^L \left\{EI\frac{\mathrm{d}^2 w_1}{\mathrm{d}x^2}\frac{\mathrm{d}^2 V}{\mathrm{d}x^2} + m\Omega^2 \int_x^L \zeta\, d\zeta \left(\frac{\mathrm{d}w_1}{\mathrm{d}x}\frac{\mathrm{d}V}{\mathrm{d}x} - e\frac{\mathrm{d}w_1}{\mathrm{d}x}\frac{\mathrm{d}\Theta}{\mathrm{d}x}\right) - \lambda(mw_1 V - mew_1\Theta)\right\} \mathrm{d}x$$

$$
\begin{aligned}
&+ w_1 \left\{ EI\frac{\mathrm{d}^3V}{\mathrm{d}x^3} - m\Omega^2 \int_x^L \zeta\, d\zeta \left(\frac{\mathrm{d}V}{\mathrm{d}x} - e\frac{\mathrm{d}\Theta}{\mathrm{d}x} \right) \right\} \Big|_0^L \\
&- \frac{\mathrm{d}w_1}{\mathrm{d}x} \left(EI\frac{\mathrm{d}^2V}{\mathrm{d}x^2} \right) \Big|_0^L = 0 \qquad (4.13)
\end{aligned}
$$

$$
\begin{aligned}
&\int_0^L \left\{ EI_w \frac{\mathrm{d}^2w_2}{\mathrm{d}x^2}\frac{\mathrm{d}^2\Theta}{\mathrm{d}x^2} - m\Omega^2 \int_x^L \zeta\, d\zeta \left(e\frac{\mathrm{d}w_2}{\mathrm{d}x}\frac{\mathrm{d}V}{\mathrm{d}x} - (e^2+r^2)\frac{\mathrm{d}w_2}{\mathrm{d}x}\frac{\mathrm{d}\Theta}{\mathrm{d}x} \right) \right. \\
&\left. + GJ\frac{\mathrm{d}w_2}{\mathrm{d}x}\frac{\mathrm{d}\Theta}{\mathrm{d}x} - \lambda \left\{ m\left(e^2+r^2\right) w_2\Theta - mew_2V \right\} \right\} \mathrm{d}x \\
&- w_2 \left\{ m\Omega^2 \int_x^L \zeta\, d\zeta \left(e\frac{\mathrm{d}V}{\mathrm{d}x}(e^2+r^2)\frac{\mathrm{d}\Theta}{\mathrm{d}x} \right) - EI_w\frac{\mathrm{d}^3\Theta}{\mathrm{d}x^3} + GJ\frac{\mathrm{d}\Theta}{\mathrm{d}x} \right\} \Big|_0^L \\
&- \frac{\mathrm{d}w_2}{\mathrm{d}x} EI_w \frac{\mathrm{d}^2\Theta}{\mathrm{d}x^2} \Big|_0^L = 0 \qquad (4.14)
\end{aligned}
$$

From Equations (4.13) and (4.14), primary variables are identified as V, $\mathrm{d}V/\mathrm{d}x$, Θ, and $\mathrm{d}\Theta/\mathrm{d}x$. Therefore V and Θ have to fulfill essential boundary conditions for the fixed end. From the essential and natural boundary conditions, Equation (4.3) and (4.4), the weak forms reduce to,

$$
\begin{aligned}
&\int_0^L \left\{ EI\frac{\mathrm{d}^2w_1}{\mathrm{d}x^2}\frac{\mathrm{d}^2V}{\mathrm{d}x^2} + m\Omega^2 \int_x^L \zeta\, d\zeta\, \frac{\mathrm{d}w_1}{\mathrm{d}x}\frac{\mathrm{d}V}{\mathrm{d}x} - m\Omega^2 e \int_x^L \zeta\, d\zeta\, \frac{\mathrm{d}w_1}{\mathrm{d}x}\frac{\mathrm{d}\theta}{\mathrm{d}x} \right. \\
&\qquad \left. -\lambda(mw_1V - mew_1\Theta) \right\} \mathrm{d}x = 0 \\
&\int_0^L \left\{ EI_w \frac{\mathrm{d}^2w_2}{\mathrm{d}x^2}\frac{\mathrm{d}^2\Theta}{\mathrm{d}x^2} - m\Omega^2 e \int_x^L \zeta\, d\zeta\, \frac{\mathrm{d}w_2}{\mathrm{d}x}\frac{\mathrm{d}V}{\mathrm{d}x} + GJ\frac{\mathrm{d}w_2}{\mathrm{d}x}\frac{\mathrm{d}\Theta}{\mathrm{d}x} \right. \\
&\left. + m\Omega^2(e^2+r^2) \int_x^L \zeta\, d\zeta\, \frac{\mathrm{d}w_2}{\mathrm{d}x}\frac{\mathrm{d}\Theta}{\mathrm{d}x} - \lambda \left\{ m\left(e^2+r^2\right) w_2\Theta - mew_2V \right\} \right\} \mathrm{d}x = 0
\end{aligned} \qquad (4.15)
$$

In the Rayleigh-Ritz method, we seek an approximate solution to Equation (4.15) in the form of a finite series:

$$
V_m = \sum_{j=1}^{m} v_j \Psi_j^{(1)} + \Psi_0^{(1)} \qquad (4.16)
$$

$$
\Theta_n = \sum_{j=1}^{n} \theta_j \Psi_j^{(2)} + \Psi_0^{(2)} \qquad (4.17)
$$

where $\Psi_0, \Psi_1, \Psi_2, ...$ are approximating functions and v_j and θ_j are undetermined parameters.

Ψ_0 fulfills the specified nonhomogeneous essential boundary conditions and $\Psi_1, \Psi_2, ...$ satisfy at least the homogeneous from of the essential boundary conditions. In the present work, orthogonal functions are used as approximating functions. To express (4.15) in the matrix form, we substitute V_m and Θ_n for V and θ and Ψ_i for w_1 and w_2, respectively. The stiffness and mass matrix are as follows:

$$\begin{bmatrix} [K^{11}] & [K^{12}] \\ [K^{12}]^T & [K^{22}] \end{bmatrix} \begin{Bmatrix} \{A\} \\ \{B\} \end{Bmatrix} - \lambda \begin{bmatrix} [M^{11}] & [M^{12}] \\ [M^{12}]^T & [M^{22}] \end{bmatrix} \begin{Bmatrix} \{A\} \\ \{B\} \end{Bmatrix} = \begin{Bmatrix} \{0\} \\ \{0\} \end{Bmatrix} \tag{4.18}$$

where

$$K_{ij}^{11} = \int_0^L \left\{ EI \frac{\mathrm{d}^2\Psi_i^{(1)}}{\mathrm{d}x^2} \frac{\mathrm{d}^2\Psi_j^{(1)}}{\mathrm{d}x^2} + m\Omega^2 \int_x^L \zeta \, d\zeta \, \frac{\mathrm{d}\Psi_i^{(1)}}{\mathrm{d}x} \frac{\mathrm{d}\Psi_j^{(1)}}{\mathrm{d}x} \right\} \mathrm{d}x \tag{4.19}$$

$$K_{ij}^{12} = -\int_0^L m\Omega^2 e \int_x^L \zeta \, d\zeta \, \frac{\mathrm{d}\Psi_i^{(1)}}{\mathrm{d}x} \frac{\mathrm{d}\Psi_j^{(2)}}{\mathrm{d}x} \mathrm{d}x \tag{4.20}$$

$$\begin{aligned} K_{ij}^{22} = \int_0^L \Bigg\{ & EI_w \frac{\mathrm{d}^2\Psi_i^{(2)}}{\mathrm{d}x^2} \frac{\mathrm{d}^2\Psi_j^{(2)}}{\mathrm{d}x^2} + GJ \frac{\mathrm{d}\Psi_i^{(2)}}{\mathrm{d}x} \frac{\mathrm{d}\Psi_j^{(2)}}{\mathrm{d}x} \\ & + m\Omega^2(e^2 + r^2) \int_x^L \zeta \, d\zeta \, \frac{\mathrm{d}\Psi_i^{(2)}}{\mathrm{d}x} \frac{\mathrm{d}\Psi_j^{(2)}}{\mathrm{d}x} \Bigg\} \mathrm{d}x \end{aligned} \tag{4.21}$$

$$M_{ij}^{11} = \int_0^L \rho A \Psi_i^{(1)} \Psi_j^{(1)} \, \mathrm{d}x \tag{4.22}$$

$$M_{ij}^{12} = -\int_0^L \rho A e \Psi_i^{(1)} \Psi_j^{(2)} \, \mathrm{d}x \tag{4.23}$$

$$M_{ij}^{22} = \int_0^L \rho A (e^2 + r^2) \Psi_i^{(2)} \Psi_j^{(2)} \, \mathrm{d}x \tag{4.24}$$

4.3 Approximating Functions

When using the Rayleigh-Ritz method, approximating functions have to fulfill essential boundary conditions. In the case of bending-torsion coupled beam, essential boundary conditions of $V = 0$, $\mathrm{d}V/\mathrm{d}x$, $\Theta = 0$, and $\mathrm{d}\Theta/\mathrm{d}x$ have to be fulfilled at the clamped base. However, Legendre and Chebyshev orthogonal polynomials by themselves cannot fulfill all

these essential boundary conditions while retaining their orthogonality. To fulfill these essential boundary conditions, artificial linear and rotational springs are introduced in the stiffness matrix and even order Legendre and Chebyshev polynomials are used. The reason that only the even order polynomials are chosen is that the odd order polynomials are more close to the mode shapes of a free-free beam and the even order polynomials are more close to the mode shapes of a cantilever beam. The additional stiffness terms to enable Legendre and Chebyshev polynomials to be used in the analysis are $\frac{1}{2}\alpha v(0)^2$, $\frac{1}{2}\beta v'(0)^2$, $\frac{1}{2}\gamma\theta(0)^2$ and $\frac{1}{2}\delta\theta'(0)^2$ where α, β, γ, and δ are the artificial spring stiffnesses. To simulate cantilever conditions, a large numerical value (up to 10^{10}) is chosen for the stiffness of artificial springs.

Integrated Legendre polynomial is linear combinations of two integrals of Legendre polynomials. The first and second terms are linear combinations of two integrals of Legendre polynomials [48].

$$I_1(x) = \frac{(1-x)}{2} \qquad\qquad I_2(x) = \frac{(1+x)}{2} \tag{4.25}$$

The rest of the polynomials $I_n(t)$ are found from the relationship [49] shown in Equation (4.26).

$$I_n(x) = \frac{1}{\sqrt{2(2n-3)}}\left(P_{n-1}(x) - P_{n-3}(x)\right) \qquad n \geq 3 \tag{4.26}$$

where $P_n(x)$ are Legendre polynomials. To fulfill essential boundary conditions of cantilever beam at $x = 0$ in cantilever Euler-Bernoulli beam, integrated Legendre Polynomials are modified to be

$$J_n(x) = I_n(x) - I_n(0), \quad n = 3, 5, \ldots \tag{4.27}$$

Karunamoorthy's modified Duncan polynomials [7] are obtained by orthogonalizing Duncan trinomials by using Gram-Schmidt process. Duncan polynomials for bending are

$$Y_n = \frac{1}{6}(n+2)(n+3)x^{n+1} - \frac{1}{3}n(n+3)x^{n+2} + \frac{1}{6}n(n+1)x^{n+3} \tag{4.28}$$

Y_n for $n = 1, 2, 3, \ldots$ satisfy the boundary conditions for a cantilever beam and are complete and linearly independent. These polynomials are orthogonalized in the interval 0 to 1 by the

Gram-Schmidt orthogonalization process and scaled so that the tip deflection is unity. The orthogonalized polynomials also satisfy the boundary conditions for a cantilever beam.

Bardell *et al.* [39] uses the special trigonometric functions in conjunction with Hermite cubics. The trigonometric functions used as hierarchical functions are

$$f_r(\xi) = \sin\left(\frac{\pi}{2}(r-4)(\xi+1)\right)\sinh\left(\frac{\pi}{2}(\xi+1)\right) \tag{4.29}$$

The eigenfunctions of a pinned-free uniform beam of Kwak are

$$V(x) = \sin\beta x + \frac{\sin\beta L}{\sinh\beta L}\sinh\beta x - \beta\left(1+\frac{\sin\beta L}{\sinh\beta L}\right)x \tag{4.30}$$

where βL are the roots of the equation $\tanh\beta L = \tan\beta L$.

Bhat's beam characteristic orthogonal polynomials consist of choosing a first polynomial $\phi_1(x)$ which satisfies both the geometrical and the natural boundary conditions of a uniform beam and obtaining the other members of the orthogonal set in the interval by using the Gram-Schmidt process as follows:

$$\begin{aligned} \phi_2(x) &= (x-B_2)\phi_1(x), \ldots, \ \phi_k(x) = (x-B_k)\phi_{k-1}(x) - C_k\phi_{k-2}(x), \\ \text{where } B_k &= \frac{\int_a^b xw(x)\phi_{k-1}^2(x)\,dx}{\int_a^b w(x)\phi_{k-1}^2(x)\,dx}, \\ C_k &= \frac{\int_a^b xw(x)\phi_{k-1}(x)\phi_{k-2}(x)\,dx}{\int_a^b w(x)\phi_{k-2}^2(x)dx} \end{aligned} \tag{4.31}$$

where $w(x)$ is the weighting function that is unity for uniform beams. When $\phi_1(x)$ satisfies both geometrical and natural boundary conditions, the additional polynomials generated by Gram-Schmidt orthogonalization satisfy only the geometric boundary conditions.

Chapter 5

Results

Orthogonal functions shown in the previous chapter are examined for their performances as basis functions for the Rayleigh-Ritz method employed to find natural frequencies of both non-rotating and rotating beams. MATHEMATICA [1] is used in generating the mass and the stiffness matrices and getting eigenvalues for natural frequencies in the Rayleigh-Ritz method. MATHEMATICA analysis was done using Silicon Graphics Octane workstation. For the reference purpose, the finite element method results for a channel beam cases are obtained using NASTRAN finite element method package and are compared with results from Rayleigh-Ritz method using MATHEMATICA.

5.1 Timoshenko Beam

Natural frequencies of Timoshenko beam for non-rotating and rotating conditions are studied prior to bending-torsion coupled beam for the verification and the performance test of orthogonal polynomials.

First, the natural frequencies of cantilever Timoshenko Beam ($L/H = 100$) obtained

[1] MATHEMATICA is a registered trademark of Wolfram Research Co.

using various orthogonal polynomials are shown in Table 5.1. The results show good agreement between the results obtained in this study using various orthogonal polynomials and those available in the reference in lowest two modes. However, the Hermite cubic and Kwak's eigenfunction cases deviate greatly from the reference results from the third mode onwards. From these results, it seems that simpler orthogonal polynomials are better suited in the natural frequencies of a cantilever Timoshenko beam. These polynomials require less effort in integration for generating the mass and the stiffness matrices.

In the case of rotating cantilever Timoshenko beams, orthogonal functions show results in good agreement to the reference results. Especially, the simple Legendre and Chebyshev polynomials indicate a good efficiency in getting results, due to the ease of performing various integrations needed in determining stiffness and mass matrices. Bardell's and Kwak's functions, however, do not show a good efficiency in getting results, mainly due to an inordinate time consumed in the integration of trigonometric functions. Also, Legendre, Chebyshev, Integrated Legendre polynomials show results, which are identical to each other when the same number of polynomials are used. While Legendre and Chebyshev polynomials take less time in calculation, other functions give less accurate results with more CPU time consumption. The natural frequencies of a rotating cantilever Timoshenko Beam ($L/r_g = 10$, $R = 3$, and $\alpha = 10$) are shown in the Table 5.2. Figures 5.1 through 5.4 show first through fourth modes shapes of rotating Timoshenko beam obtained by the Rayleigh-Ritz method using Karunamoorthy's modified Duncan polynomials.

5.2 Bending-Torsion Coupled Beam

In the bending-torsion coupled beam analysis, three cases are studied: (i) free-free beam, (ii) a cantilever, and (iii) a rotating cantilever beam.

5.2.1 Free-Free Beam Case

For the free-free bending-torsion coupled beam, Table 5.3 shows the comparison of the results obtained using various orthogonal polynomials to those given in the reference [2]. Figure 5.5 through 5.8 show mode shapes obtained using Legendre polynomials and Figure 5.9 through 5.10 show mode shapes obtained using NASTRAN. Among various orthogonal polynomials tested, integrated Legendre polynomials show the least close approximation to the reference results. Even in the approximations obtained by Legendre and Chebyshev polynomials, the first normal mode which was found in both the reference and by NASTRAN Finite element package analysis is not found with the Rayleigh-Ritz method. In the Rayleigh-Ritz method, it is very important that the assumed shape functions form a complete set so as to represent all the modes of the structure. The results obtained from orthogonal polynomials missing out one mode in current case seems to be due to the fact that tried orthogonal polynomial shape functions fail to represent all the modes.

5.2.2 A Cantilever Case

For the vibration of bending-torsion coupled beam in the cantilever case, most of the orthogonal functions used show very good agreements as can be seen in Table 5.4 to the reference which also uses Euler-Bernoulli beam theory for bending. For Legendre and Chebyshev polynomials cases, artificial spring of stiffness 10^7 is added to the stiffness term of (4.19) and (4.21). Figures 5.11 through 5.14 show mode shapes obtained by Rayleigh-Ritz method using Karunamoorthy's modified Duncan polynomials and Figures 5.15 through 5.16 shows mode shapes obtained by NASTRAN. Among orthogonal functions used in the analysis, beam characteristic orthogonal polynomials show most close approximations but Kwak's eigenfunctions and Karunamoorthy's modified Duncan polynomials show somewhat different results from the other orthogonal functions and the reference [3]. Natural frequencies obtained by NASTRAN also show some deviation from the results given in the reference and from the results obtained from the Rayleigh-Ritz method. This seems to be due to the

fact that the elements used in the NASTRAN analysis are 2 dimensional plate elements and allow all types of complicating effects such as the shear deformation and rotatory inertia along with better representation of warping effect.

5.2.3 A Rotating Cantilever Case

Natural Frequencies of the flexural-torsional coupled vibration of cantilever Bernoulli-Euler Channel Beam in the rotating condition are shown in Table 5.5. Figures 5.17 through 5.20 show mode shapes obtained by Rayleigh-Ritz method using Karunamoorthy's modified Duncan polynomials and Figures 5.21 and 5.22 show mode shapes obtained by using NASTRAN. The results obtained using orthogonal polynomials show close agreement with respect to each other. Beam characteristic orthogonal polynomials show the closest approximations to the NASTRAN results. However, the beam characteristic polynomials require a lot of calculation time in getting the coefficients of polynomials and generating the mass and the stiffness matrices by integration as the number of polynomials used are increased.

The results obtained from the Rayleigh-Ritz method using orthogonal functions deviate from the results obtained from the NASTRAN finite element package. Figures 5.23 through 5.27 show vertical and torsional mode shapes obtained by NASTRAN. When examining these mode shapes and comparing them to those obtained from the Rayleigh-Ritz method shown in Figure 5.17 through 5.20, it is noticed that there is another normal mode in the NASTRAN analysis as shown in 5.25 which is not found in the analysis using the Rayleigh-Ritz method. Also, the shapes of normal modes are slightly different for the NASTRAN analysis and the Rayleigh-Ritz analysis in the vertical deflection modes. Only the mode shapes of first and second modes of Rayleigh-Ritz method is close to those of the NASTRAN analysis. However, the torsional mode shapes of the first, third, and fourth modes of the Rayleigh-Ritz analysis are very close to those obtained from the NASTRAN analysis. In these modes, the location of peaks in mode shapes are very close to each other.

The reason that there is another normal mode in the NASTRAN analysis is due to

the fact that the second mode which is found in the NASTRAN analysis was not correctly represented by any of the orthogonal polynomials. Moreover, Figure 5.28 shows the side view of deformation at the tip on the 4th normal mode. The front view of Figure 5.28 show apparent effect of warping on the cross section but does not show section deformation when we see the side view. Since warping stiffness is considered in the analysis using Rayleigh-Ritz method, the deviation of results is due to missing mode which cannot be represented by orthogonal polynomials. Therefore, in the case of the rotating cantilever bending-torsion coupled beam, at least the first mode could be correctly found with the Rayleigh-Ritz method using orthogonal functions but other modes were overestimated in the results obtained using the Rayleigh-Ritz method.

In Figure 5.29, natural frequencies obtained by different number of polynomials are shown. The case shown in the figure is the natural frequency of the fourth mode shape of the rotating bending-torsion coupled beam. In the figure, the results obtained using Chebyshev, Karunamoorthy's modified Ducan and beam characteristic orthogonal polynomials are compared to each other. Among orthogonal polynomials used, Karunamoorthy's modified Duncan polynomial and beam characteristic polynomials, which fulfill more boundary condition at the first approximating mode shape, show a faster convergence than the Chebyshev polynomials which fulfill essential boundary condition using artificial spring.

To examine the effect of rotation, the natural frequencies of first mode shapes of coupled flexural-torsional vibration are compared to each other in Figure 5.30. Obtained results show close agreement to each other. Results from the NASTRAN analysis show slightly higher natural frequency estimation at higher rotation speed than the results by the Rayleigh-Ritz method using various orthogonal polynomials.

Next, the natural frequencies are obtained and compared for different length of the flexural-torsional coupled vibration of a rotating beam. Also, the results obtained using Rayleigh-Ritz method are compared to the results obtained using NASTRAN analysis. The results are plotted in Figure 5.31. The figure shows that natural frequencies obtained using

NASTRAN analysis shows lower values than those using Rayleigh-Ritz method for shorter beams. This seems to be due to the fact that shear and rotation effect is not accounted in the analysis using Rayleigh-Ritz method.

Table 5.1: Cantilever Timoshenko Beam (N is the number of polynomials used in the case of Rayleigh-Ritz method using orthogonal polynomials and the number of elements in the case of FEM, $L/H = 100$)

Methods	1st Mode	2nd Mode	3rd Mode	4th Mode	N	Integration
Exact	3.516	22.023	61.618	120.615		
Legendre	3.516	22.023	61.618	120.617	10	Exact
Chebyshev	3.516	22.023	61.618	120.617	10	”
Integrated Legendre	3.513	21.892	62.224	124.590	10	”
Modified Duncan	3.566	22.225	61.723	119.337	10	”
Bardell’s Hermite cubic	3.400	21.982	61.029	116.834	10	Numerical
Kwak’s eigenfunctions	3.830	24.004	67.166	132.008	15	”

Table 5.2: Natural frequencies of a rotating cantilever Timoshenko beam (the number of approximating functions used $N = 5$, T is the CPU time consumed in calculation)

Methods	1st Mode	2nd Mode	3rd Mode	4th Mode	5th Mode	T (sec)	Integration
Yokoyama [10]	23.050	45.598	67.716	73.076			
Legendre	23.036	45.455	67.045	72.573	94.858	5.3	Exact
Chebyshev	23.036	45.455	67.045	72.573	94.858	4.3	”
Integrated Legendre	23.036	45.455	67.045	72.573	94.858	54.8	”
Modified Duncan	23.051	46.225	67.345	74.847	92.533	64.9	”
Bardell’s functions	23.607	46.270	68.275	74.976	94.434	444.9	Numerical
Kwak’s functions	24.157	47.488	70.270	77.265	98.379	42.6	”

Table 5.3: The natural frequencies of a Free-Free channel (N=10)

Method	3rd Mode	4th Mode	5th Mode	6th Mode
Bishop *et al.*[2]	342.13	371.62	721.16	1247.0
Legendre	-	369.66	768.75	1389.72
Chebyshev	-	369.66	768.75	1389.72
Integrated Legendre	-	369.66	768.75	1389.72
Beam Characteristic	-	369.66	768.75	1389.72
NASTRAN	337.5	350.2	710.7	1222.0

Table 5.4: The natural frequencies of coupled flexural torsional vibration of a short cantilever beam (750 CQUAD4 elements used in the NASTRAN analysis)

Polynomials	1	2	3	4	5	N	T(sec)	Integration
Bercin and Tanaka [3]	24.03	88.54	131.41	358.57	549.83			
Legendre	24.03	88.45	131.64	360.34	550.21	10	34.5	Exact
Chebyshev	24.03	88.45	131.64	360.34	550.21	10	55.2	”
Integrated Legendre	24.03	88.45	131.58	359.84	549.93	10	56.5	”
Orthogonalized Duncan	24.02	88.44	131.40	358.55	549.21	10	122.6	”
Beam characteristic	24.03	88.44	131.44	366.62	549.49	5	284.4	”
Bardell’s functions	24.24	89.55	131.48	358.84	549.53	10	497.2	Numerical
Kwak’s functions	24.83	91.83	136.66	374.21	571.93	10	72.6	”
NASTRAN	22.91	84.55	126.30	390.01	555.40			FEM

Table 5.5: Natural frequencies of the flexural-torsional coupled vibration of rotating slender cantilever beam (Ω = 600 rpm, 392 CQUAD4 elements used in the NASTRAN analysis, channel specifications from [47]).

Polynomials	1	2	3	4	5	N	T(sec)	Integration
Legendre	15.802	55.397	123.519	220.014	351.397	10	36.9	Exact
Chebyshev	15.708	56.241	123.317	219.823	351.207	10	53.8	”
Integrated Legendre	15.862	56.320	126.293	225.340	358.124	10	55.0	”
Modified Duncan	15.770	55.386	122.891	217.854	343.495	10	120.5	”
Beam Characteristic	15.770	55.373	122.754	217.659	343.423	10	216.9	”
Bardell’s functions	16.135	56.695	126.382	224.910	355.337	10	517.3	Numerical
Kwak’s functions	16.067	58.805	131.972	234.604	372.020	10	167.7	”
NASTRAN	15.755	46.738, 59.468	114.505	199.538	304.306	-	-	FEM

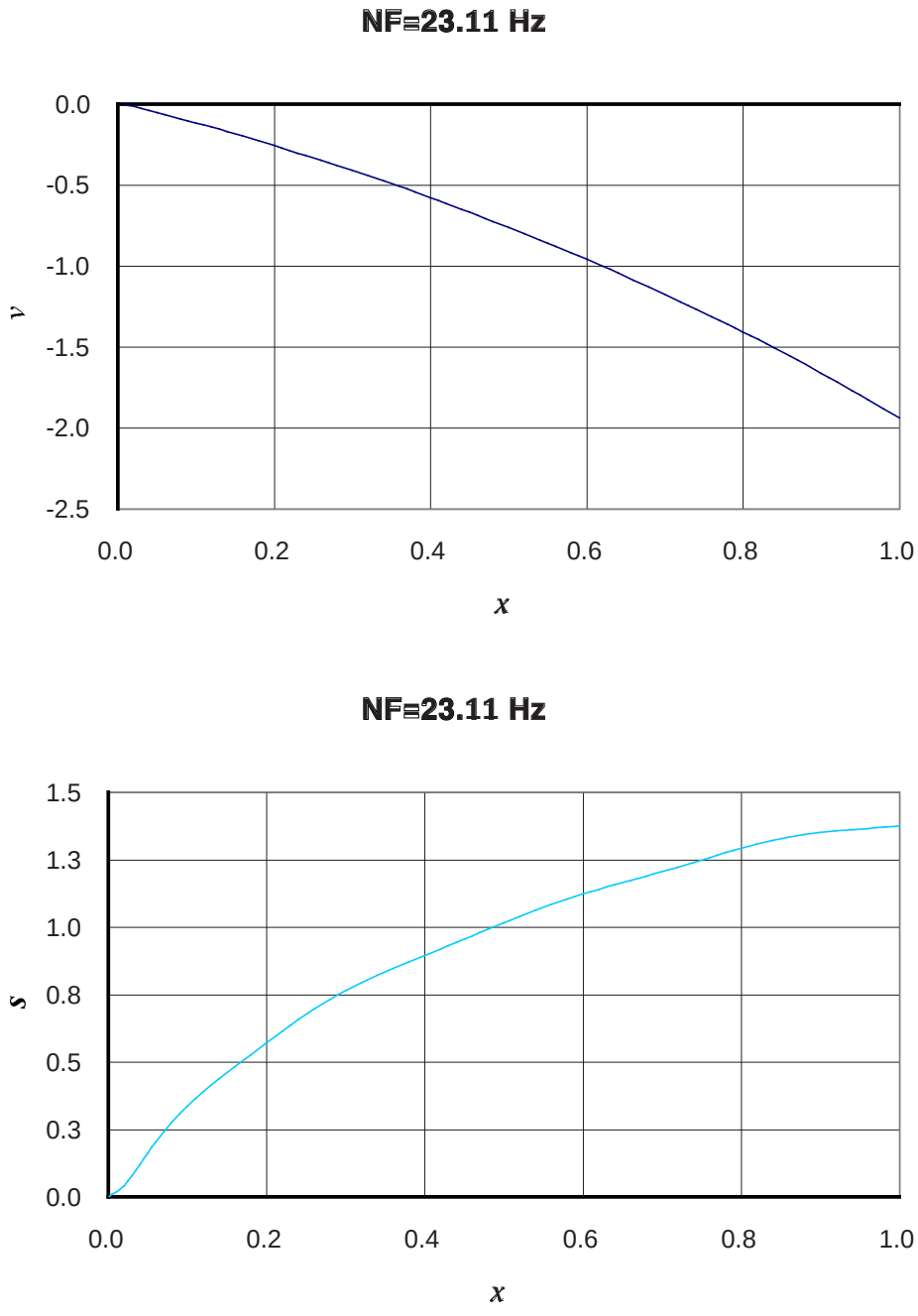

Figure 5.1: The first mode shapes, as obtained by the Rayleigh-Ritz method using Karunamoorthy's modified Duncan polynomials, for a rotating Timoshenko beam

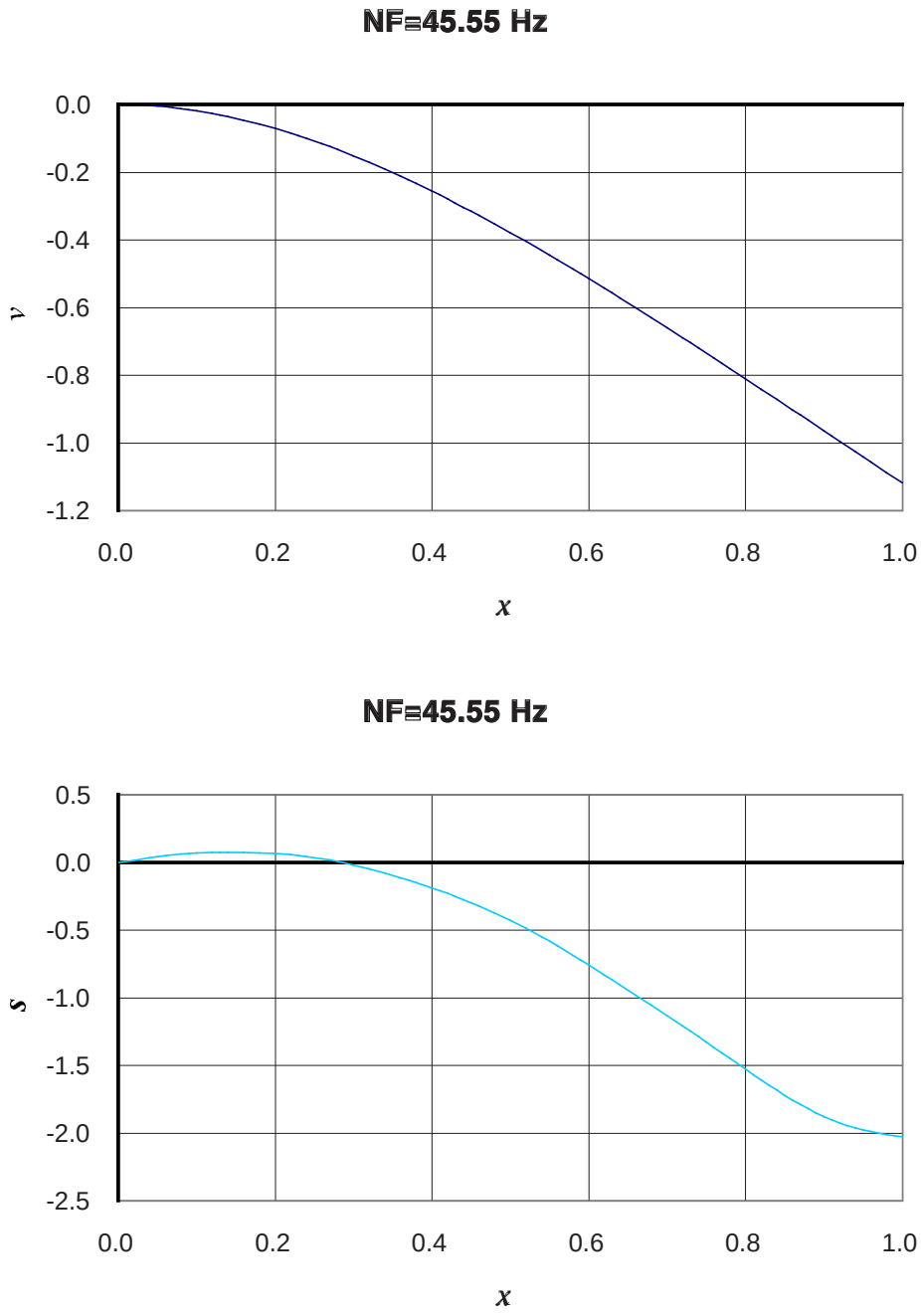

Figure 5.2: The second mode shapes, as obtained by the Rayleigh-Ritz method using Karunamoorthy's modified Duncan polynomials, for a rotating Timoshenko beam

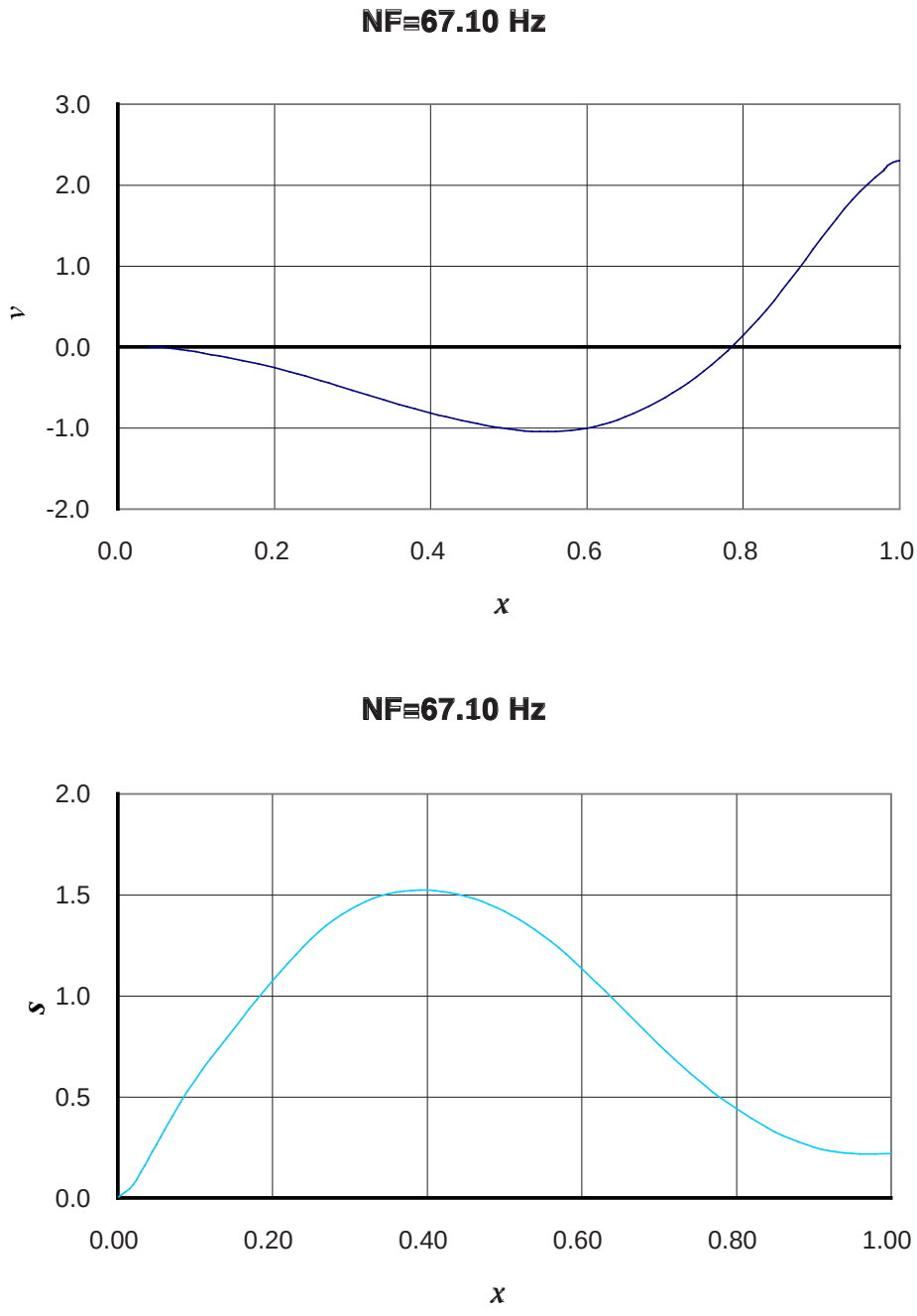

Figure 5.3: The third mode shapes, as obtained by the Rayleigh-Ritz method using Karunamoorthy's modified Duncan polynomials, for a rotating Timoshenko beam

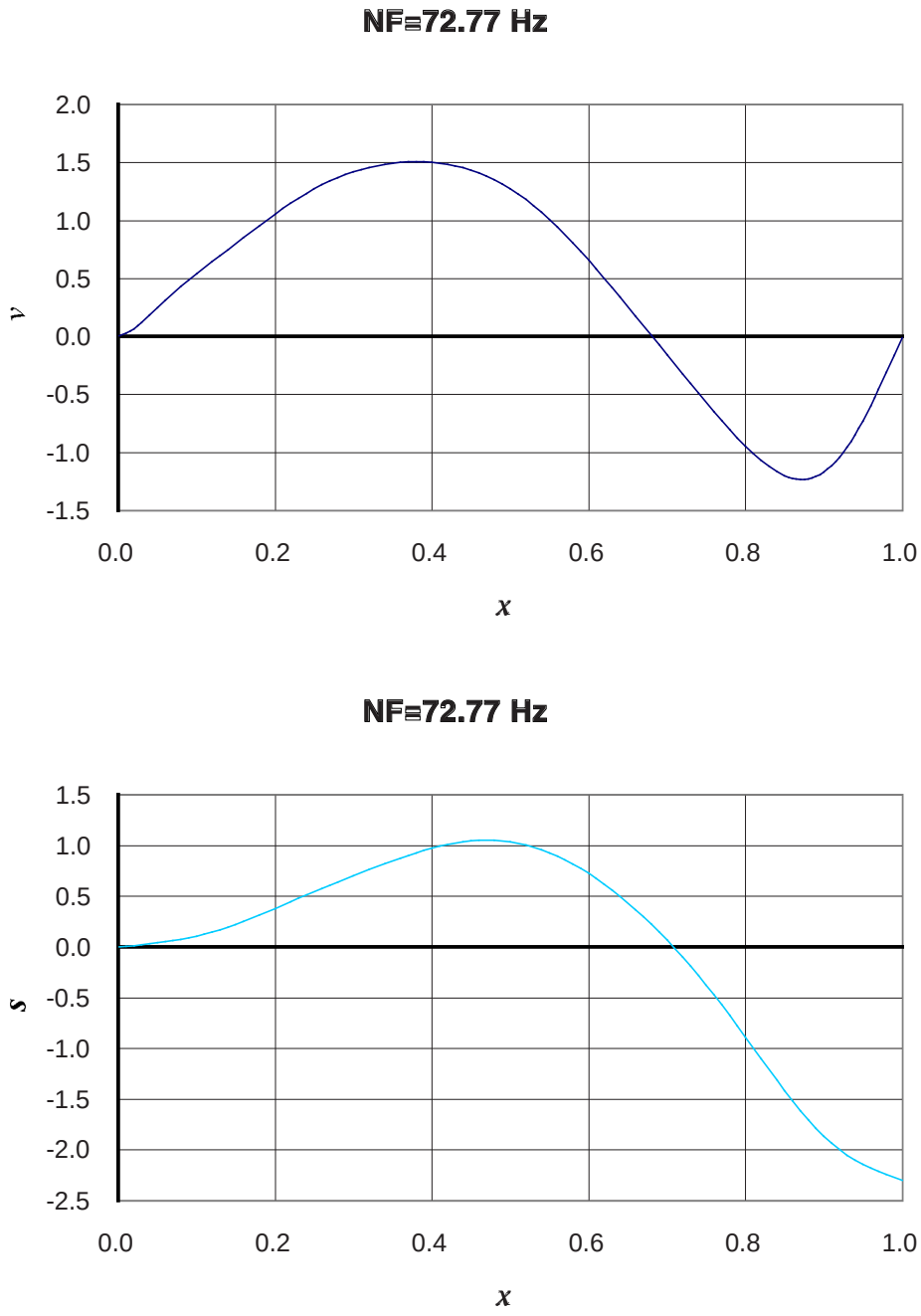

Figure 5.4: The fourth mode shapes, as obtained by the Rayleigh-Ritz method using Karunamoorthy's modified Duncan polynomials, for a rotating Timoshenko beam

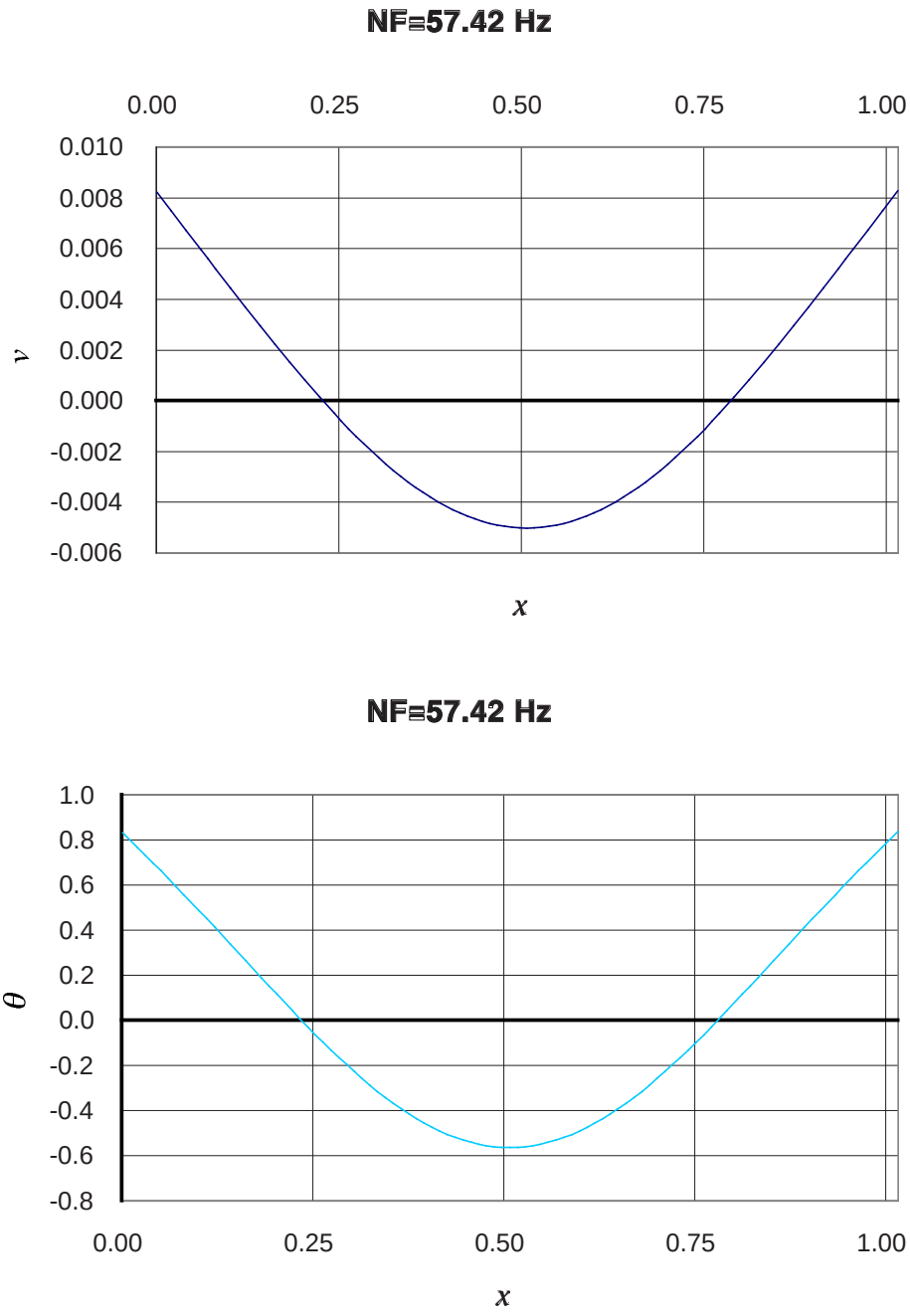

Figure 5.5: The first mode shapes, as obtained by the Rayleigh-Ritz method using Legendre polynomials, for a Free-Free Channel Beam

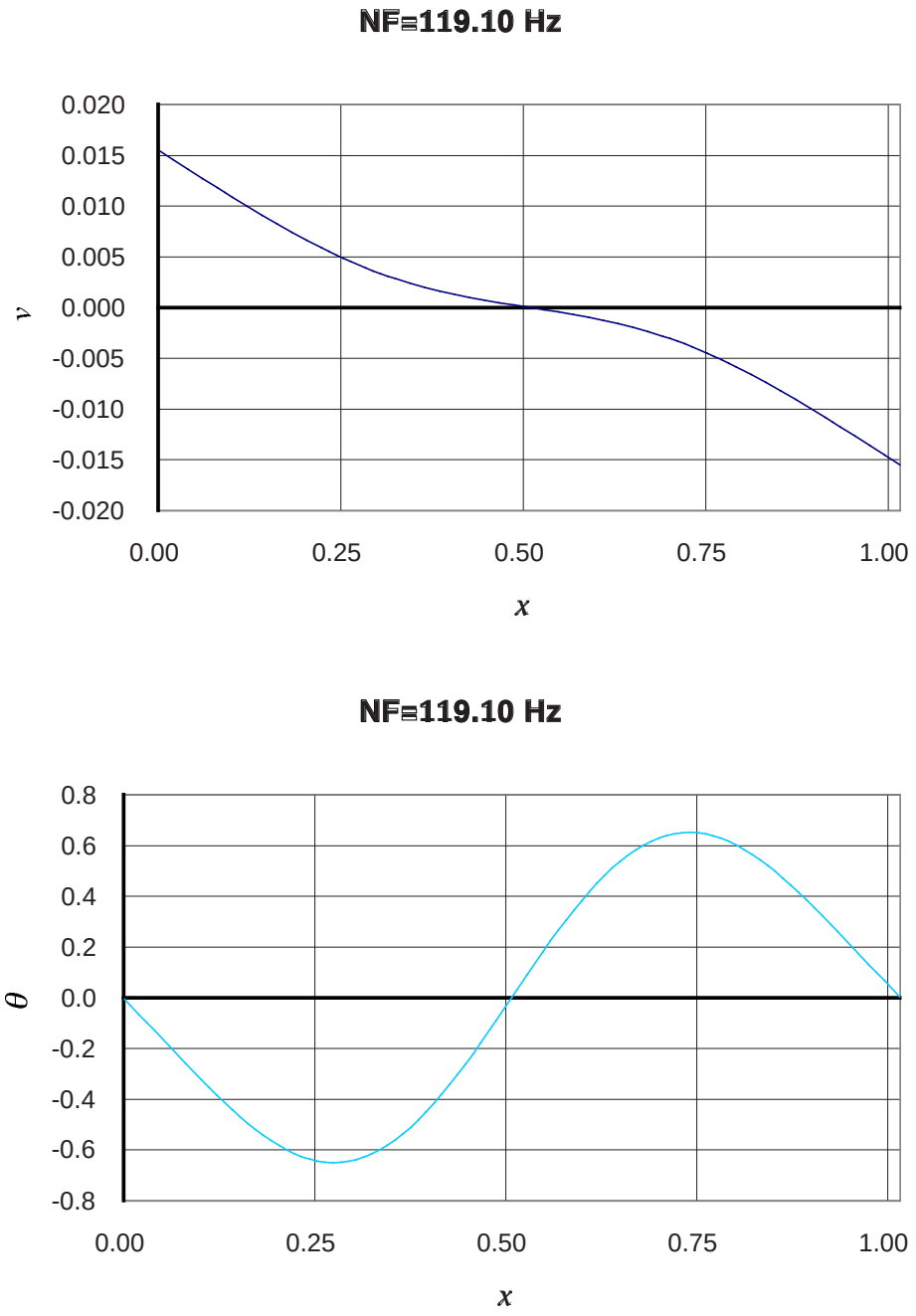

Figure 5.6: The second mode shapes, as obtained by the Rayleigh-Ritz method using Legendre polynomials, for a Free-Free Channel Beam

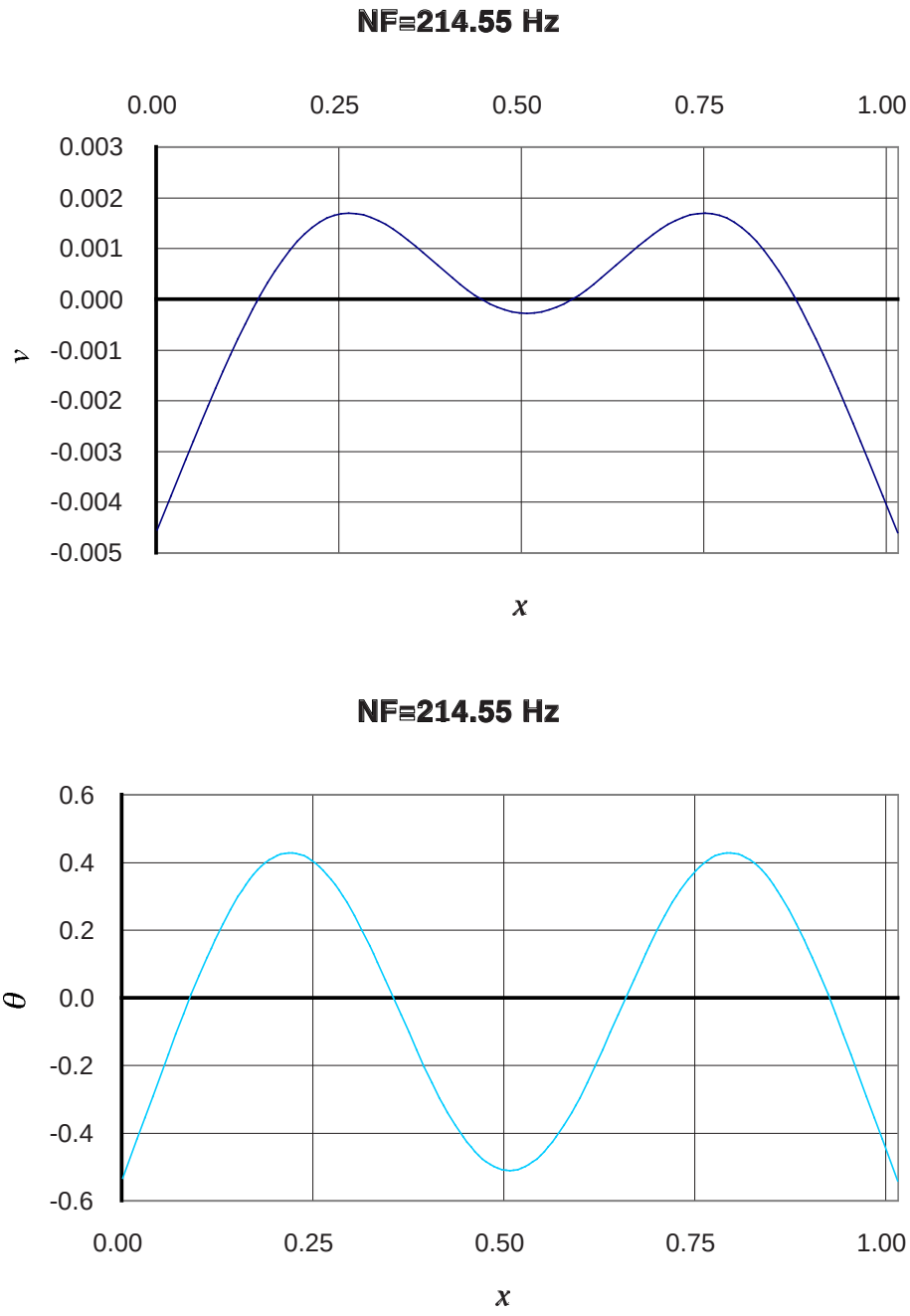

Figure 5.7: The third mode shapes, as obtained by the Rayleigh-Ritz method using Legendre polynomials, for a Free-Free Channel Beam

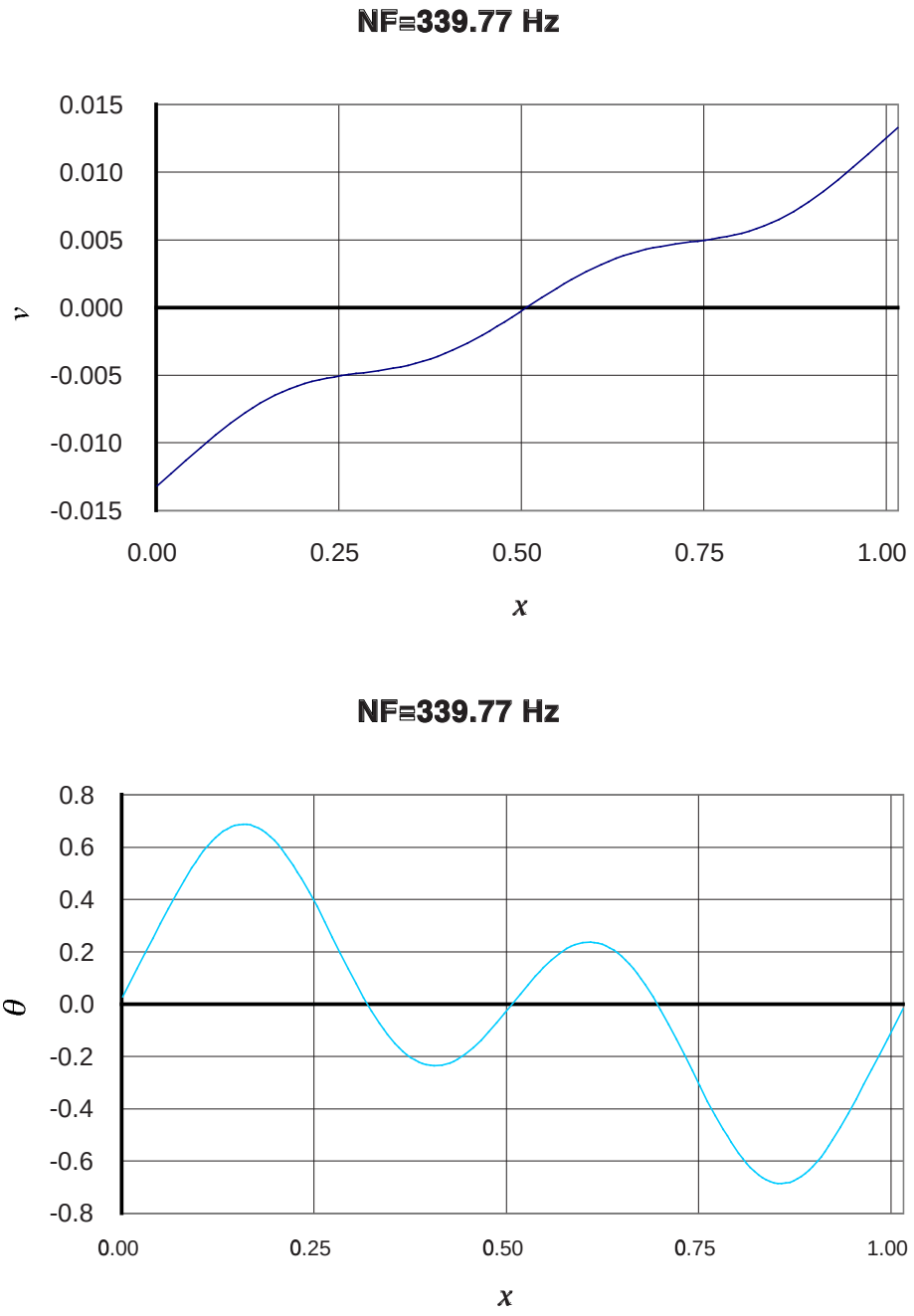

Figure 5.8: The fourth mode shapes, as obtained by the Rayleigh-Ritz method using Legendre polynomials, for a Free-Free Channel Beam

Mode 1, (NF=337.5 Hz)

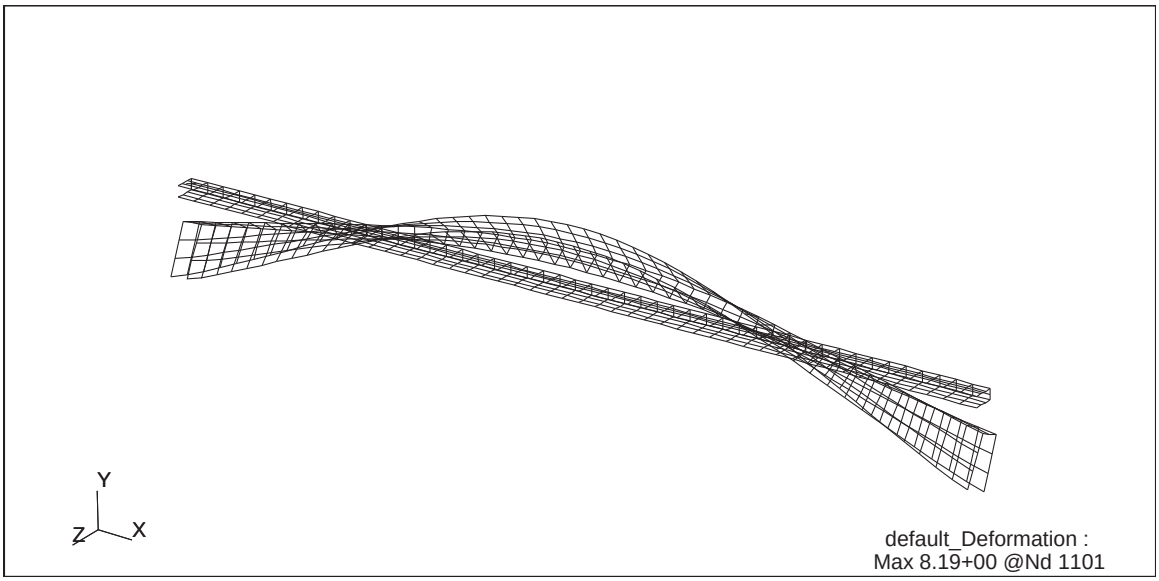

Mode 2, (NF=350.2 Hz)

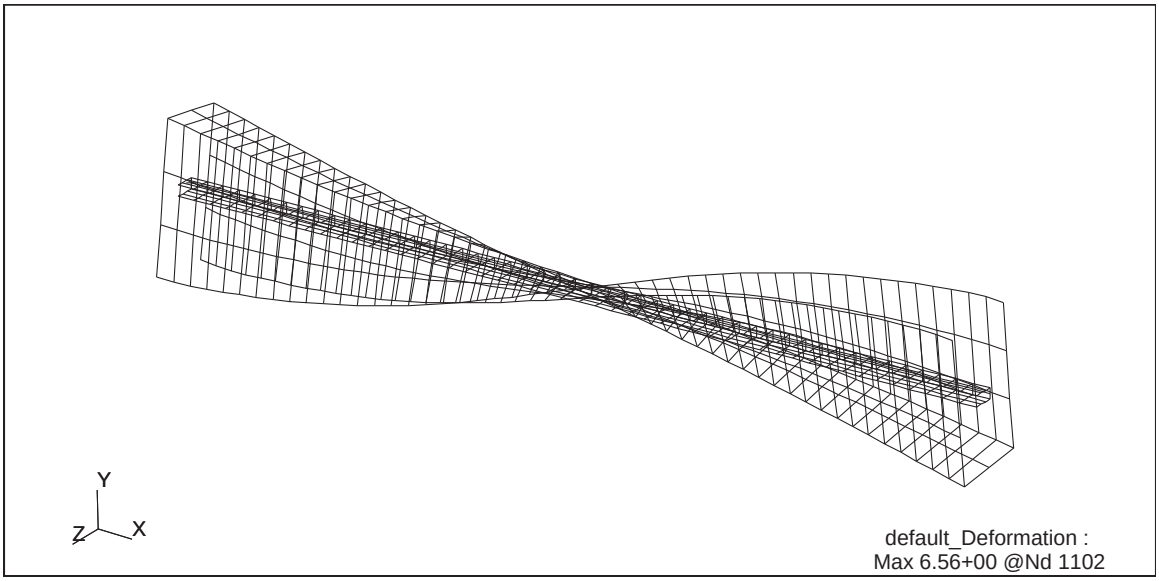

Figure 5.9: The first and second mode shapes of free-free channel beam case as obtained by the NASTRAN analysis

Mode 3, (NF=710.6 Hz)

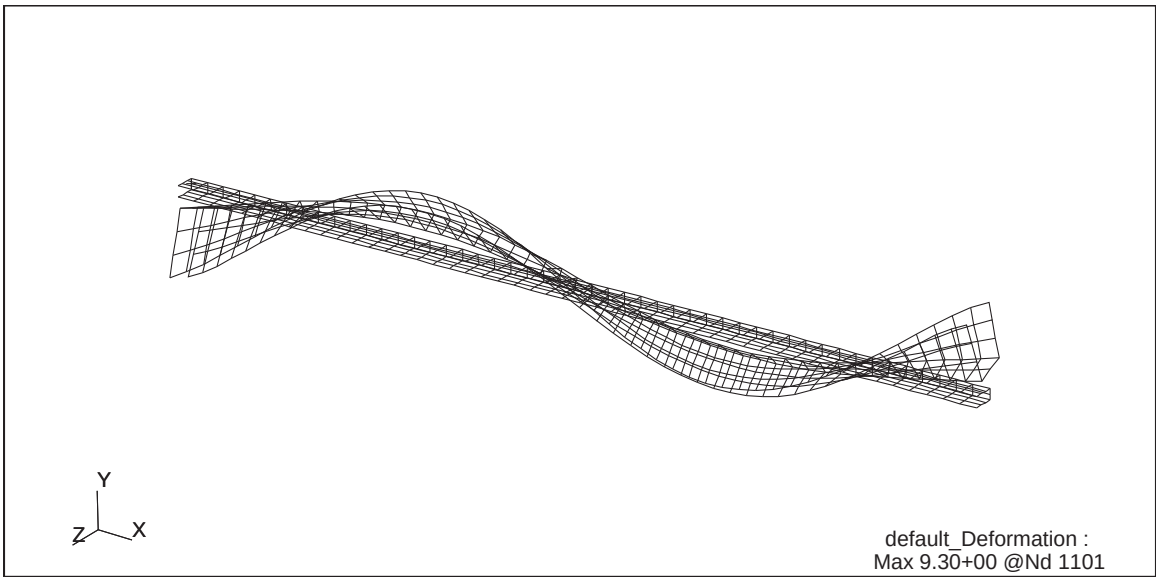

Mode 4, (NF=1221.0 Hz)

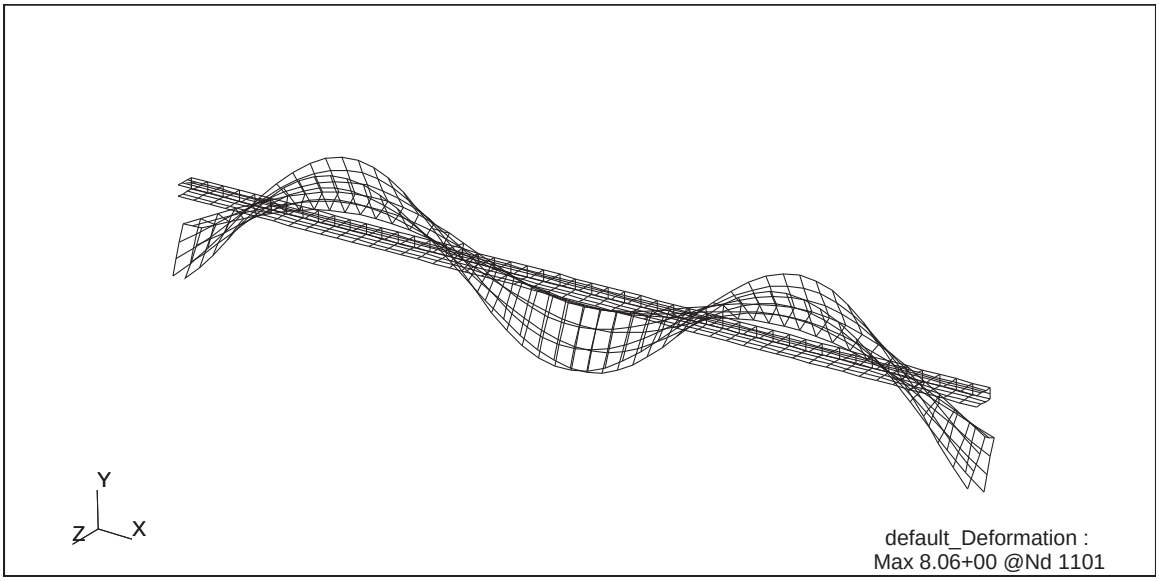

Figure 5.10: The third and fourth mode shapes of free-free channel beam case as obtained by the NASTRAN analysis

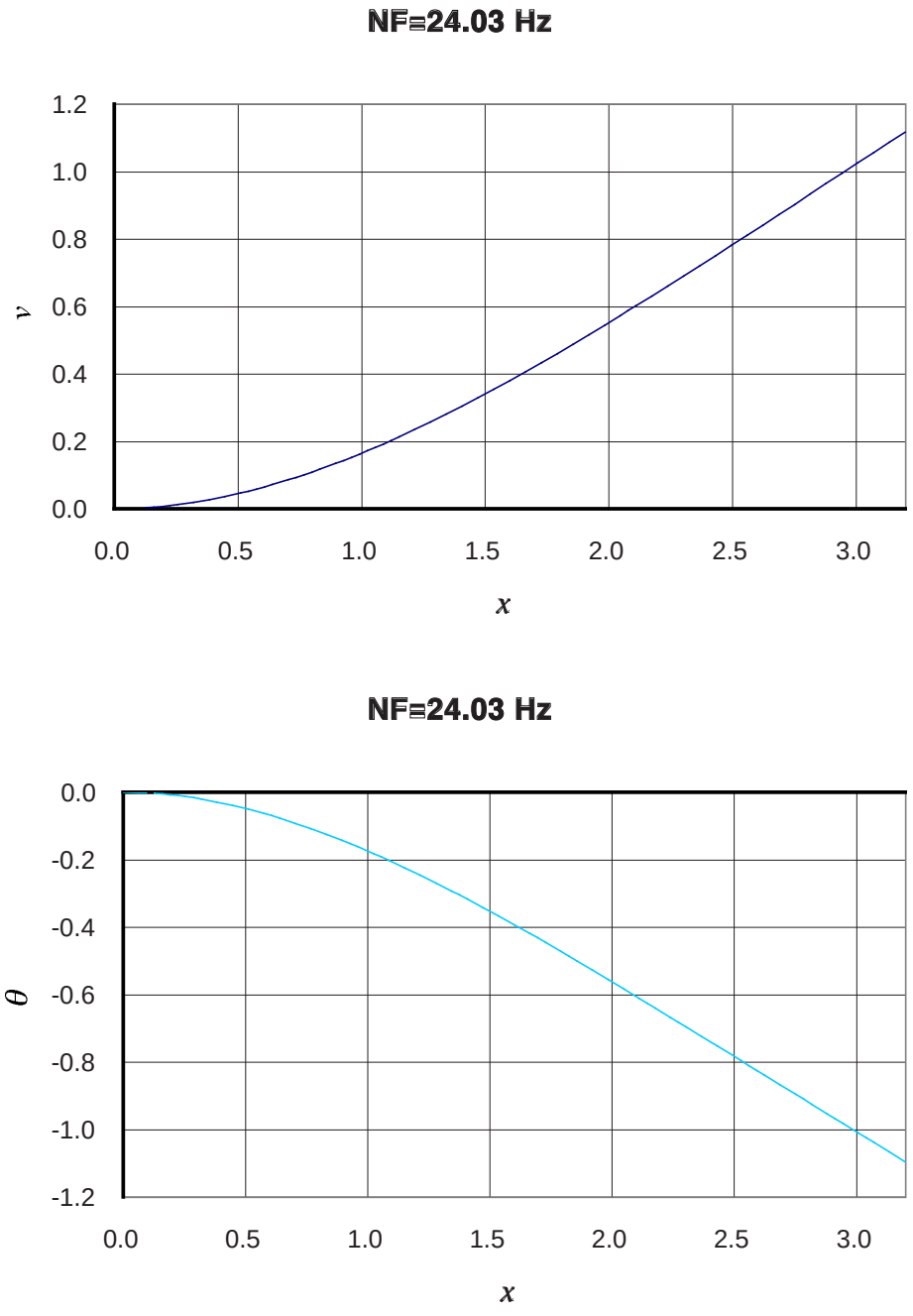

Figure 5.11: The first mode shapes of a bending-torsion coupled cantilever beam as obtained by the Rayleigh-Ritz method using Karunamoorthy's modified Duncan polynomials

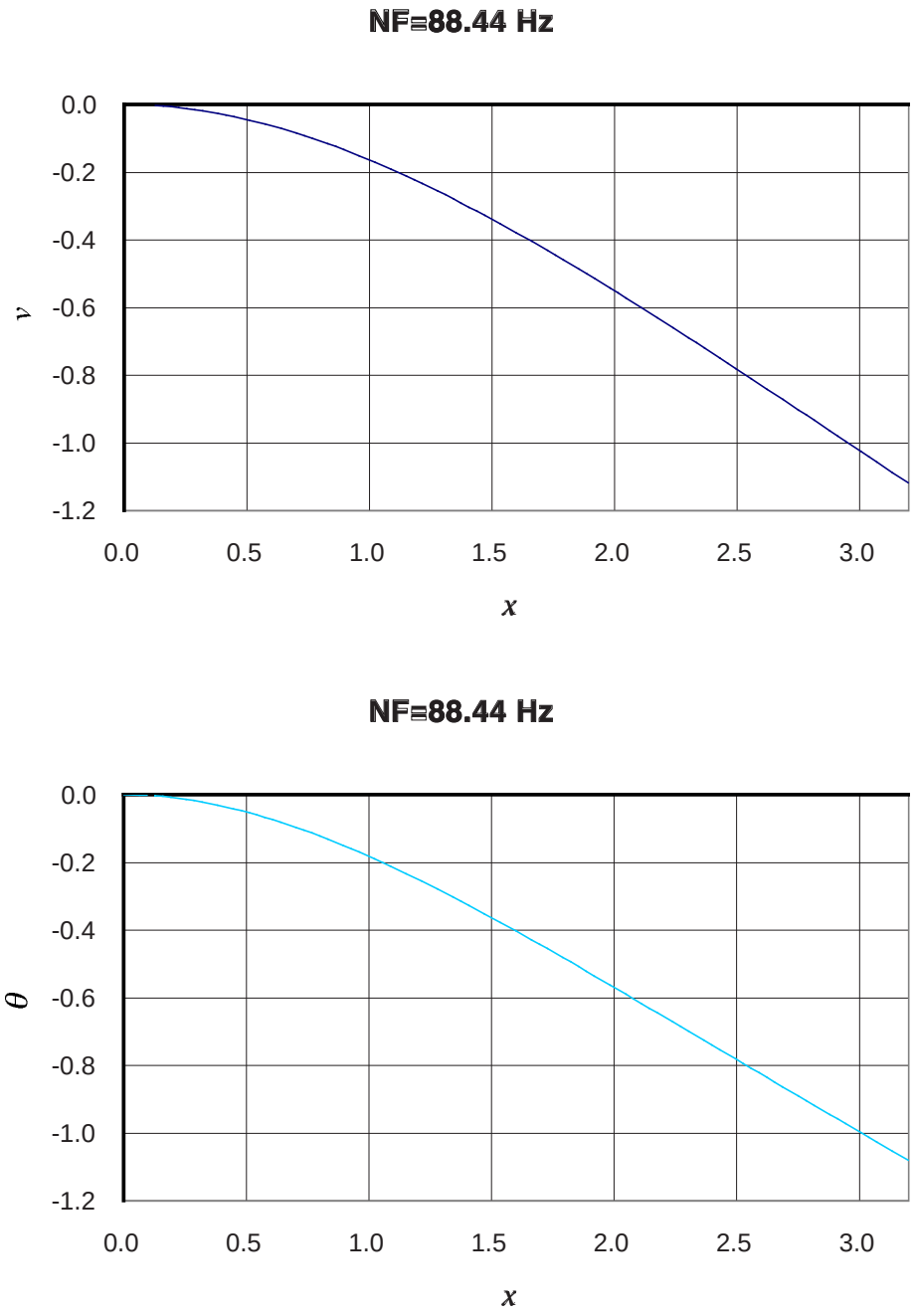

Figure 5.12: The second mode shapes of a bending-torsion coupled cantilever beam as obtained by the Rayleigh-Ritz method using Karunamoorthy's modified Duncan polynomials

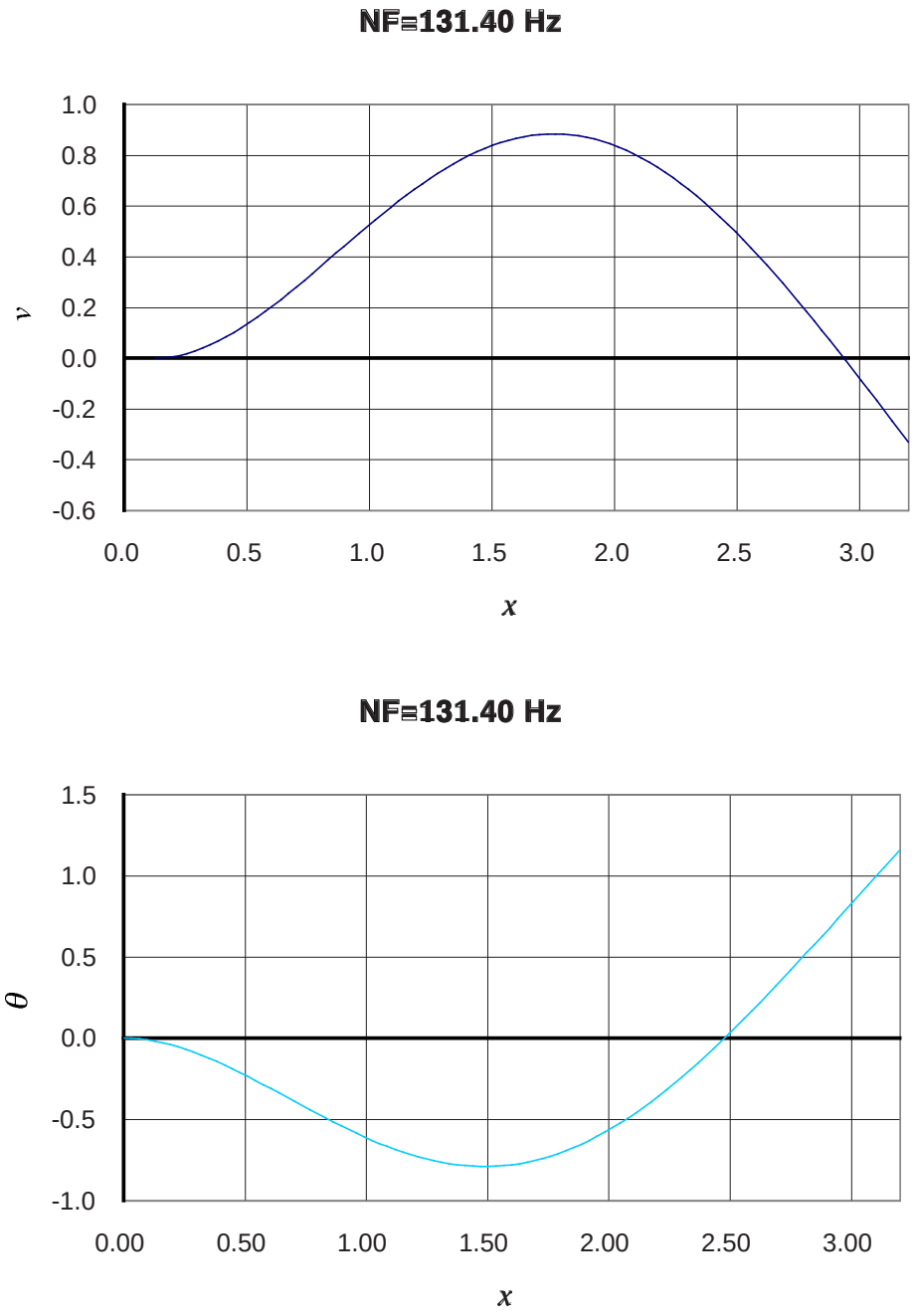

Figure 5.13: The third mode shapes of a bending-torsion coupled cantilever beam as obtained by the Rayleigh-Ritz method using Karunamoorthy's modified Duncan polynomials

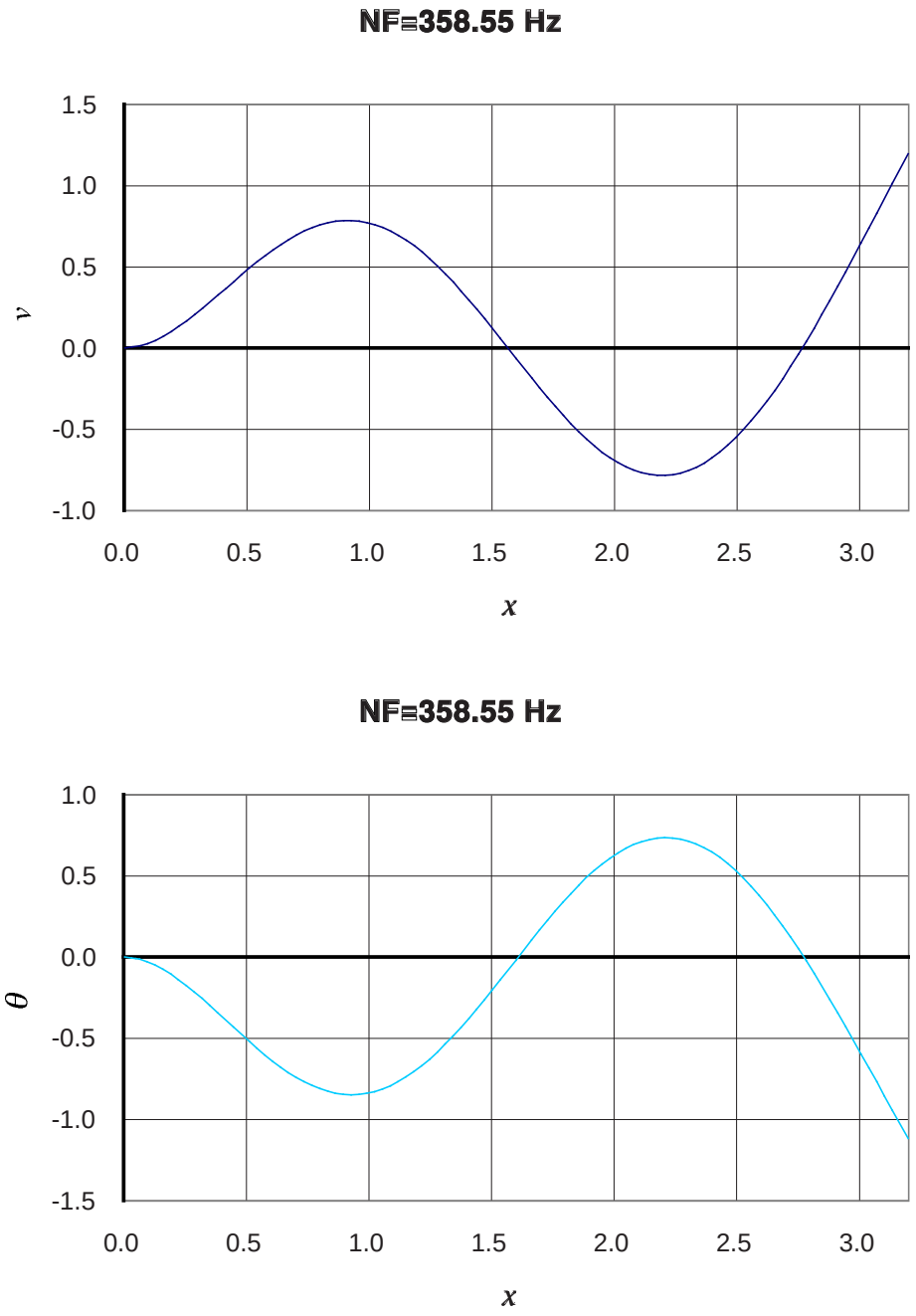

Figure 5.14: The fourth mode shapes of a bending-torsion coupled cantilever beam as obtained by the Rayleigh-Ritz method using Karunamoorthy's modified Duncan polynomials

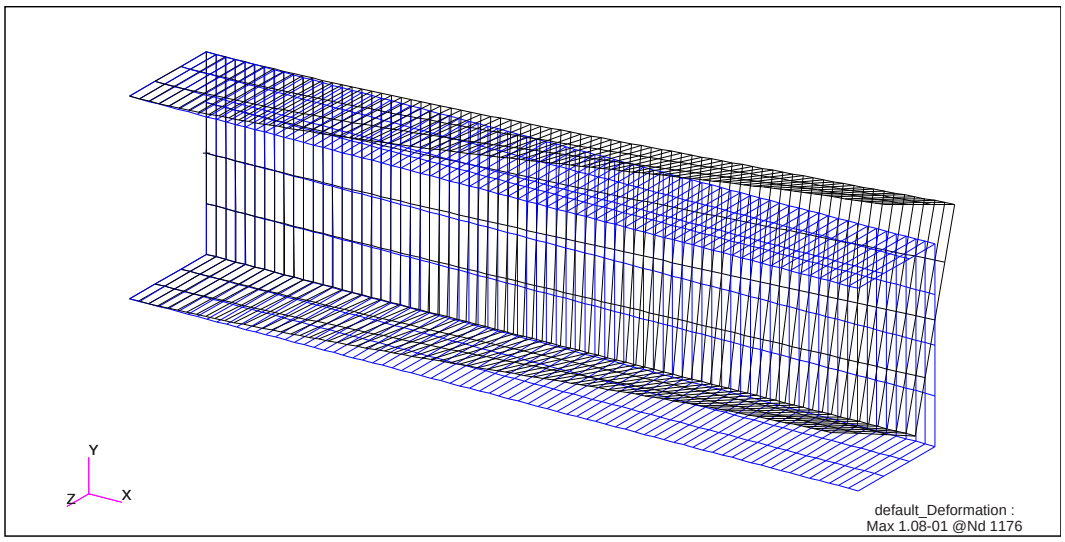

Mode 1, NF=23 Hz

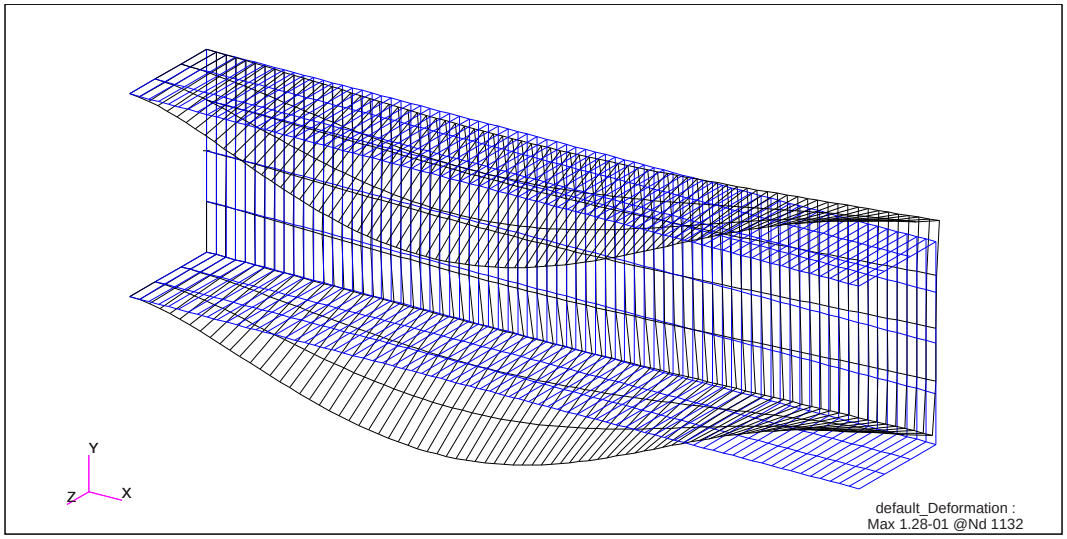

Mode 2, NF=85 Hz

Figure 5.15: The first and second mode shapes, as obtained by the NASTRAN analysis, for a short cantilever channel beam

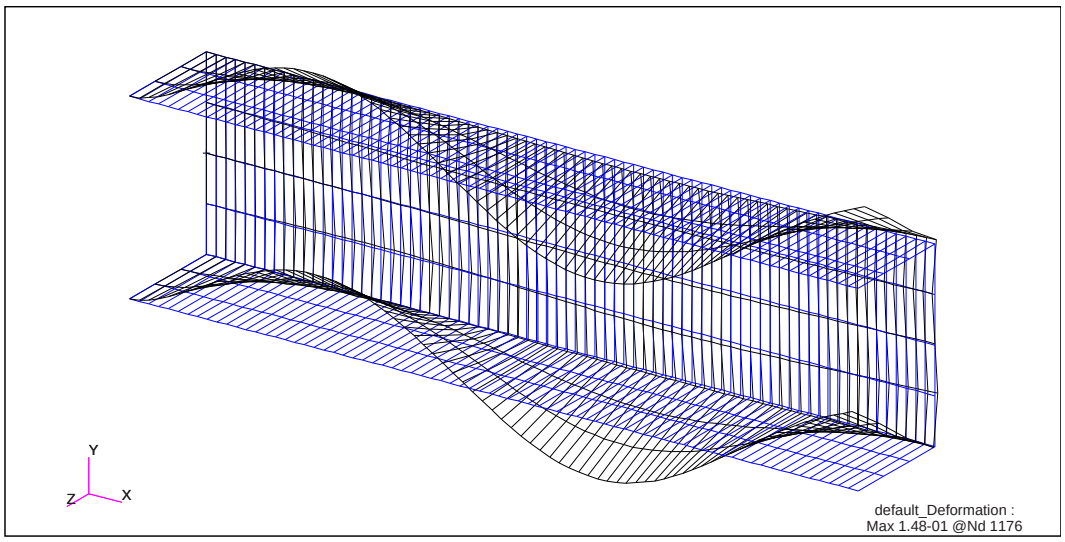

Mode 3, NF=126 Hz

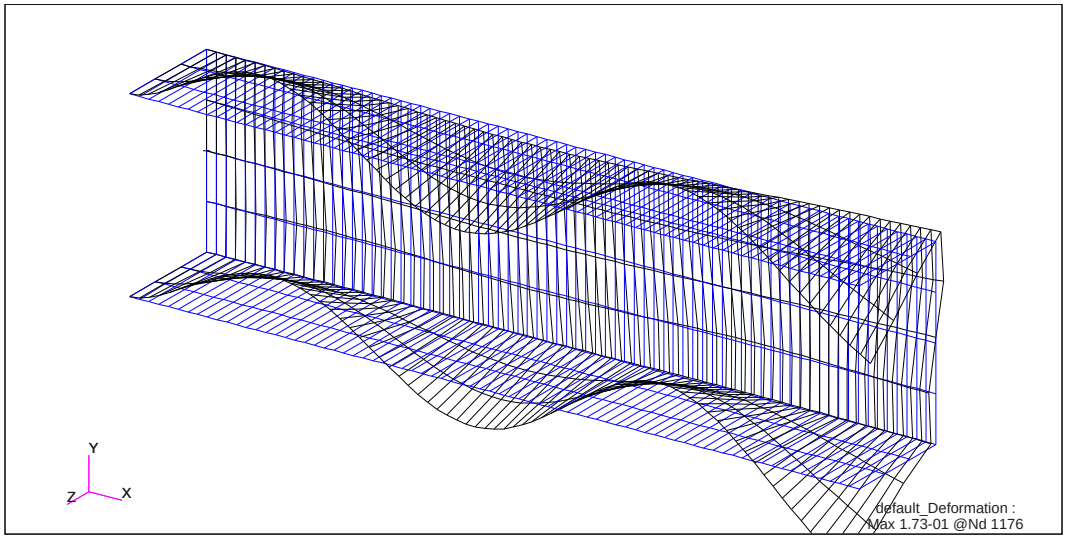

Mode 4, NF=175 Hz

Figure 5.16: The third and fourth mode shapes, as obtained by the NASTRAN analysis, for a short cantilever channel beam

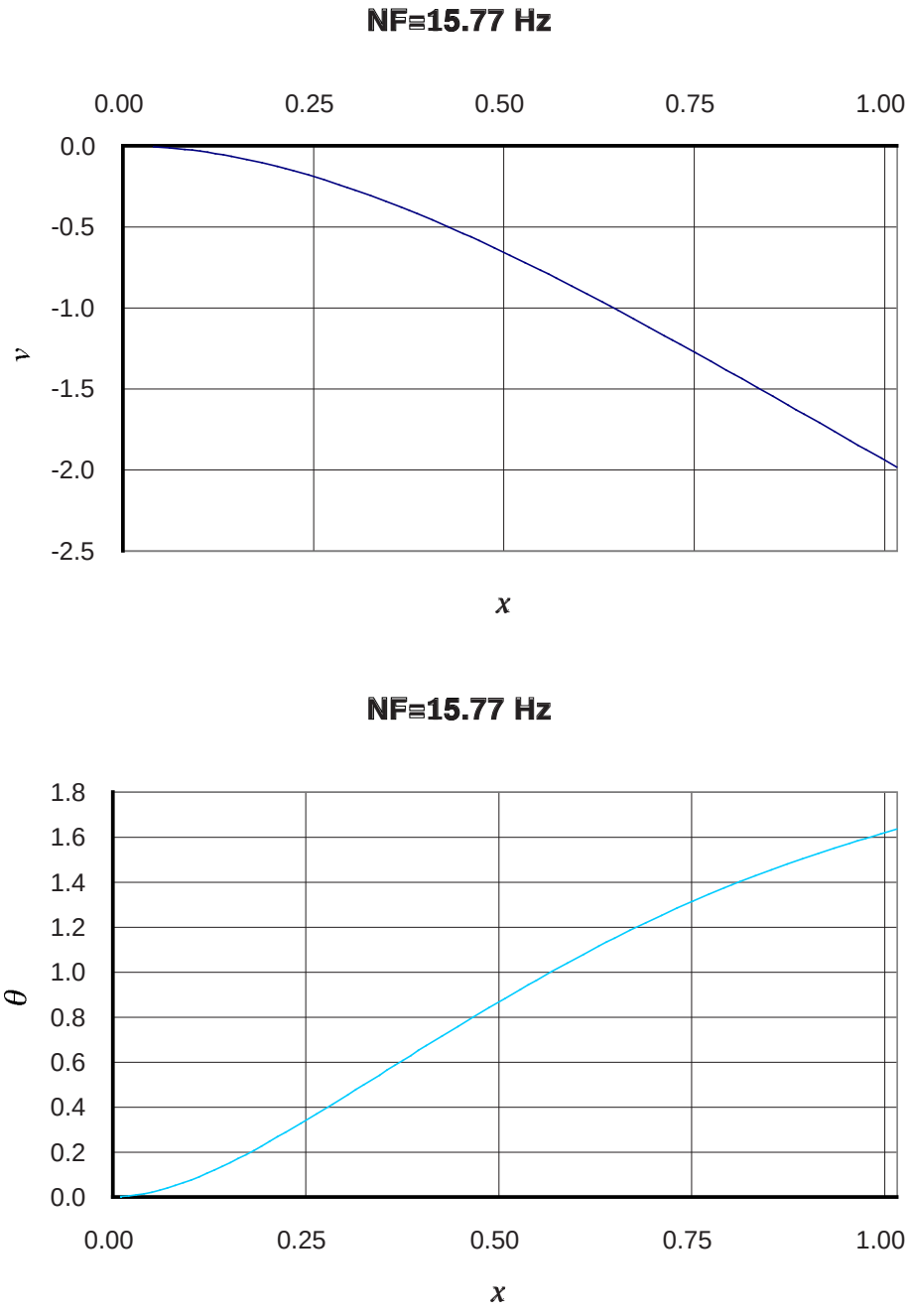

Figure 5.17: The first mode shapes of a rotating slender bending-torsion coupled cantilever channel beam as obtained using Karunamoorthy's modified Duncan polynomials (Ω = 600rpm)

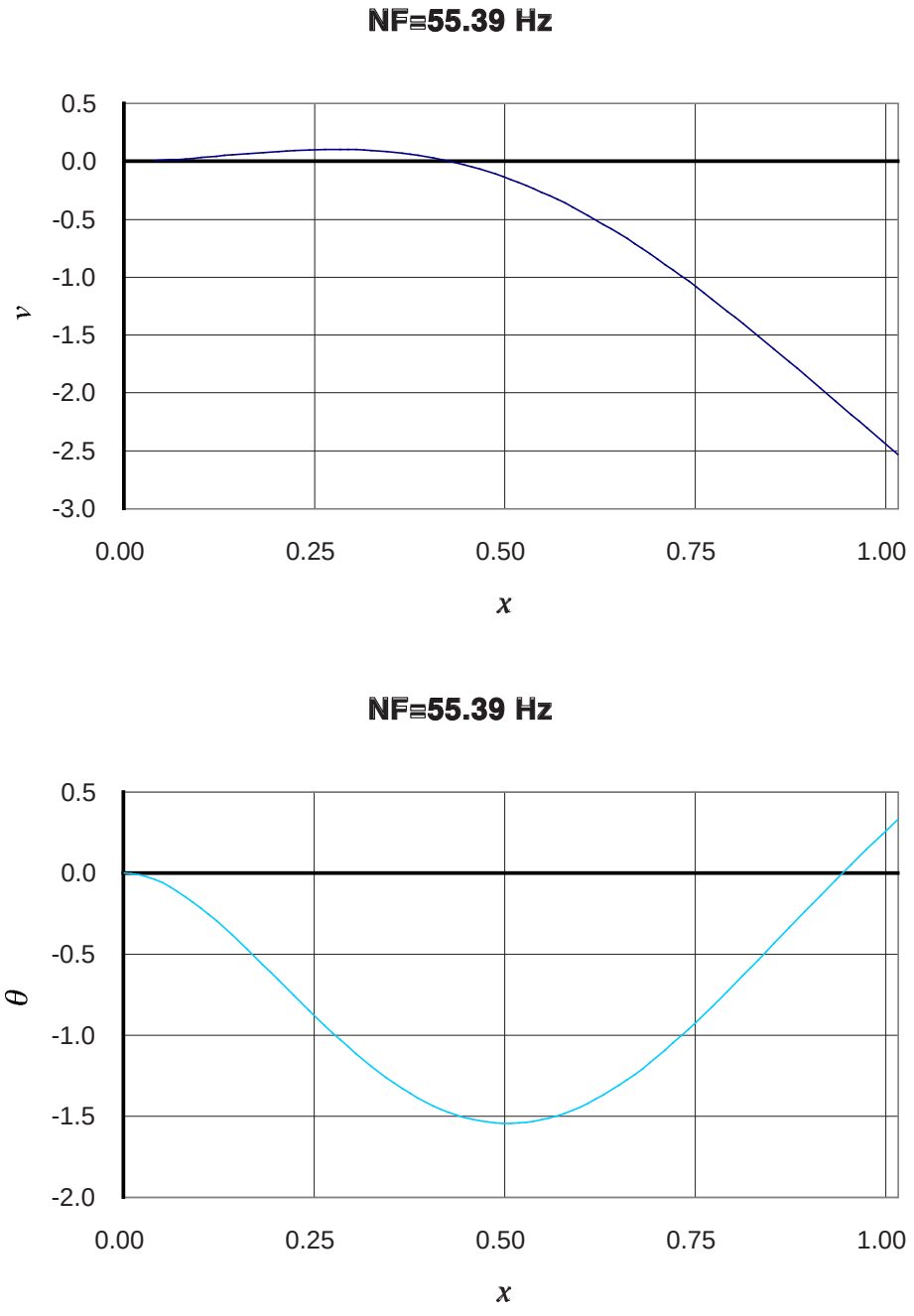

Figure 5.18: The second mode shapes of a rotating slender bending-torsion coupled cantilever channel beam as obtained using Karunamoorthy's modified Duncan polynomials (Ω = 600rpm)

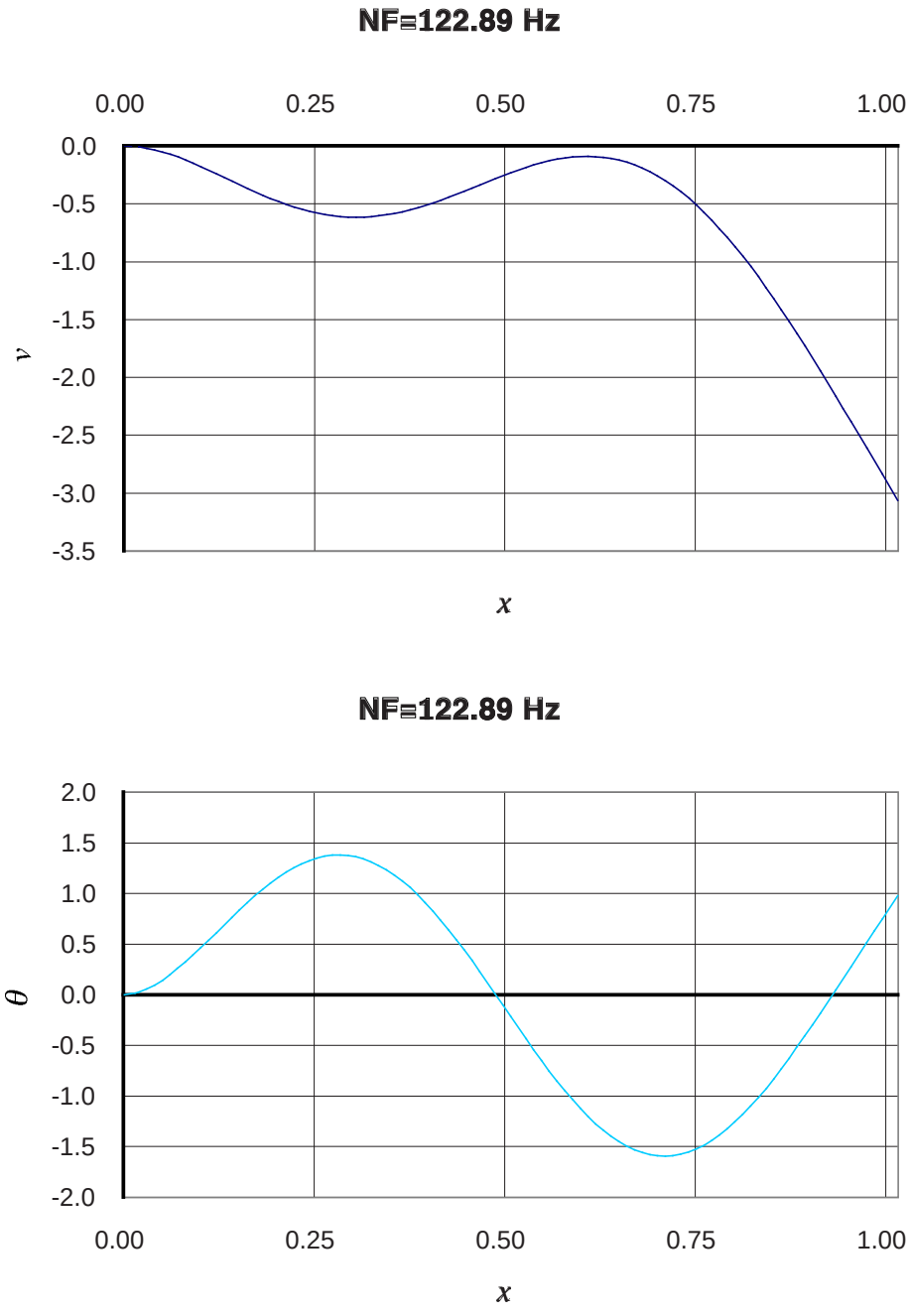

Figure 5.19: The third mode shapes of a rotating slender bending-torsion coupled cantilever channel beam as obtained using Karunamoorthy's modified Duncan polynomials (Ω = 600rpm)

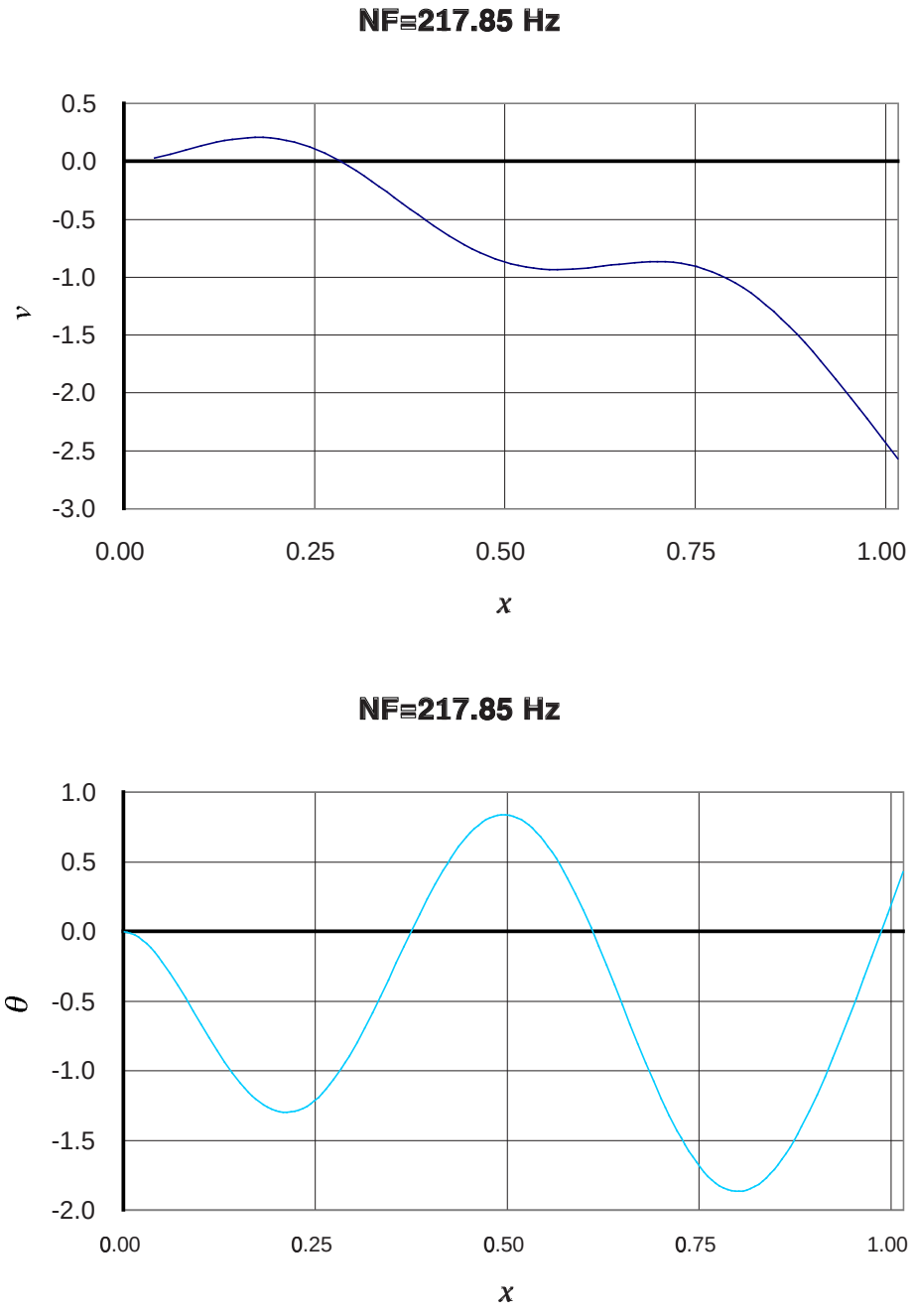

Figure 5.20: The fourth mode shapes of a rotating slender bending-torsion coupled cantilever channel beam as obtained using Karunamoorthy's modified Duncan polynomials (Ω = 600rpm)

Mode 1, (NF=15.61 Hz)

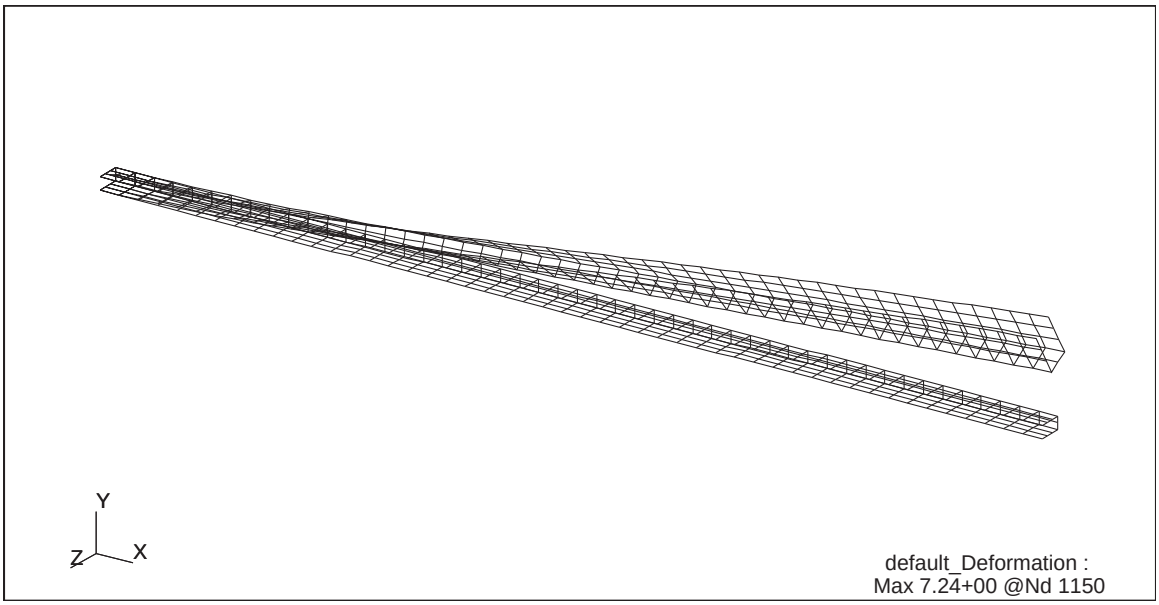

Mode 2, (NF=59.47 Hz)

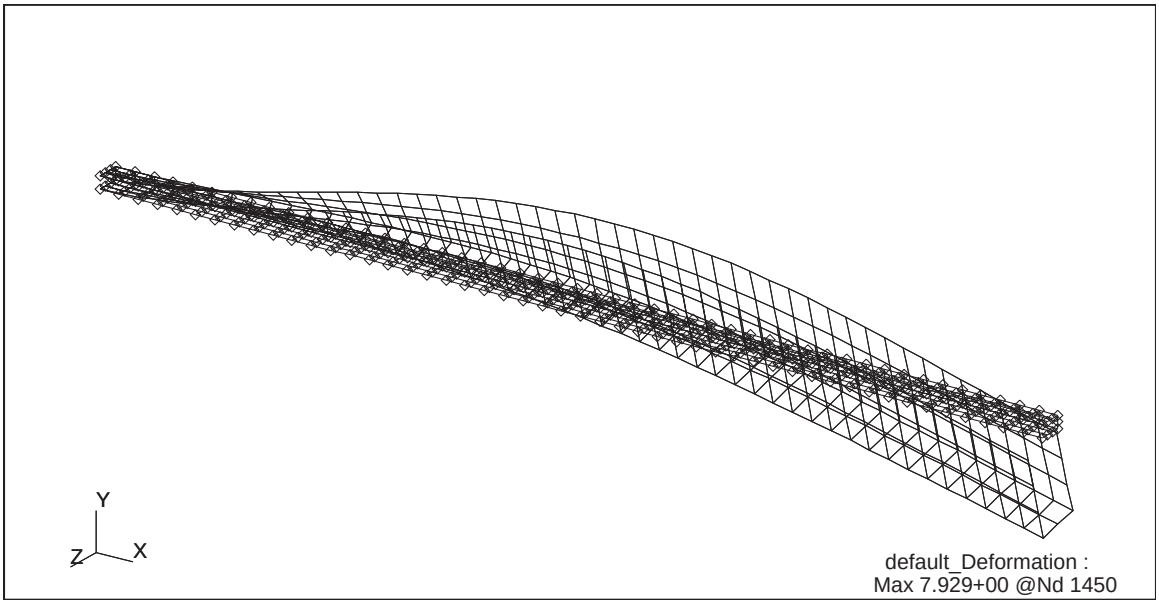

Figure 5.21: The first and second mode shapes of a rotating cantilever channel beam as obtained by the NASTRAN analysis ($\Omega = 600$rpm)

Mode 3, (NF=114.51 Hz)

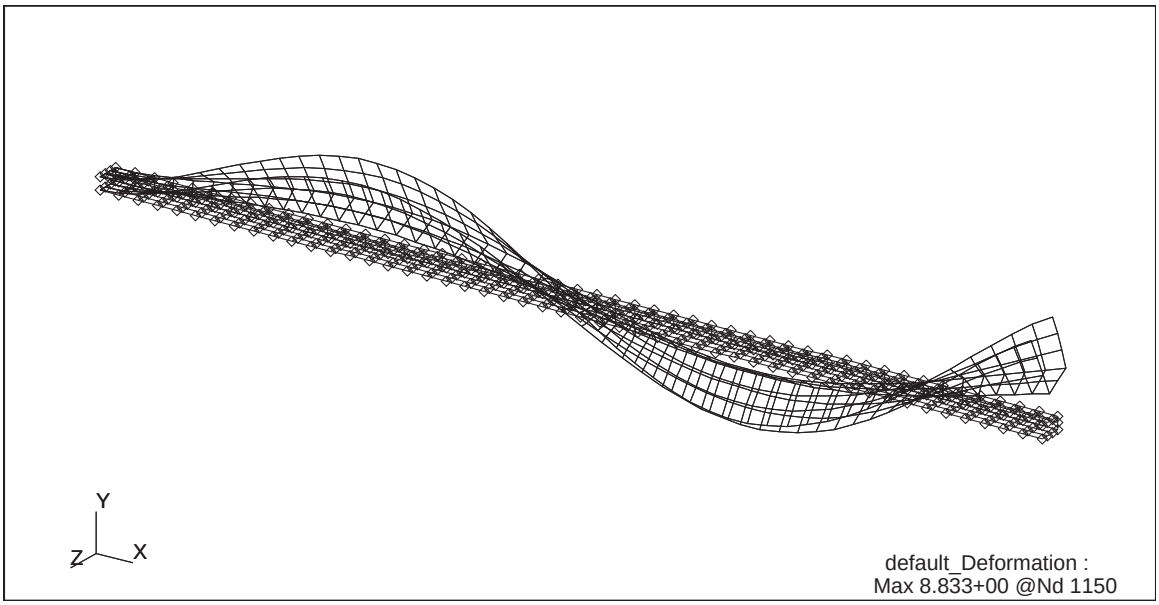

Mode 4, (NF=199.54 Hz)

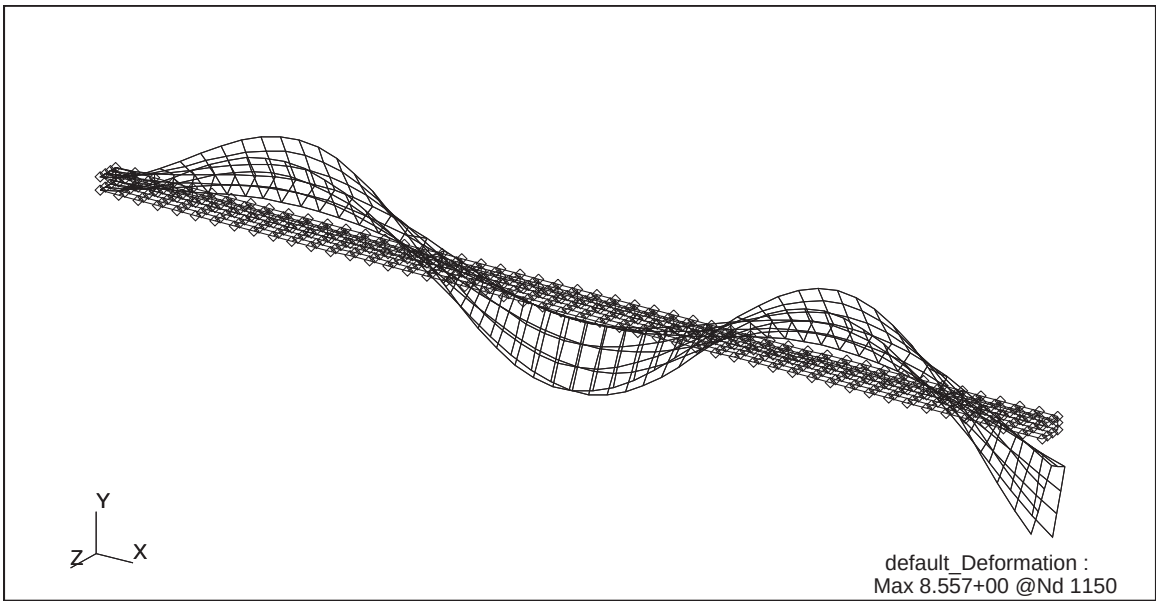

Figure 5.22: The third and fourth mode shapes of a rotating cantilever channel beam as obtained by the NASTRAN analysis ($\Omega = 600$rpm)

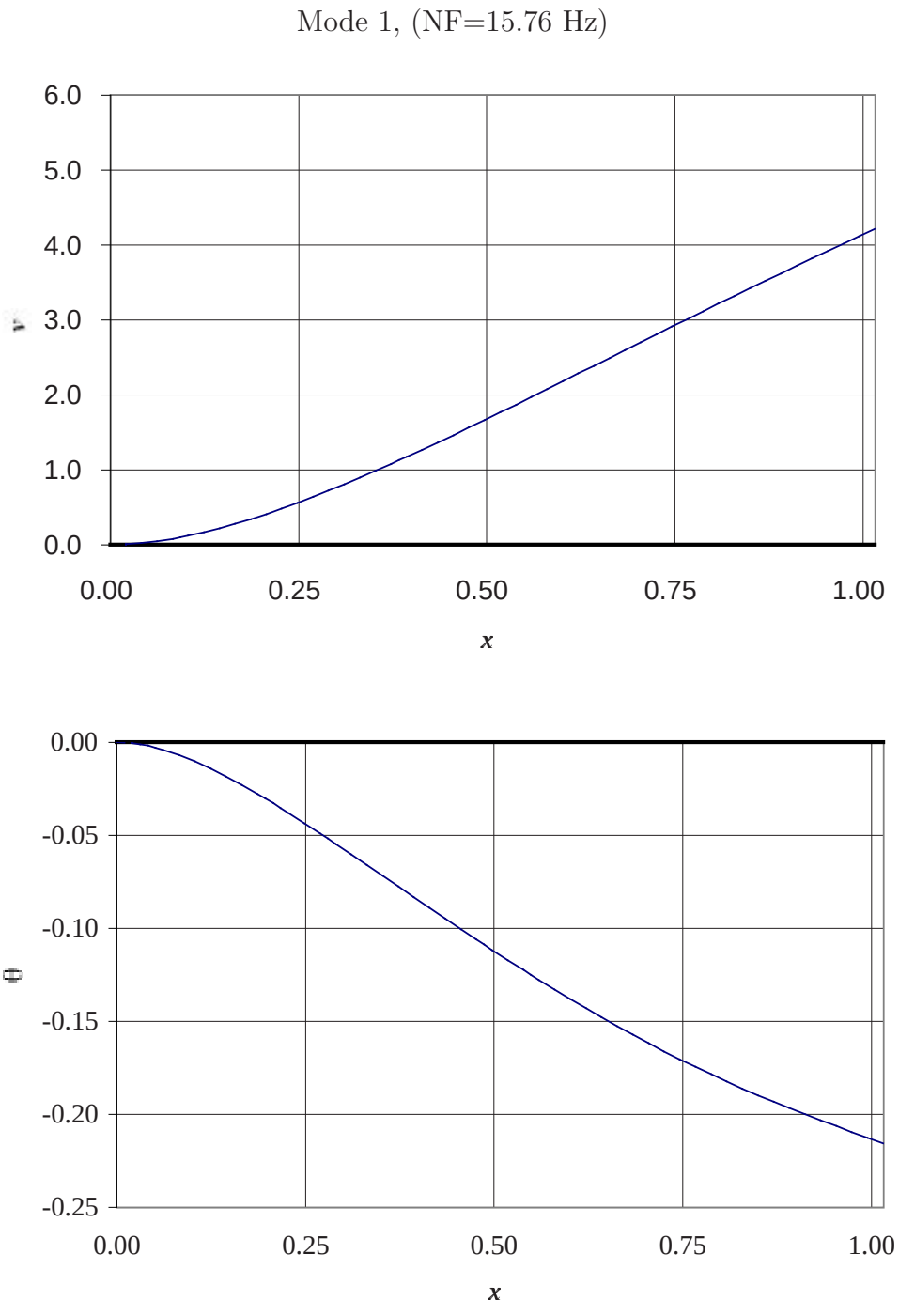

Figure 5.23: The first normal mode shapes of a rotating bending-torsion coupled slender cantilever channel beam as obtained by the NASTRAN analysis ($\Omega = 600$ rpm)

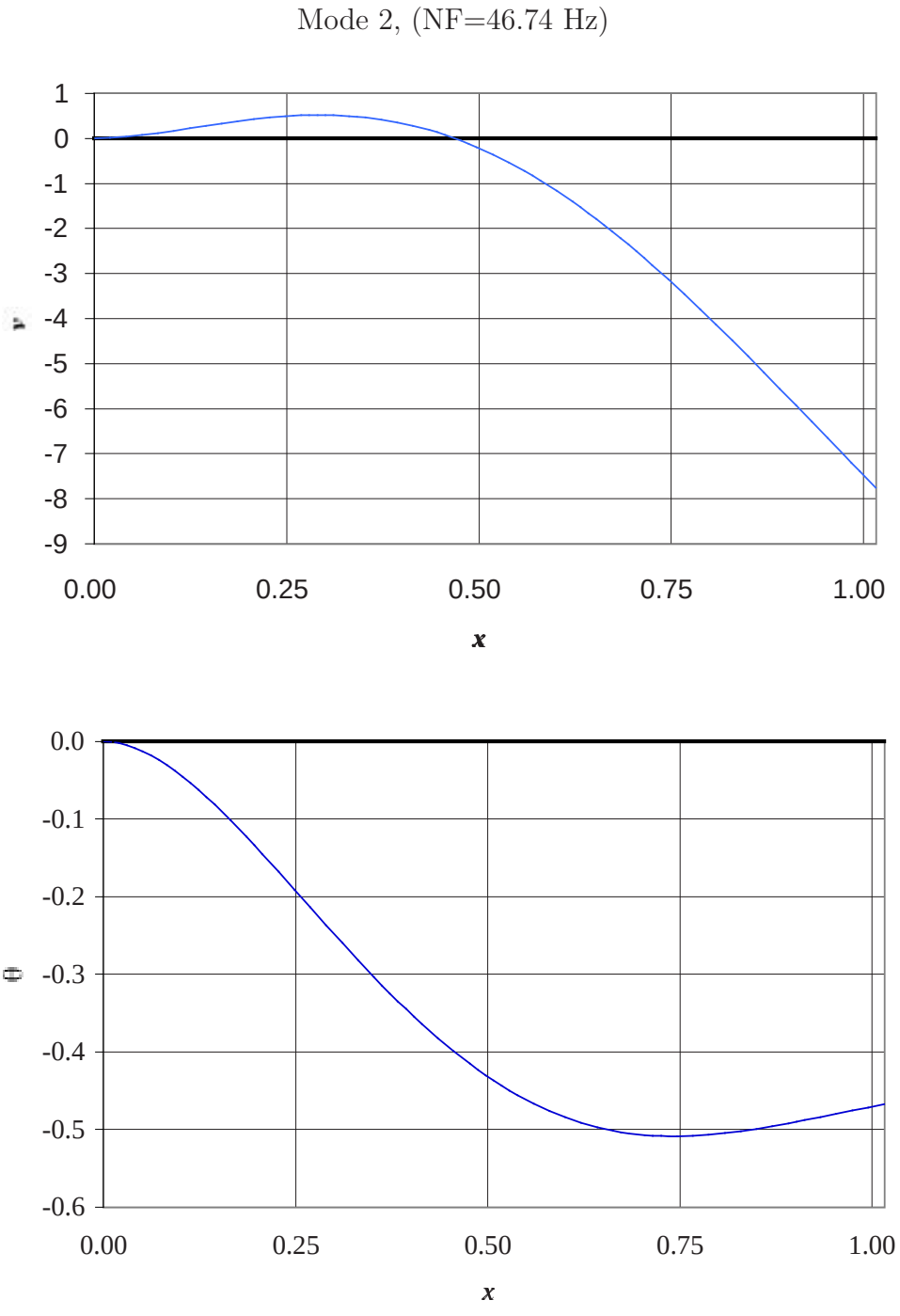

Figure 5.24: The second normal mode shapes of a rotating bending-torsion coupled slender cantilever channel beam as obtained by the NASTRAN analysis ($\Omega = 600$ rpm)

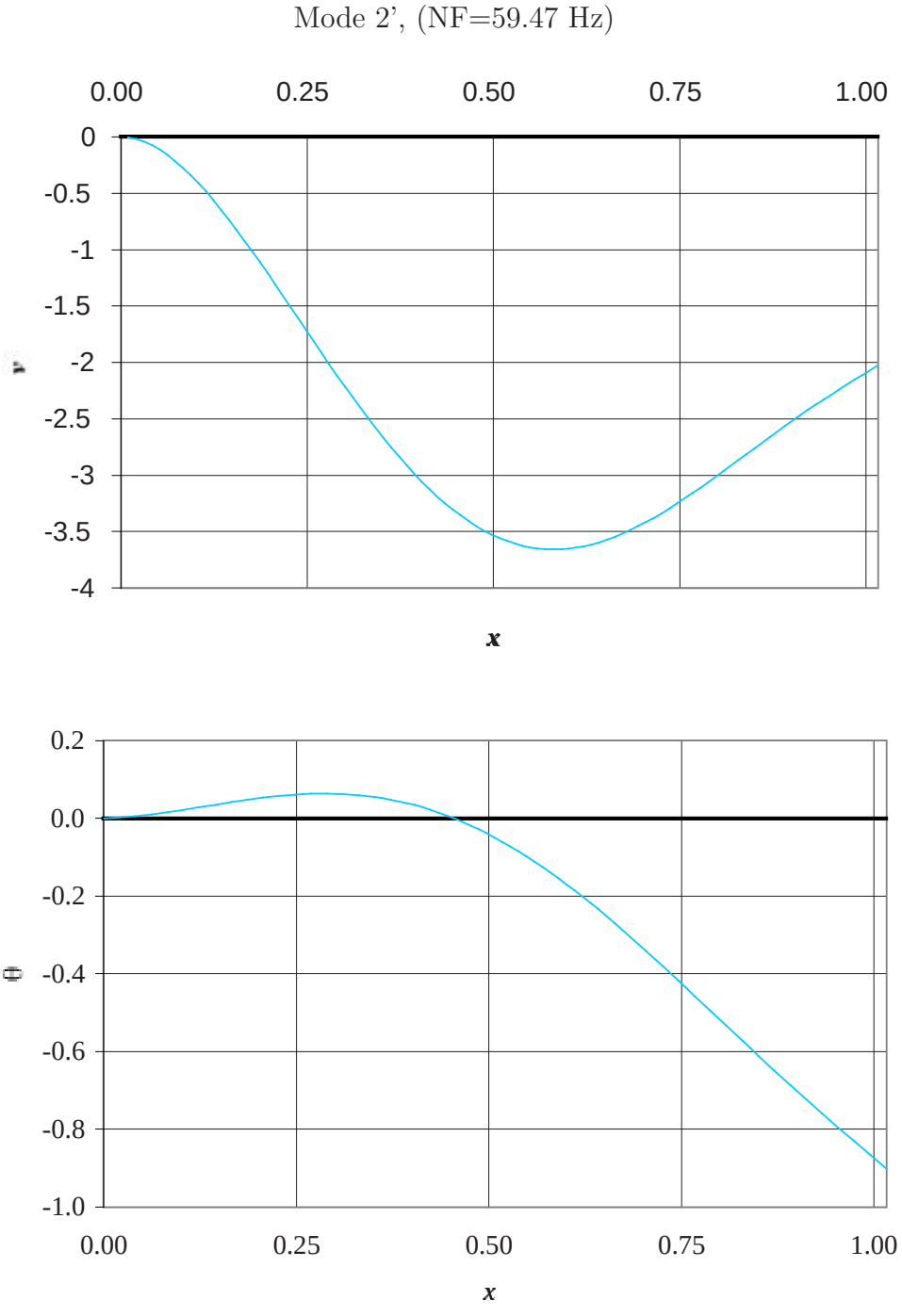

Figure 5.25: Another second normal mode shapes of a rotating bending-torsion coupled slender cantilever channel beam as obtained by the NASTRAN analysis ($\Omega = 600$ rpm)

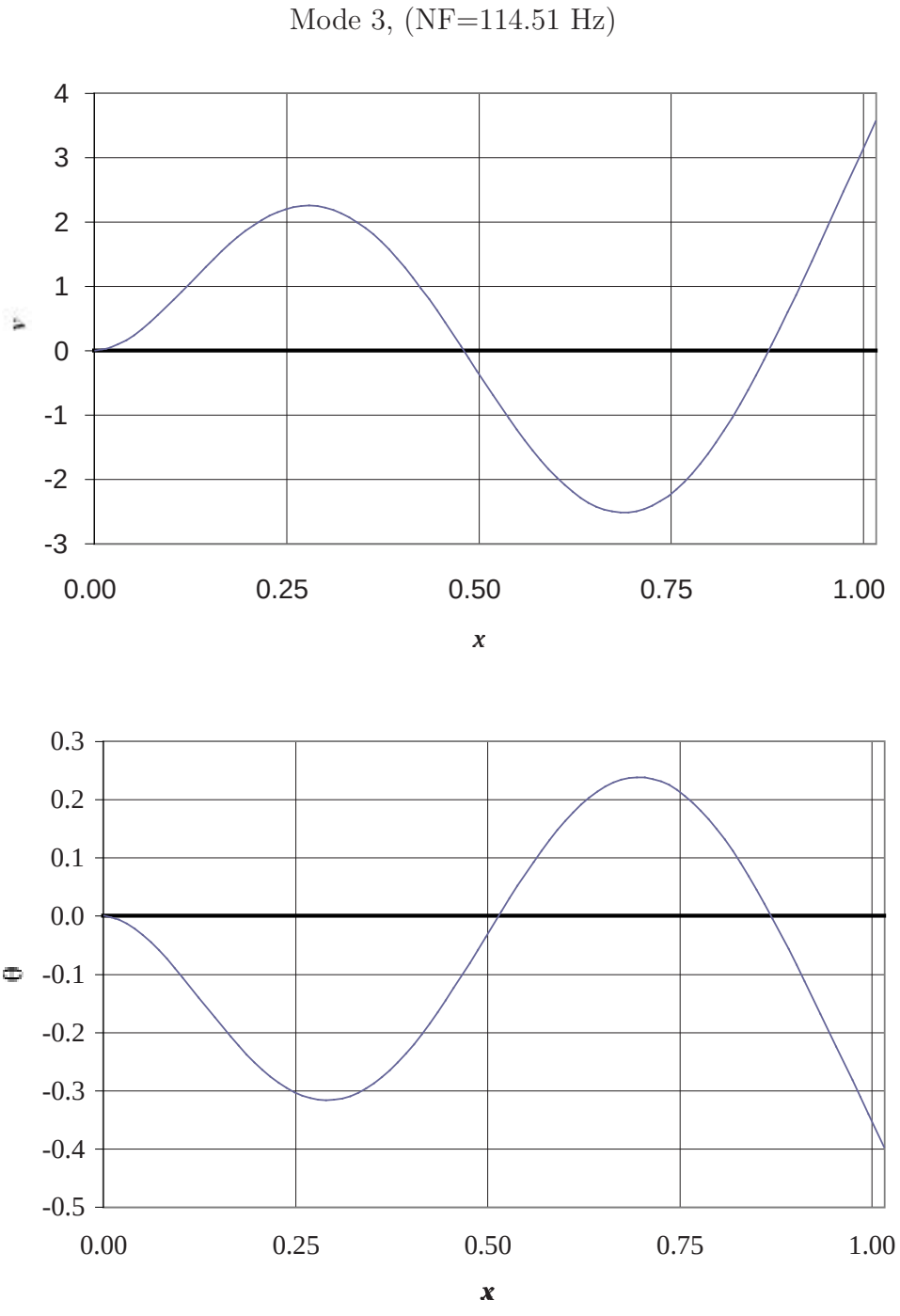

Figure 5.26: The third normal mode shapes of a rotating bending-torsion coupled slender cantilever channel beam as obtained by the NASTRAN analysis ($\Omega = 600$ rpm)

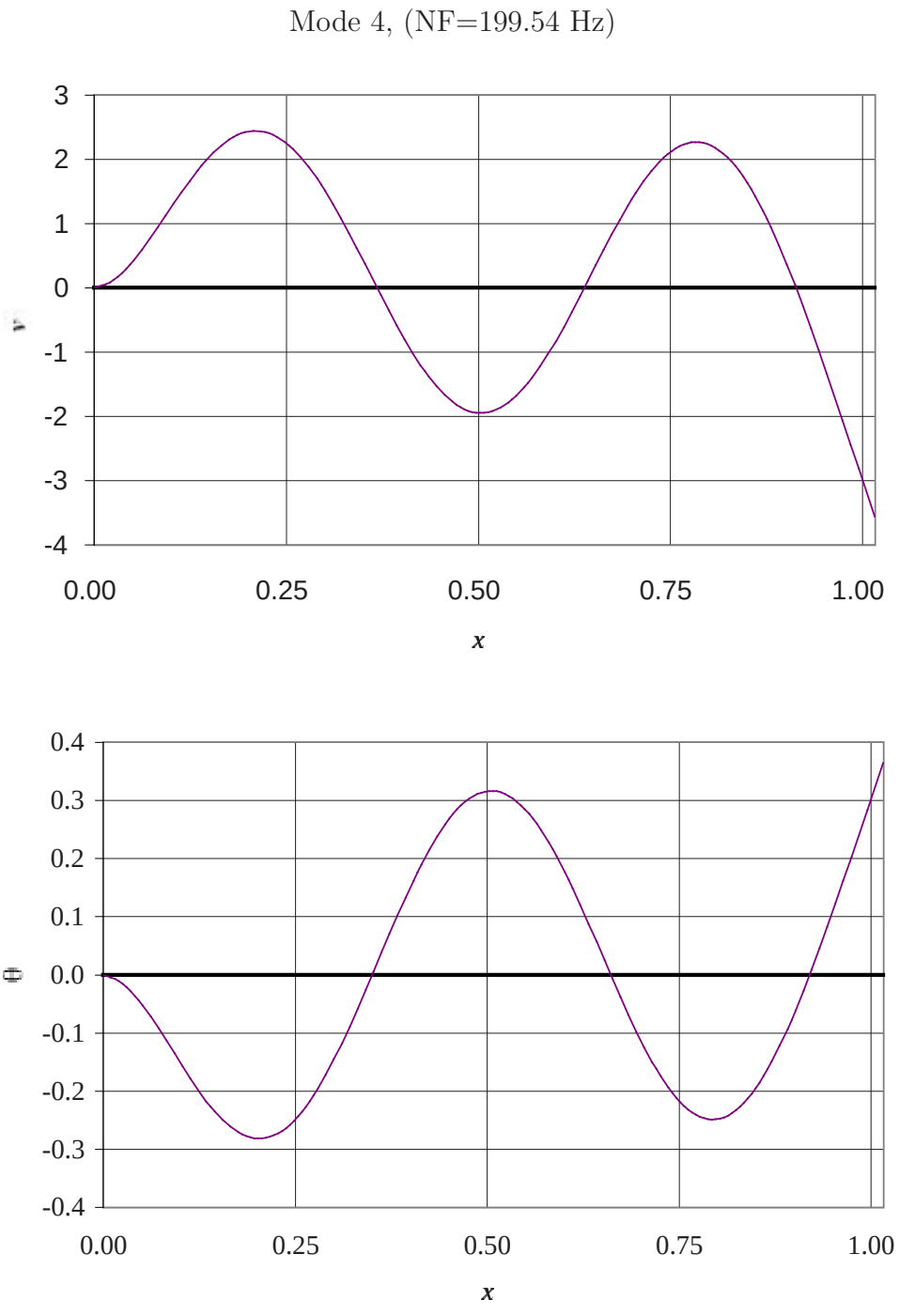

Figure 5.27: The fourth normal mode shapes of a rotating bending-torsion coupled slender cantilever channel beam aS obtained by the NASTRAN analysis ($\Omega = 600$ rpm)

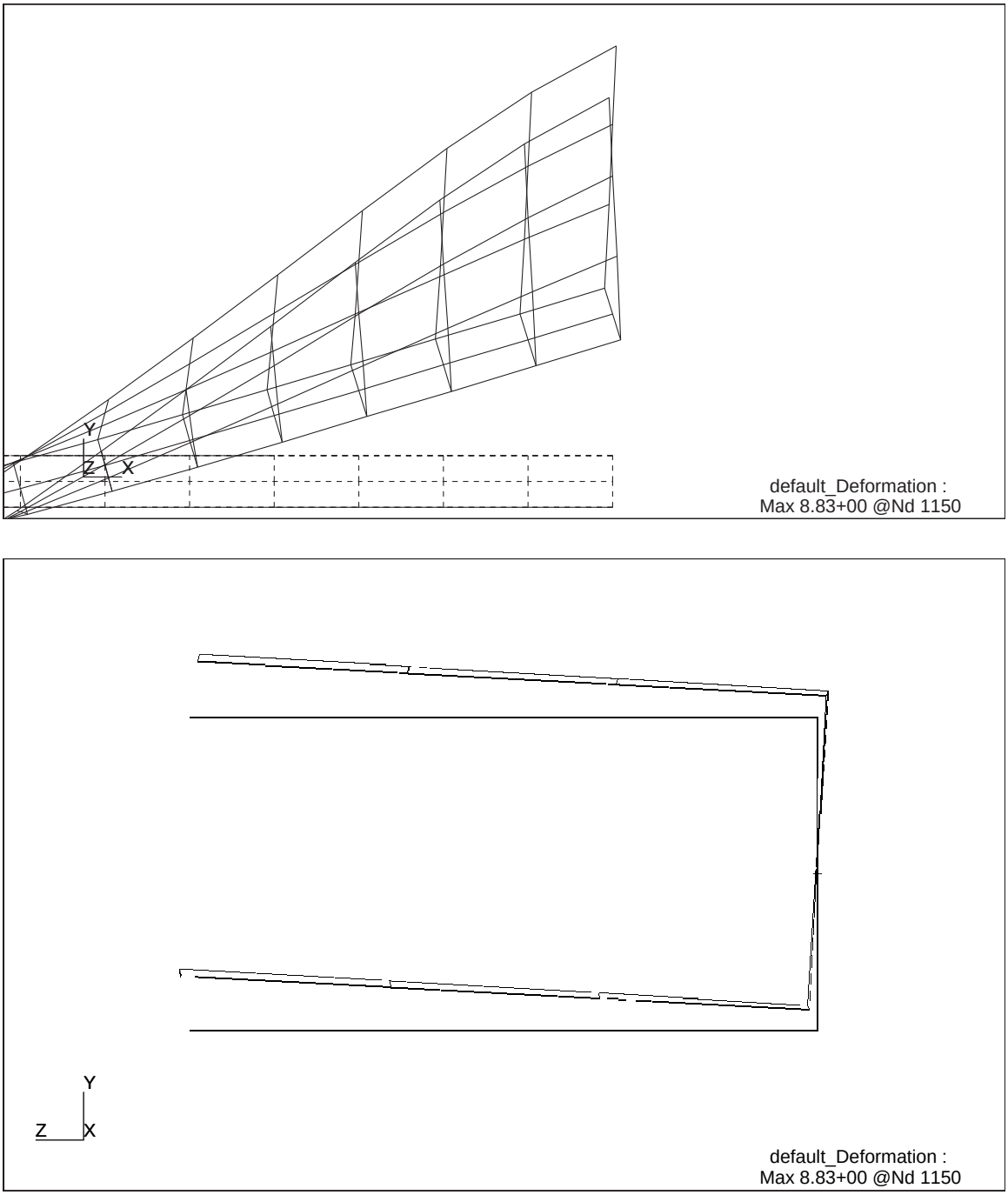

Figure 5.28: Tip deformation shape in the 4th normal mode of a rotating bending-torsion coupled beam as obtained by the NASTRAN analysis ($\Omega = 600$rpm)

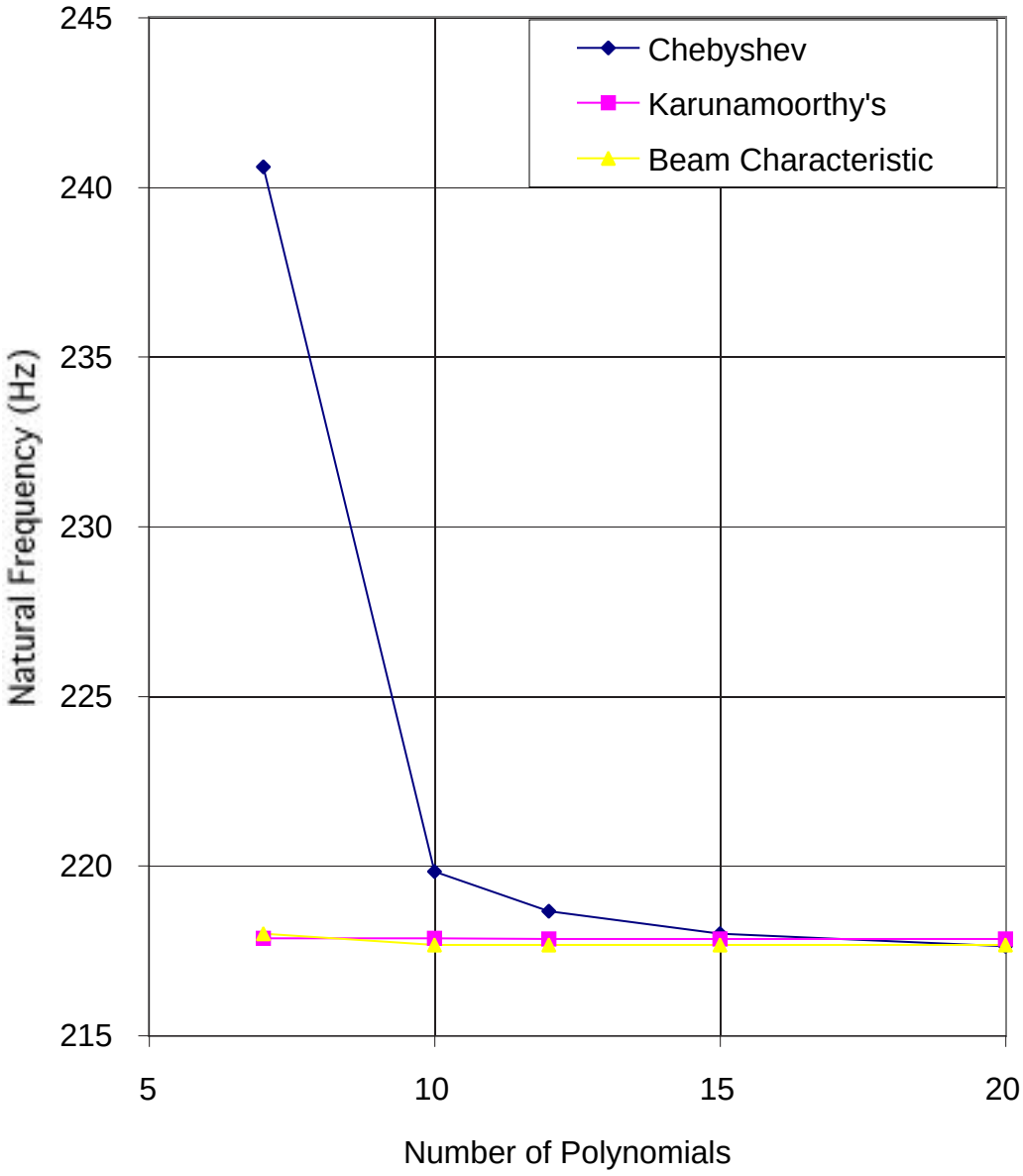

Figure 5.29: The fourth mode, as obtained by using different number of polynomials, for coupled flexural-torsional vibration of a slender channel beam ($\Omega = 600$ rpm)

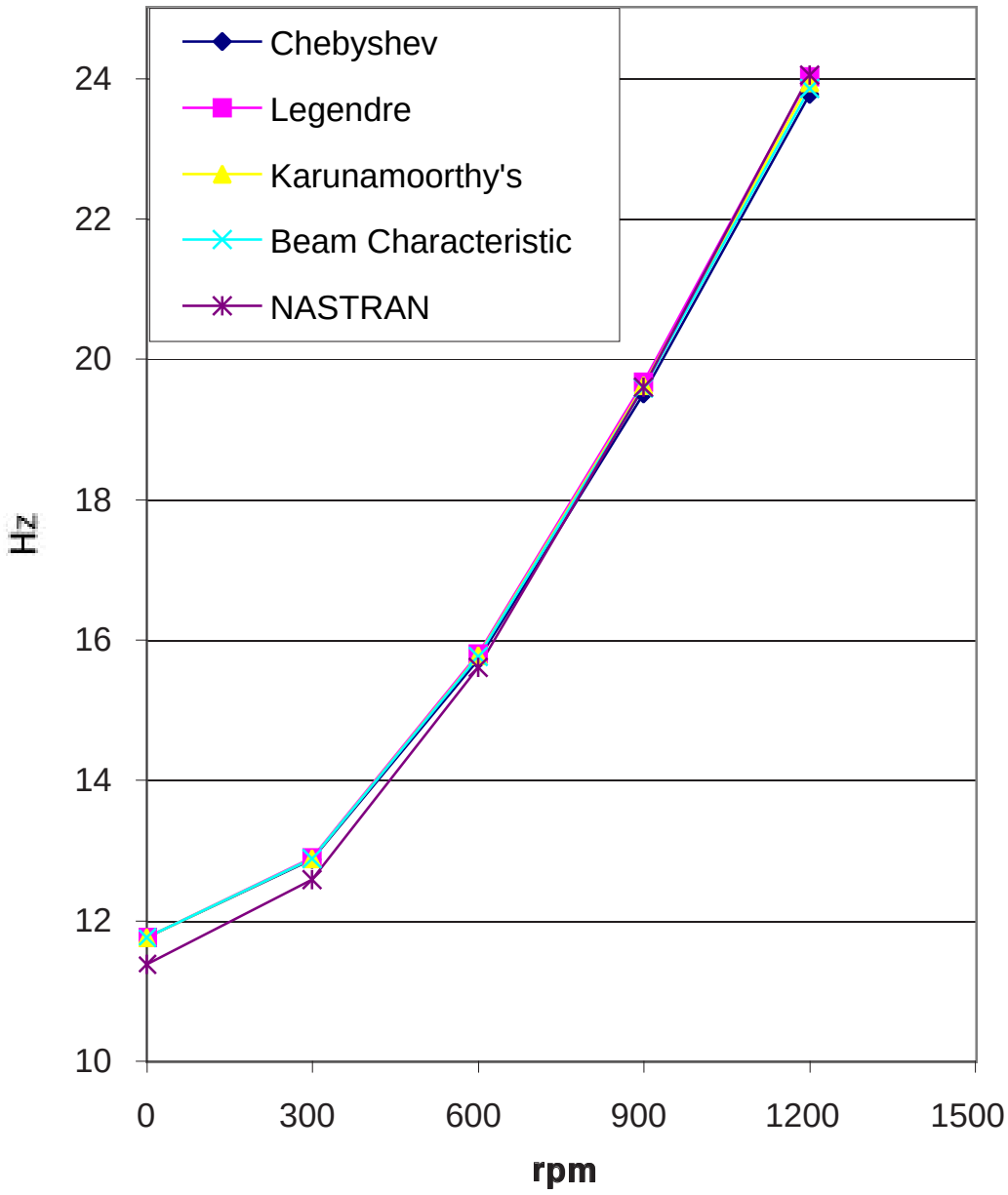

Figure 5.30: Natural frequencies of the first mode of coupled flexural-torsional vibration for different rotating speeds

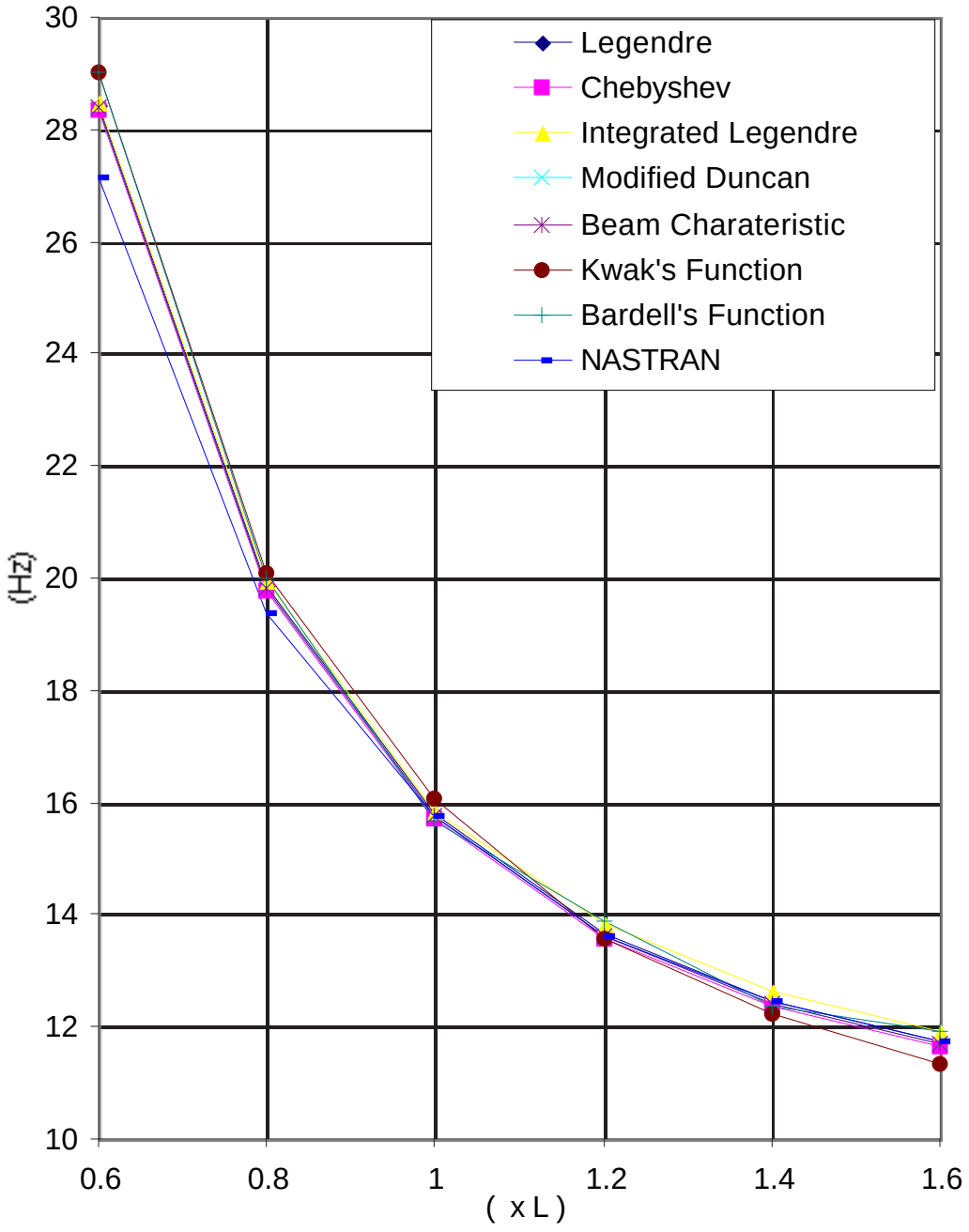

Figure 5.31: Natural frequencies of the first mode of rotating coupled flexural-torsional vibration for different lengths ($\Omega = 600$rpm)

Chapter 6

Summary and Conclusion

Various orthogonal polynomials were examined to evaluate their performance in determining the natural frequencies of normal modes in bending-torsion coupled rotating beam and other different cases and loadings. Tested orthogonal polynomials show good approximations compared to other orthogonal functions which contains trigonometric functions in finding normal modes of non-rotating and rotating beams. Among tested orthogonal functions, simple Legendre polynomials gave best efficiency in getting results. This is mainly because of ease of integration when these polynomials are used. Bardell and Kwak's orthogonal functions, which do not use polynomials completely, do not show good efficiency in getting results due to the enormous time consumed in the integration of trigonometric functions when generating the mass and stiffness matrices. Also, these orthogonal functions give less accurate approximations compared to orthogonal polynomials when the same number of approximating functions are used. Beam characteristic orthogonal polynomials show most accurate results and faster convergence but they require calculation time in generating assumed mode polynomials for different boundary conditions. Overall, orthogonal polynomials show good efficiency in finding natural frequencies of various beam boundary conditions with the least effort and time even though orthogonal polynomials have shown some limitations as in the case of not finding every normal modes of coupled flexural-torsional vibration of the free-free

channel beam.

The developed method here can be extended to analyze natural modes of coupled vibrations including axial and lateral vibrations along with flexural-torsional vibrations. Moreover, coupled vibrations of multi-cell composite thin-walled beams can be analyzed using the developed method. Moreover, more efficient method to fulfill essential boundary conditions and explicit addition of warping function in the strain-displacement relation should be explored in the future work

Bibliography

Bibliography

[1] Dokumaci, E., "An exact solution for coupled bending and torsion vibrations of uniform beams having single cross-sectional symmetry," *Journal of Sound and Vibration*, Vol. 119, No. 3, 1987, pp. 443-449.

[2] Bishop, R. E. D., Cannon, S. M., and Miao, S., "On Coupled Bending and Torsional Vibration of Uniform Beams," *Journal of Sound and Vibration*, Vol. 131, No. 3, 1989, pp. 457-464.

[3] Bercin, A. N. and Tanaka, M., "Coupled Flexural-Torsional Vibrations of Timoshenko Beams," *Journal of Sound and Vibration*, Vol. 207, No. 1, 1997, pp. 47-59.

[4] Young, T. H. and Liou, G. T., "Coriolis Effect on the Vibration of a Cantilever Plate With Time-Varying Rotating Speed," *Journal of Vibration and Acoustics*, Vol. 114, 1992, pp. 232-241.

[5] Leissa, A. W., and Co. C. M., "Coriolis Effects on the Vibrations of Rotating Beams and Plates," *Proceedings of Twelfth Southeastern Conference on Theoretical and Applied Mechanics*, 1984, pp. 508-513.

[6] Love, A. E. H., *A Treatise on the Mathematical Theory of Elasticity*, Dover Publications Inc., New York, 1927.

[7] Timoshenko, S. P., *History of Strength of Materials*, Dover Publications Inc, New York, 1953.

[8] Strutt, J. W., *Theory of Sound*, Macmillan Publications, London, 1877,

[9] Timoshenko, S. P. "On the correction for shear of the differential equation for transverse vibrations of bars of uniform cross-section," *Philosophical Magazine*, 1921, pp. 744.

[10] Timoshenko, S. P., "On the transverse vibrations of bars of uniform cross-section," *Philosophical Magazine*, 1922, pp. 125.

[11] Singhvi, S. and Kapania, R. K., "Comparison of Simple and Chebyshev Polynomials in Rayleigh-Ritz Analysis," *Journal of Engineering Mechanics*, ASCE, Vol. 120, N. 10, 1994, pp.2126

[12] Kruszewski, E. T., "Effects of transverse shear and rotary inertia on the natural frequencies of a uniform beam," *National Advisory Committee for Aeronautics*, 1909.

[13] Traill-Nash, R. W. and Collar A. R., "The effects of shear flexibility and rotatory inertia on the bending vibrations of beams," *Quarterly Journal of Mechanics and Applied Mathematics*, Vol 6, 1953, pp. 186-213.

[14] Huang, T. C., "The effect of rotatory inertia and of shear deformation on the frequency and normal mode equations of uniform beams with simple end conditions," *Journal of Applied Mechanics*, 1961. pp. 579-584.

[15] Dolph, C. L., "On the Timoshenko theory of transverse beam vibrations," *Quarterly of Applied Mathematics*, 1954, Vol. 12, pp. 175-187.

[16] Herrmann, G., "Forced motions of Timoshenko beam theory," *Journal of Applied Mechanics*, Vol. 77, 1955, pp. 53-56.

[17] Davies, R. M., "The frequency of transverse vibration of a loaded fixed-free bar III. The effect of rotatory inertia of the bar," *Philosophical Magazine*, 1937, pp. 563.

[18] Fan, H. and Widera, G. E. O., "Refined Engineering Beam Theory Based on the Asymptotic Expansion Approach," *AIAA Journal*, Vol. 29, Mar., 1991, pp. 444-449.

[19] Boyce, W. E., Diprima, R. C., and Handelman, G. H., "Vibrations of rotating beams of constant section." Proc. 2nd U.S. Natl Cong. Appl. Mech., 1954, pp. 165.

[20] Carnegie, W., "Vibrations of rotating cantilever blading: theoretical approaches to the frequency problem based on energy methods," *Journal of Mechanical Engineering Science*, Vol 1, 1959, pp.235-240

[21] Schilhansl, M. J., "Bending frequency of a rotating cantilever beam," *Journal of Applied Mechanics*, Vol. 25, 1958, pp. 28-30.

[22] Rubinstein, N. and Stadter, J. T., "Bounds to bending frequencies of a rotating beam," *Journal of the Franklin Institute*, Vol. 294, 1972, pp. 217.

[23] Pnuelli, D., "Natural bending frequency comparable to rotational frequency in rotating cantilever beam," *Journal of Applied Mechanics*, Vol. 39, 1972, pp. 602-604.

[24] Lo, H., Goldberg, J. E., and Bogdanoff, J. L., "Effect of small hub radius change on bending frequencies of a rotating beam." *Journal of Applied Mechanics*, Vol.27, 1960, pp. 548

[25] Boyce, W. E. and Handelman, G. H., "Vibrations of rotating beams with tip mass," *Z. Angew. Math. Phys.*, Vol. 12, 1961., pp. 369

[26] Kumar, R., "Vibrations of space booms under centrifugal force field," *Trans. C.A.S.I.*, Vol.7, 1974, pp. 1.

[27] Stafford, R. O. and Giurgiutiu, V., "Semi-analytic methods for rotating Timoshenko beams," *International Journal of Mechanical Sciences*, Vol. 17, 1975, pp. 719.

[28] McDaniel, T. J., and Murthy, V. R., "Bounds on the dynamic characteristics of rotating beams," *AIAA Journal*, Vol. 15, 1977, pp. 439.

[29] Subrahmanyam, K. B., Kulkarni, S. V., and Rao, J. S., "Coupled bending-torsion vibrations of rotating blades of asymmetric aerofoil cross section with allowance for shear

deflection and rotary inertia by use of the Reissner method," *Journal of Sound and Vibration*, Vol. 75, 1981, pp. 17-36.

[30] Bhat, R. B., "Transverse vibrations of a rotating uniform cantilever beam with tip mass as predicted by using beam characteristic orthogonal polynomials in the Rayleigh-Ritz method," *Journal of Sound and Vibration*, Vol. 105, No. 2, 1986, pp. 199-210.

[31] Chihara, T. S. *Introduction to Orthogonal Polynomials* Gordon and Breach, London, 1978.

[32] Shames, I. H. and Dym, C. L. *Energy and Finite Element Methods in Structural Mechanics* Hemisphere Publishing Co., 1985.

[33] Bazoune, A. and Khulief, Y. A., "A finite beam element for vibration analysis of rotating tapered Timoshenko beams," *Journal of Sound and Vibration*, Vol. 156, No. 1, 1992, pp. 141-164.

[34] Yokoyama, T., "Free vibration characteristics of rotating Timoshenko beams," *International Journal of Mechanical Sciences*, Vol. 30, No. 10, 1988, pp. 743-755.

[35] Bishop, R. E. D. and Price, W. G., "Coupled bending and twisting of a Timoshenko beam," *Journal of Sound and Vibration*, Vol. 50, 1977, pp.469-477.

[36] Banerjee, J. R. and Fisher S. A.,"Coupled Bending-Torsional Dynamic Stiffness Matrix for Axially Loaded Beam Elements," *International Journal for Numerical Methods in Engineering*, Vol. 33, 1992, pp. 739-751.

[37] Adam, C., "Forced vibrations of elastic bending-torsion coupled beams," *Journal of Sound and Vibration*, Vol. 221, No. 2, 1999, pp. 273-287.

[38] Karunamoorthy, S. N., Peters, D. A., and Barwey, D., "Orthogonal Polynomials for Energy Methods in Rotary Wing Structural Dynamics," *Journal of the American Helicopter Society*, Jul. 1993. pp. 93-98.

[39] Bardell, N. S., Dunsdon, J. M., and Langley, R. S., "Free Vibration of Thin, Isotropic, Open, Conical Panels," *Journal of Sound and Vibration*, Vol. 217, No. 2, 1993, pp. 297-320.

[40] Kwak, M.K., "New Admissible Functions for the Dynamic Analysis of a Slewing Flexible Beam," *Journal of Sound and Vibration*, Vol. 210, No. 5, 1998, pp. 581-592.

[41] Amabili, M. and Garziera, R., "A technique for the systematic choice of admissible functions in the Rayleigh-Ritz method," *Journal of Sound and Vibration*, Vol. 224, No. 3, 1999, pp. 519-539.

[42] Ruta, P., "Application of Chebyshev series to solution of non-prismatic beam vibration problems," *Journal of Sound and Vibration*, Vol. 227, No. 2, 1999, pp. 449-467.

[43] Chihara, T. S., *Introduction to Orthogonal Polynomials*, Gordon and Breach, London, 1978.

[44] Murray, N. W., *Introduction to the Theory of Thin-Walled Structures*. Oxford, New York, 1984.

[45] Megson, T. H. G., *Aircraft Structures for Engineering Students*, 2nd Ed. Halsted Press, 1990.

[46] Timoshenko, S., Young, D. H., and Weaver, Jr. W., *Vibration Problems in Engineering*, 4th Ed. Wiley, New York, 1974.

[47] Bishop, R. E. D., Price, W. G., and Zhang, Xicheng, "On the Structural Dynamics of a Vlasov Beam," Proceedings of the Royal Society, London, A388, 1983, pp.49-73.

[48] Park, S. and Kapania, R. K., "Comparison of various orthogonal polynomials in hp-version time finite element method," AIAA Journal, Vol. 36, No. 4, Apr. 1998, pp. 651-655.

[49] Szabó, B. and Babuška, I., *Finite Element Analysis*, John Wiley & Sons, New York, 1991.

Appendix A

MATHEMATICA Input

a) Natural frequencies of rotating cantilever Timoshenko beam by Rayleigh-Ritz method using Legendre polynomials

```
j = 0; n = 10; L =.; h =.; rs =.; rg =.; psi =.; kd =.; r = 3;
Do[j ++;
        p[j] = LegendreP[i, x / L];
        Print[p[j]];
        , {i, 1, n * 2, 2}]

Do[pd1[i] = D[p[i], x], {i, 1, n}]
start = TimeUsed[]
k = Table[0, {i, 1, 2 * n - 1}, {j, 1, 2 * n - 1}];
kc = Table[0, {i, 1, n}, {j, 1, n}];
kw = Table[0, {i, 1, n}, {j, 1, n}];

Do[Do[
  k[[i, j]] = (5 / 13 * kd / rg^2) * Integrate[pd1[i] * pd1[j], {x, 0, L}]
        , {j, i, n}], {i, 1, n}]

Do[Do[
        k[[i, n + j]] = (5 / 13 * kd / rg^2) * Integrate[pd1[i] * p[j], {x, 0, L}]
                    , {j, 1, n - 1}], {i, 1, n}]

Do[Do[
        k[[n + i, n + j]] = Integrate[pd1[i] * pd1[j], {x, 0, L}]
          + (5 / 13 * kd / rg^2) * Integrate[p[i] * p[j], {x, 0, L}]
                , {j, i, n - 1}], {i, 1, n - 1}]

Do[Do[
        kc[[i, j]] = Integrate[Integrate[y, {y, r + x, r + 1}] * pd1[i] * pd1[j], {x, 0, L}]
        , {j, 1, n}], {i, 1, n}]

Do[Do[
        kw[[i, j]] = Integrate[p[i] * p[j], {x, 0, L}]
        , {j, 1, n}], {i, 1, n}]

Do[
Do[
    k[[i, j]] = k[[j, i]]
    , {j, 1, i - 1}]
, {i, 2, 2 * n - 1}]

Do[Do[
        k[[i, j]] += rs^2 * (kc[[i, j]] - Sin[psi]^2 * kw[[i, j]])
        , {j, 1, n}], {i, 1, n}]

MatrixForm[k]
```

```
mt = Table[0, {i, 1, 2 * n - 1}, {j, 1, 2 * n - 1}];
Do[Do[
    mt[[i, j]] = Integrate[p[i] * p[j], {x, 0, L}];
    , {j, i, n}], {i, 1, n}]
Do[Do[
        mt[[n + i, n + j]] = rg^2 * mt[[i, j]]
            , {j, i, n - 1}], {i, 1, n - 1}]
Do[Do[
    mt[[i, j]] = mt[[j, i]]
    , {j, 1, i - 1}]
, {i, 2, 2 * n - 1}]

MatrixForm[mt]



L = 1;
rs = 0;
psi = 0;
r = 0;
kd = 0.85;
rg = 1 / 10;
N[Eigenvalues[Inverse[mt].k]^(1 / 2)]



end = TimeUsed[];
Print["CPU Time Used = ", end - start, " sec"]
```

b) Natural frequencies of bending-torsion coupled rotating cantilever Bernoulli-Euler channel beam by Rayleigh-Ritz method using Karunamoorthy's modified Duncan polynomials

```
<< LinearAlgebra`Orthogonalization`

L =.; rs =.; el =.; elw =.; gj =.; y =.; mm =. ; ee =.; rr =.;

n = 10;
yp = Table[0, {i, 1, n}];
Do[
 Print[yp[[i]] =
   1 / 6 * (i + 2) (i + 3) * x^ (i + 1) - 1 / 3 * i * (i + 3) * x^ (i + 2) + 1 / 6 * i * (i + 1) * x^ (i + 3)]
 ,
 {i,
  1,
  n}]

ot = GramSchmidt[yp, InnerProduct Æ (Integrate[#1 #2, {x, 0, 1}] &)];


Do[
 sc = ot[[i]] /. x Æ 1;
 Print[p[i] = Expand[ot[[i]] / (sc)]]
 , {i, 1, n}]
Do[
        Print[p[i] = p[i] /. x -> x / L] // Simplify;
        , {i, 1, n}]

L = 1.016;
Plot[{p[1], p[2], p[3], p[4], p[5]}, {x, 0, L}]
L =.;
Do[
        pr[i] = -p[i];
        , {i, 1, n}]

t1 = TimeUsed[]
Do[pd1[i] = D[p[i], x], {i, 1, n}]
Do[pd2[i] = D[pd1[i], x], {i, 1, n}]

Do[pd1r[i] = D[pr[i], x], {i, 1, n}]
Do[pd2r[i] = D[pd1r[i], x], {i, 1, n}]
```

```
k = Table[0, {i, 1, 2*n}, {j, 1, 2*n}];

Do[Do[
  kp = pd1[i]*pd1[j] /. x Æ 0;
  k[[i, j]] = el*Integrate[pd2[i]*pd2[j], {x, 0, L}]
    + mm*rs^2*Integrate[Integrate[y, {y, x, L}]*pd1[i]*pd1[j], {x, 0, L}]
      + 1./2.*ks*kp
       , {j, i, n}], {i, 1, n}]

Do[Do[
  k[[i, n + j]] =
   -mm*rs^2*Integrate[Integrate[y, {y, x, L}]*ee*pd1[i]*pd1r[j], {x, 0, L}]
     , {j, i, n}], {i, 1, n}]

Do[Do[
         kp = pd1r[i]*pd1r[j] /. x Æ 0;
        k[[n + i, n + j]] = elw*Integrate[pd2r[i]*pd2r[j], {x, 0, L}]
          + gj*Integrate[pd1r[i]*pd1r[j], {x, 0, L}]
             +
    mm*rs^2*(ee^2 + rr^2)*Integrate[Integrate[y, {y, x, L}]*pd1r[i]*pd1r[j]
      , {x, 0, L}]
    + 1./2.*ks*kp
                , {j, i, n}], {i, 1, n}]

Do[
Do[
    k[[i, j]] = k[[j, i]]
    , {j, 1, i - 1}]
, {i, 2, 2*n}]



MatrixForm[k]
```

```
mt = Table[0, {i, 1, 2 * n}, {j, 1, 2 * n}];



Do[Do[

    mt[[i, j]] = mm * Integrate[p[i] * p[j], {x, 0, L}];
    , {j, i, n}], {i, 1, n}]

Do[Do[
        mt[[i, n + j]] = -mm * ee * Integrate[p[i] * pr[j], {x, 0, L}]
                    , {j, 1, n}], {i, 1, n}]

Do[Do[
        mt[[n + i, n + j]] = mm * (ee^2 + rr^2) * Integrate[pr[i] * pr[j], {x, 0, L}];
            , {j, i, n}], {i, 1, n}]


Do[Do[
    mt[[i, j]] = mt[[j, i]]
    , {j, 1, i - 1}]
, {i, 2, 2 * n}]

MatrixForm[mt]


L = 1.016;
rs =.;

el = 97.1628;
elw = 5.9388 10^ -3;
gj = 1.4189 10^ -1;
y =.
mm = 0.10472;
ee = 0.02187;
rr = Sqrt[(5.4197 10^ -12) / (4.032 10^ -5)]


rs = 0;
mtk = Inverse[mt].k;

ev = N[Eigenvalues[mtk]^(1 / 2)] / (2 * Pi)

MatrixForm[evt = Eigenvectors[mtk]];
t2 = TimeUsed[];
Print["CPU Time Used is", t2 - t1, "sec"];


Print["Rotating Speed = ", rs = 10, " radian/sec"]
Print["               = ", N[rs / (2 * Pi)], " rev/sec"]
mtk = Inverse[mt].k;

ev = N[Eigenvalues[mtk]^(1 / 2)] / (2 * Pi)
    rs =.
```

```
ks = 10^7;
Print["Rotating Speed = ", rs = 5, " rev/sec"]
Print["               = ", N[rs = rs * (2 * Pi)], " rad/sec"]
mtk = Inverse[mt].k;

{ev, evt} = Eigensystem[mtk];
evalue = N[ev^ (1 / 2) / (2 * Pi)]

Print["Rotating Speed = ", rs = 15, " rev/sec"]
Print["               = ", N[rs = rs * (2 * Pi)], " rad/sec"]
mtk = Inverse[mt].k;

{ev, evt} = Eigensystem[mtk];
evalue = N[ev^ (1 / 2) / (2 * Pi)]

ks = 10^7;
Print["Rotating Speed = ", rs = 20, " rev/sec"]
Print["               = ", N[rs = rs * (2 * Pi)], " rad/sec"]
mtk = Inverse[mt].k;

{ev, evt} = Eigensystem[mtk];
evalue = N[ev^ (1 / 2) / (2 * Pi)]

Print["Rotating Speed = ", rs = 10, " rev/sec"]
Print["               = ", N[rs = rs * (2 * Pi)], " rad/sec"]
mtk = Inverse[mt].k;

{ev, evt} = Eigensystem[mtk];
evalue = N[ev^ (1 / 2) / (2 * Pi)]


tbc = Table[0, {i, 1, 51}, {j, 1, 3}];
Do[md[i] = 0;
 md2[i] = 0;
 Do[md2[i] += pr[j] * evt[[i, n + j]];
  md[i] += p[j] * evt[[i, j]];, {j, 1, n}];
 ki = 2 * n - i + 1;
 str = Print["Mode", ki, "  w=", N[ev[[i]]^(1 / 2) / (2 * Pi)]];
 md[i] =
  Expand[Simplify[Normalize[md[i], InnerProduct Æ (Integrate[#1 #2, {x, 0, L}] &)]]];
 md2[i] = Expand[Simplify[Normalize[md2[i],
     InnerProduct Æ (Integrate[#1 #2, {x, 0, L}] &)]]];
 gp[ki] = Plot[md[i], {x, 0, L}, AxesLabel Æ {"x", "v"},
   GridLines Æ Automatic, PlotRange Æ All];
 kc = 0;
 Do[kc++;
  tbc[[kc, 1]] = xi;
  tbc[[kc, 2]] = md[i] /. x Æ xi;
  tbc[[kc, 3]] = md2[i] /. x Æ xi;
  , {xi, 0, 1.016, 1.016 / 50}];
 Print[MatrixForm[tbc]];
 gp2[ki] = Plot[md2[i], {x, 0, L},
   AxesLabel Æ {"x", "Theta"}, GridLines Æ Automatic, PlotRange Æ All];
 , {i, 2 * n, 2 * n - 5, -1}]
```

Appendix B

MATHEMATICA Matrix Output

a) Stiffness matrix obtained for rotating bending - torsion coupled beam by Rayleigh Ritz method using Karunamoorthy's modified Duncan polynomials. (5 polynomials are used)

$$\begin{pmatrix}
\frac{16ei}{5L^3}+\frac{122}{405}L\,mm\,rs^2 & -\frac{544ei}{285L^3}+\frac{478Lmmrs^2}{2565} & \frac{2752ei}{2499L^3}-\frac{130006Lmmrs^2}{562275} & -\frac{17936ei}{24269L^3}+\frac{9301462Lmmrs^2}{60065775} \\
-\frac{544ei}{285L^3}+\frac{478Lmmrs^2}{2565} & \frac{264944ei}{1805L^3}+\frac{110114Lmmrs^2}{59565} & -\frac{1549712ei}{15827L^3}-\frac{188998Lmmrs^2}{1187025} & \frac{32065408ai}{461111L^3}-\frac{10935915eLmmrs^2}{126805525} \\
\frac{2752ei}{2499L^3}-\frac{130006Lmmrs^2}{562275} & -\frac{1549712ei}{15827L^3}-\frac{188998Lmmrs^2}{1187025} & \frac{124047248ei}{99127L^3}+\frac{20923562Lmmrs^2}{3865953} & -\frac{11194242812ei}{144440055L^3}-\frac{46690866Lmmrs^2}{31768121} \\
-\frac{17936ei}{24269L^3}+\frac{9301462Lmmrs^2}{60065775} & \frac{32065408ai}{461111L^3}-\frac{10935915eLmmrs^2}{126805525} & -\frac{11194242812ei}{144440055L^3}-\frac{46690866Lmmrs^2}{31768121} & \frac{2156981073806ei}{4627734265L^3}+\frac{4240959862Lmmrs^2}{420703115} \\
\frac{15408ei}{28631L^3}-\frac{8621674Lmmrs^2}{70861725} & -\frac{28377344ai}{543989L^3}+\frac{98714558Lmmrs^2}{149596975} & \frac{16854492384ei}{23849623L^3}-\frac{3174978Lmmrs^2}{2204587} & -\frac{1102242723003688ei}{38216515645L^3}-\frac{351764866Lmmrs^2}{99263677}
\end{pmatrix}$$

$$\begin{pmatrix}
\frac{122}{405}ee\,L\,mm\,rs^2 & 0 & 0 & 0 \\
\frac{478eeLmmrs^2}{2565} & \frac{110114eeLmmrs^2}{59565} & 0 & 0 \\
-\frac{130006eeLmmrs^2}{562275} & -\frac{188998eeLmmrs^2}{1187025} & \frac{20923562eeLmmrs^2}{3865953} & 0 \\
\frac{9301462eeLmmrs^2}{60065775} & -\frac{10935915eeLmmrs^2}{126805525} & -\frac{46690866eeLmmrs^2}{31768121} & \frac{4240959862eeLmmrs^2}{420703115} \\
-\frac{8621674eeLmmrs^2}{70861725} & \frac{98714558eeLmmrs^2}{149596975} & -\frac{3174978eeLmmrs^2}{2204587} & -\frac{351764866eeLmmrs^2}{99263677}
\end{pmatrix}$$

$$\begin{pmatrix}
\frac{15408ei}{28631L^3}-\frac{8621674Lmmrs^2}{70861725} & \frac{122}{405}ee\,L\,mm\,rs^2 & \frac{478eeLmmrs^2}{2565} \\
-\frac{28377344ai}{543989L^3}+\frac{98714558Lmmrs^2}{149596975} & 0 & \frac{110114eeLmmrs^2}{59565} \\
\frac{16854492384ei}{23849623L^3}-\frac{3174978Lmmrs^2}{2204587} & 0 & 0 \\
-\frac{1102242723003688ei}{38216515645L^3}-\frac{351764866Lmmrs^2}{99263677} & 0 & 0 \\
\frac{111425702445872ei}{9017075771L^3}+\frac{2140941765461mmrs^2}{13935480737} & 0 & 0 \\
0 & \frac{16eiw}{5L^3}+\frac{8gi}{7L}+\frac{122}{405}L\,mm\,(ee^2+rr^2)\,rs^2 & -\frac{544eiw}{285L^3}+\frac{243gi}{133L}+\frac{478Lmm\,(ee^2+rr^2)\,rs^2}{2565} \\
0 & -\frac{544eiw}{285L^3}+\frac{243gi}{133L}+\frac{478Lmm\,(ee^2+rr^2)\,rs^2}{2565} & \frac{264944eiw}{1805L^3}+\frac{189610gi}{22743L}+\frac{110114Lmm\,(ee^2+rr^2)\,rs^2}{59565} \\
0 & \frac{2752eiw}{2499L^3}+\frac{6577gi}{7497L}-\frac{130006Lmm\,(ee^2+rr^2)\,rs^2}{562275} & -\frac{1549712eiw}{15827L^3}+\frac{3562568gi}{712215L}-\frac{188998Lmm\,(ee^2+rr^2)\,rs^2}{1187025} \\
0 & -\frac{17936eiw}{24269L^3}+\frac{1792846gi}{1092105L}+\frac{9301462Lmm\,(ee^2+rr^2)\,rs^2}{60065775} & \frac{32065408aiw}{461111L^3}+\frac{218474028gi}{76083315L}-\frac{10935915eLmm\,(ee^2+rr^2)\,rs^2}{126805525} \\
\frac{2140941765461eeLmmrs^2}{13935480737} & \frac{15408eiw}{28631L^3}+\frac{2159870gi}{19841283L}-\frac{8621674Lmm\,(ee^2+rr^2)\,rs^2}{70861725} & -\frac{28377344aiw}{543989L^3}+\frac{1927287114gi}{33068805L}+\frac{98714558Lmm\,(ee^2+rr^2)\,rs^2}{149596975}
\end{pmatrix}$$

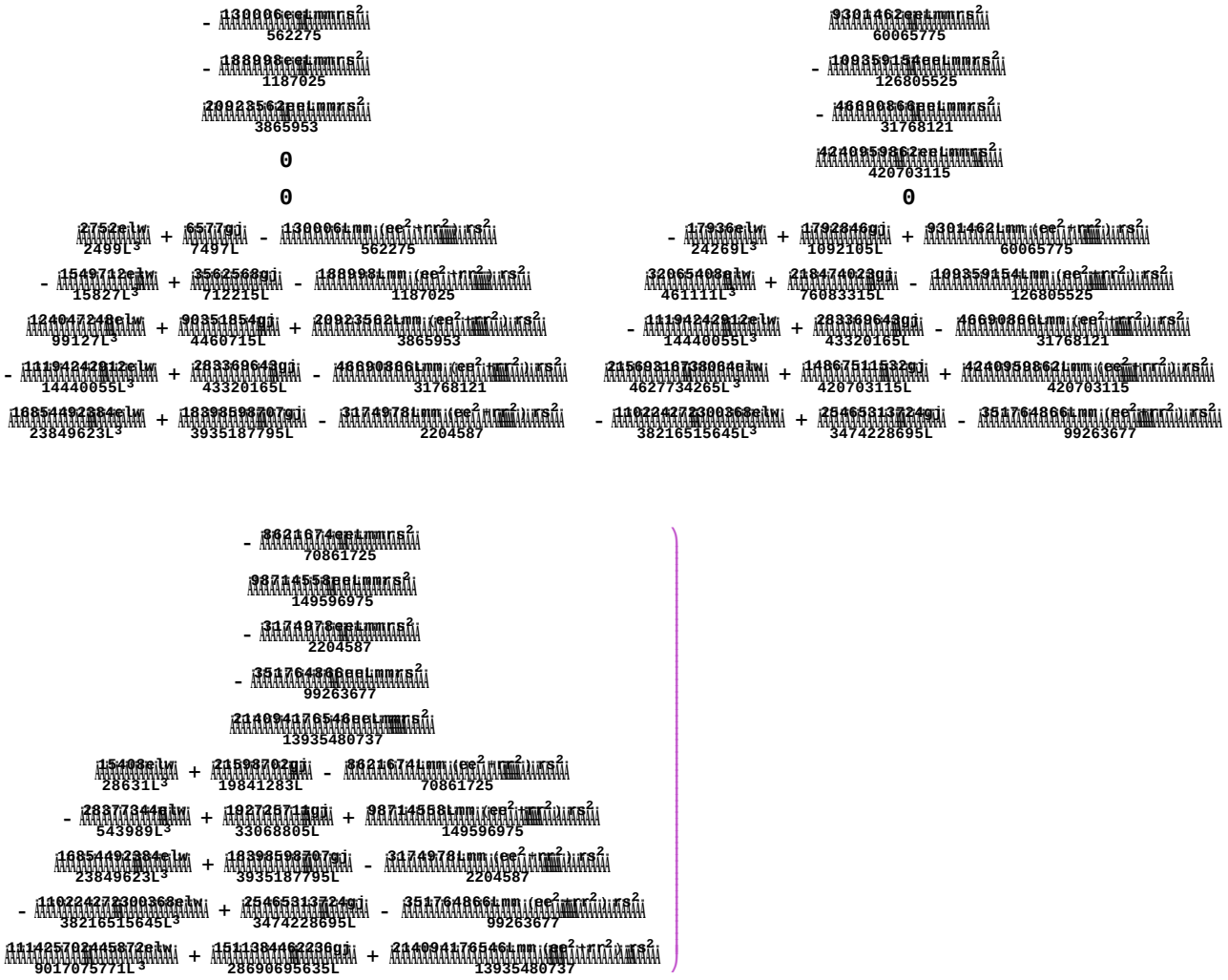

b) Mass matrix obtained for rotating bending - torsion coupled beam by Rayleigh Ritz method using Karunamoorthy's modified Duncan polynomials. (5 polynomials are used)

$$\begin{pmatrix}
\frac{104\,L\,mm}{405} & 0 & 0 & 0 & 0 & \frac{104\,ee\,L\,mm}{405} & 0 \\
0 & \frac{16952\,L\,mm}{59565} & 0 & 0 & 0 & 0 & \frac{16952\,ee\,L\,mm}{59565} \\
0 & 0 & \frac{1109704\,L\,mm}{3865953} & 0 & 0 & 0 & 0 \\
0 & 0 & 0 & \frac{108948424\,L\,mm}{420703115} & 0 & 0 & 0 \\
0 & 0 & 0 & 0 & \frac{3230173544\,L\,mm}{13935480737} & 0 & 0 \\
\frac{104\,ee\,L\,mm}{405} & 0 & 0 & 0 & 0 & \frac{104}{405}\,L\,mm\,(ee^2+rr^2) & 0 \\
0 & \frac{16952\,ee\,L\,mm}{59565} & 0 & 0 & 0 & 0 & \frac{16952\,L\,mm\,(ee^2+rr^2)}{59565} \\
0 & 0 & \frac{1109704\,ee\,L\,mm}{3865953} & 0 & 0 & 0 & 0 \\
0 & 0 & 0 & \frac{108948424\,ee\,L\,mm}{420703115} & 0 & 0 & 0 \\
0 & 0 & 0 & 0 & \frac{3230173544\,ee\,L\,mm}{13935480737} & 0 & 0
\end{pmatrix}$$

$$\begin{pmatrix}
0 & 0 & 0 \\
0 & 0 & 0 \\
\frac{1109704\,ee\,L\,mm}{3865953} & 0 & 0 \\
0 & \frac{108948424\,ee\,L\,mm}{420703115} & 0 \\
0 & 0 & \frac{3230173544\,ee\,L\,mm}{13935480737} \\
0 & 0 & 0 \\
0 & 0 & 0 \\
\frac{1109704\,L\,mm\,(ee^2+rr^2)}{3865953} & 0 & 0 \\
0 & \frac{108948424\,L\,mm\,(ee^2+rr^2)}{420703115} & 0 \\
0 & 0 & \frac{3230173544\,L\,mm\,(ee^2+rr^2)}{13935480737}
\end{pmatrix}$$

Appendix C

NASTRAN Input

```
$ Normal Modes Analysis, Database
TIME 10
DIAG 8
SOL 103
CEND
$
SUBTITLE=R Center at the centroid
Label=Channel Beam BSROEU
$
$SEALL = ALL
$SUPER = ALL
$ECHO = NONE
$MAXLINES = 999999999
$SUBCASE 1
$ Subcase name : Default
SPC=1
load=232
VECTOR(SORT1,REAL)=ALL
SPCFORCES(SORT1,REAL)=ALL
$DISPLACEMENT=ALL
$ Static Analysis
subcase 100
   load=232
   elforce=all
$ Dynamic Analysis
subcase 200
   statsub=100
   METHOD=1
$
BEGIN BULK
$PARAM    POST    -1
$PARAM    PATVER  3.
$PARAM    AUTOSPC YES
$PARAM   COUPMASS -1
$PARAM    K6ROT   0.
$PARAM    WTMASS  1.
$PARAM,NOCOMPS,-1
$PARAM   PRTMAXIM YES
param   autospc yes
param,  post,   -1
$       2#      3#      4#      5#      6#      7#      8#
$
EIGRL    1                        20
$ Rotation Effect
$       2#      3#      4#      5#      6#      7#      8#
RFORCE  232     1500            0.00001 0.      1.      0.
GRID   1500         0.     0.     0.01016
$ Elements and Element Properties for region : pshell.900
$       2#      3#      4#      5#      6#      7#      8#
PSHELL   900     800     6.35-4  800             800
$ Description of Material :
$       2#      3#      4#      5#      6#      7#      8#
$$MAT1    800             6.89+10         2.618+10        .316
MAT1    800         6.89+10      2.618+10.316  2597.
$$ Pset: "pshell.900" will be imported as: "pshell.900"
CQUAD4   1       900     1101    1102    1202    1201    0.      0.
CQUAD4   2       900     1102    1103    1203    1202    0.      0.
CQUAD4   3       900     1103    1104    1204    1203    0.      0.
CQUAD4   4       900     1104    1105    1205    1204    0.      0.
CQUAD4   5       900     1105    1106    1206    1205    0.      0.
CQUAD4   6       900     1106    1107    1207    1206    0.      0.
CQUAD4   7       900     1107    1108    1208    1207    0.      0.
CQUAD4   8       900     1108    1109    1209    1208    0.      0.
```

```
CQUAD4   9       900     1109    1110    1210    1209    0.      0.
CQUAD4   10      900     1110    1111    1211    1210    0.      0.
CQUAD4   11      900     1111    1112    1212    1211    0.      0.
CQUAD4   12      900     1112    1113    1213    1212    0.      0.
CQUAD4   13      900     1113    1114    1214    1213    0.      0.
CQUAD4   14      900     1114    1115    1215    1214    0.      0.
CQUAD4   15      900     1115    1116    1216    1215    0.      0.
CQUAD4   16      900     1116    1117    1217    1216    0.      0.
CQUAD4   17      900     1117    1118    1218    1217    0.      0.
CQUAD4   18      900     1118    1119    1219    1218    0.      0.
CQUAD4   19      900     1119    1120    1220    1219    0.      0.
CQUAD4   20      900     1120    1121    1221    1220    0.      0.
CQUAD4   21      900     1121    1122    1222    1221    0.      0.
CQUAD4   22      900     1122    1123    1223    1222    0.      0.
CQUAD4   23      900     1123    1124    1224    1223    0.      0.
CQUAD4   24      900     1124    1125    1225    1224    0.      0.
CQUAD4   25      900     1125    1126    1226    1225    0.      0.
CQUAD4   26      900     1126    1127    1227    1226    0.      0.
CQUAD4   27      900     1127    1128    1228    1227    0.      0.
CQUAD4   28      900     1128    1129    1229    1228    0.      0.
CQUAD4   29      900     1129    1130    1230    1229    0.      0.
CQUAD4   30      900     1130    1131    1231    1230    0.      0.
CQUAD4   31      900     1131    1132    1232    1231    0.      0.
CQUAD4   32      900     1132    1133    1233    1232    0.      0.
CQUAD4   33      900     1133    1134    1234    1233    0.      0.
CQUAD4   34      900     1134    1135    1235    1234    0.      0.
CQUAD4   35      900     1135    1136    1236    1235    0.      0.
CQUAD4   36      900     1136    1137    1237    1236    0.      0.
CQUAD4   37      900     1137    1138    1238    1237    0.      0.
CQUAD4   38      900     1138    1139    1239    1238    0.      0.
CQUAD4   39      900     1139    1140    1240    1239    0.      0.
CQUAD4   40      900     1140    1141    1241    1240    0.      0.
CQUAD4   41      900     1141    1142    1242    1241    0.      0.
CQUAD4   42      900     1142    1143    1243    1242    0.      0.
CQUAD4   43      900     1143    1144    1244    1243    0.      0.
CQUAD4   44      900     1144    1145    1245    1244    0.      0.
CQUAD4   45      900     1145    1146    1246    1245    0.      0.
CQUAD4   46      900     1146    1147    1247    1246    0.      0.
CQUAD4   47      900     1147    1148    1248    1247    0.      0.
CQUAD4   48      900     1148    1149    1249    1248    0.      0.
CQUAD4   49      900     1149    1150    1250    1249    0.      0.
CQUAD4   50      900     1201    1202    1302    1301    0.      0.
CQUAD4   51      900     1202    1203    1303    1302    0.      0.
CQUAD4   52      900     1203    1204    1304    1303    0.      0.
CQUAD4   53      900     1204    1205    1305    1304    0.      0.
CQUAD4   54      900     1205    1206    1306    1305    0.      0.
CQUAD4   55      900     1206    1207    1307    1306    0.      0.
CQUAD4   56      900     1207    1208    1308    1307    0.      0.
CQUAD4   57      900     1208    1209    1309    1308    0.      0.
CQUAD4   58      900     1209    1210    1310    1309    0.      0.
CQUAD4   59      900     1210    1211    1311    1310    0.      0.
CQUAD4   60      900     1211    1212    1312    1311    0.      0.
CQUAD4   61      900     1212    1213    1313    1312    0.      0.
CQUAD4   62      900     1213    1214    1314    1313    0.      0.
CQUAD4   63      900     1214    1215    1315    1314    0.      0.
CQUAD4   64      900     1215    1216    1316    1315    0.      0.
CQUAD4   65      900     1216    1217    1317    1316    0.      0.
CQUAD4   66      900     1217    1218    1318    1317    0.      0.
CQUAD4   67      900     1218    1219    1319    1318    0.      0.
CQUAD4   68      900     1219    1220    1320    1319    0.      0.
CQUAD4   69      900     1220    1221    1321    1320    0.      0.
CQUAD4   70      900     1221    1222    1322    1321    0.      0.
CQUAD4   71      900     1222    1223    1323    1322    0.      0.
```

```
CQUAD4   72      900     1223    1224    1324    1323    0.      0.
CQUAD4   73      900     1224    1225    1325    1324    0.      0.
CQUAD4   74      900     1225    1226    1326    1325    0.      0.
CQUAD4   75      900     1226    1227    1327    1326    0.      0.
CQUAD4   76      900     1227    1228    1328    1327    0.      0.
CQUAD4   77      900     1228    1229    1329    1328    0.      0.
CQUAD4   78      900     1229    1230    1330    1329    0.      0.
CQUAD4   79      900     1230    1231    1331    1330    0.      0.
CQUAD4   80      900     1231    1232    1332    1331    0.      0.
CQUAD4   81      900     1232    1233    1333    1332    0.      0.
CQUAD4   82      900     1233    1234    1334    1333    0.      0.
CQUAD4   83      900     1234    1235    1335    1334    0.      0.
CQUAD4   84      900     1235    1236    1336    1335    0.      0.
CQUAD4   85      900     1236    1237    1337    1336    0.      0.
CQUAD4   86      900     1237    1238    1338    1337    0.      0.
CQUAD4   87      900     1238    1239    1339    1338    0.      0.
CQUAD4   88      900     1239    1240    1340    1339    0.      0.
CQUAD4   89      900     1240    1241    1341    1340    0.      0.
CQUAD4   90      900     1241    1242    1342    1341    0.      0.
CQUAD4   91      900     1242    1243    1343    1342    0.      0.
CQUAD4   92      900     1243    1244    1344    1343    0.      0.
CQUAD4   93      900     1244    1245    1345    1344    0.      0.
CQUAD4   94      900     1245    1246    1346    1345    0.      0.
CQUAD4   95      900     1246    1247    1347    1346    0.      0.
CQUAD4   96      900     1247    1248    1348    1347    0.      0.
CQUAD4   97      900     1248    1249    1349    1348    0.      0.
CQUAD4   98      900     1249    1250    1350    1349    0.      0.
CQUAD4   99      900     1301    1302    1402    1401    0.      0.
CQUAD4   100     900     1302    1303    1403    1402    0.      0.
CQUAD4   101     900     1303    1304    1404    1403    0.      0.
CQUAD4   102     900     1304    1305    1405    1404    0.      0.
CQUAD4   103     900     1305    1306    1406    1405    0.      0.
CQUAD4   104     900     1306    1307    1407    1406    0.      0.
CQUAD4   105     900     1307    1308    1408    1407    0.      0.
CQUAD4   106     900     1308    1309    1409    1408    0.      0.
CQUAD4   107     900     1309    1310    1410    1409    0.      0.
CQUAD4   108     900     1310    1311    1411    1410    0.      0.
CQUAD4   109     900     1311    1312    1412    1411    0.      0.
CQUAD4   110     900     1312    1313    1413    1412    0.      0.
CQUAD4   111     900     1313    1314    1414    1413    0.      0.
CQUAD4   112     900     1314    1315    1415    1414    0.      0.
CQUAD4   113     900     1315    1316    1416    1415    0.      0.
CQUAD4   114     900     1316    1317    1417    1416    0.      0.
CQUAD4   115     900     1317    1318    1418    1417    0.      0.
CQUAD4   116     900     1318    1319    1419    1418    0.      0.
CQUAD4   117     900     1319    1320    1420    1419    0.      0.
CQUAD4   118     900     1320    1321    1421    1420    0.      0.
CQUAD4   119     900     1321    1322    1422    1421    0.      0.
CQUAD4   120     900     1322    1323    1423    1422    0.      0.
CQUAD4   121     900     1323    1324    1424    1423    0.      0.
CQUAD4   122     900     1324    1325    1425    1424    0.      0.
CQUAD4   123     900     1325    1326    1426    1425    0.      0.
CQUAD4   124     900     1326    1327    1427    1426    0.      0.
CQUAD4   125     900     1327    1328    1428    1427    0.      0.
CQUAD4   126     900     1328    1329    1429    1428    0.      0.
CQUAD4   127     900     1329    1330    1430    1429    0.      0.
CQUAD4   128     900     1330    1331    1431    1430    0.      0.
CQUAD4   129     900     1331    1332    1432    1431    0.      0.
CQUAD4   130     900     1332    1333    1433    1432    0.      0.
CQUAD4   131     900     1333    1334    1434    1433    0.      0.
CQUAD4   132     900     1334    1335    1435    1434    0.      0.
CQUAD4   133     900     1335    1336    1436    1435    0.      0.
CQUAD4   134     900     1336    1337    1437    1436    0.      0.
```

```
CQUAD4   135     900     1337    1338    1438    1437    0.      0.
CQUAD4   136     900     1338    1339    1439    1438    0.      0.
CQUAD4   137     900     1339    1340    1440    1439    0.      0.
CQUAD4   138     900     1340    1341    1441    1440    0.      0.
CQUAD4   139     900     1341    1342    1442    1441    0.      0.
CQUAD4   140     900     1342    1343    1443    1442    0.      0.
CQUAD4   141     900     1343    1344    1444    1443    0.      0.
CQUAD4   142     900     1344    1345    1445    1444    0.      0.
CQUAD4   143     900     1345    1346    1446    1445    0.      0.
CQUAD4   144     900     1346    1347    1447    1446    0.      0.
CQUAD4   145     900     1347    1348    1448    1447    0.      0.
CQUAD4   146     900     1348    1349    1449    1448    0.      0.
CQUAD4   147     900     1349    1350    1450    1449    0.      0.
CQUAD4   148     900     1401    1402    1502    1501    0.      0.
CQUAD4   149     900     1402    1403    1503    1502    0.      0.
CQUAD4   150     900     1403    1404    1504    1503    0.      0.
CQUAD4   151     900     1404    1405    1505    1504    0.      0.
CQUAD4   152     900     1405    1406    1506    1505    0.      0.
CQUAD4   153     900     1406    1407    1507    1506    0.      0.
CQUAD4   154     900     1407    1408    1508    1507    0.      0.
CQUAD4   155     900     1408    1409    1509    1508    0.      0.
CQUAD4   156     900     1409    1410    1510    1509    0.      0.
CQUAD4   157     900     1410    1411    1511    1510    0.      0.
CQUAD4   158     900     1411    1412    1512    1511    0.      0.
CQUAD4   159     900     1412    1413    1513    1512    0.      0.
CQUAD4   160     900     1413    1414    1514    1513    0.      0.
CQUAD4   161     900     1414    1415    1515    1514    0.      0.
CQUAD4   162     900     1415    1416    1516    1515    0.      0.
CQUAD4   163     900     1416    1417    1517    1516    0.      0.
CQUAD4   164     900     1417    1418    1518    1517    0.      0.
CQUAD4   165     900     1418    1419    1519    1518    0.      0.
CQUAD4   166     900     1419    1420    1520    1519    0.      0.
CQUAD4   167     900     1420    1421    1521    1520    0.      0.
CQUAD4   168     900     1421    1422    1522    1521    0.      0.
CQUAD4   169     900     1422    1423    1523    1522    0.      0.
CQUAD4   170     900     1423    1424    1524    1523    0.      0.
CQUAD4   171     900     1424    1425    1525    1524    0.      0.
CQUAD4   172     900     1425    1426    1526    1525    0.      0.
CQUAD4   173     900     1426    1427    1527    1526    0.      0.
CQUAD4   174     900     1427    1428    1528    1527    0.      0.
CQUAD4   175     900     1428    1429    1529    1528    0.      0.
CQUAD4   176     900     1429    1430    1530    1529    0.      0.
CQUAD4   177     900     1430    1431    1531    1530    0.      0.
CQUAD4   178     900     1431    1432    1532    1531    0.      0.
CQUAD4   179     900     1432    1433    1533    1532    0.      0.
CQUAD4   180     900     1433    1434    1534    1533    0.      0.
CQUAD4   181     900     1434    1435    1535    1534    0.      0.
CQUAD4   182     900     1435    1436    1536    1535    0.      0.
CQUAD4   183     900     1436    1437    1537    1536    0.      0.
CQUAD4   184     900     1437    1438    1538    1537    0.      0.
CQUAD4   185     900     1438    1439    1539    1538    0.      0.
CQUAD4   186     900     1439    1440    1540    1539    0.      0.
CQUAD4   187     900     1440    1441    1541    1540    0.      0.
CQUAD4   188     900     1441    1442    1542    1541    0.      0.
CQUAD4   189     900     1442    1443    1543    1542    0.      0.
CQUAD4   190     900     1443    1444    1544    1543    0.      0.
CQUAD4   191     900     1444    1445    1545    1544    0.      0.
CQUAD4   192     900     1445    1446    1546    1545    0.      0.
CQUAD4   193     900     1446    1447    1547    1546    0.      0.
CQUAD4   194     900     1447    1448    1548    1547    0.      0.
CQUAD4   195     900     1448    1449    1549    1548    0.      0.
CQUAD4   196     900     1449    1450    1550    1549    0.      0.
CQUAD4   197     900     1501    1502    1602    1601    0.      0.
```

```
CQUAD4   198     900     1502    1503    1603    1602    0.      0.
CQUAD4   199     900     1503    1504    1604    1603    0.      0.
CQUAD4   200     900     1504    1505    1605    1604    0.      0.
CQUAD4   201     900     1505    1506    1606    1605    0.      0.
CQUAD4   202     900     1506    1507    1607    1606    0.      0.
CQUAD4   203     900     1507    1508    1608    1607    0.      0.
CQUAD4   204     900     1508    1509    1609    1608    0.      0.
CQUAD4   205     900     1509    1510    1610    1609    0.      0.
CQUAD4   206     900     1510    1511    1611    1610    0.      0.
CQUAD4   207     900     1511    1512    1612    1611    0.      0.
CQUAD4   208     900     1512    1513    1613    1612    0.      0.
CQUAD4   209     900     1513    1514    1614    1613    0.      0.
CQUAD4   210     900     1514    1515    1615    1614    0.      0.
CQUAD4   211     900     1515    1516    1616    1615    0.      0.
CQUAD4   212     900     1516    1517    1617    1616    0.      0.
CQUAD4   213     900     1517    1518    1618    1617    0.      0.
CQUAD4   214     900     1518    1519    1619    1618    0.      0.
CQUAD4   215     900     1519    1520    1620    1619    0.      0.
CQUAD4   216     900     1520    1521    1621    1620    0.      0.
CQUAD4   217     900     1521    1522    1622    1621    0.      0.
CQUAD4   218     900     1522    1523    1623    1622    0.      0.
CQUAD4   219     900     1523    1524    1624    1623    0.      0.
CQUAD4   220     900     1524    1525    1625    1624    0.      0.
CQUAD4   221     900     1525    1526    1626    1625    0.      0.
CQUAD4   222     900     1526    1527    1627    1626    0.      0.
CQUAD4   223     900     1527    1528    1628    1627    0.      0.
CQUAD4   224     900     1528    1529    1629    1628    0.      0.
CQUAD4   225     900     1529    1530    1630    1629    0.      0.
CQUAD4   226     900     1530    1531    1631    1630    0.      0.
CQUAD4   227     900     1531    1532    1632    1631    0.      0.
CQUAD4   228     900     1532    1533    1633    1632    0.      0.
CQUAD4   229     900     1533    1534    1634    1633    0.      0.
CQUAD4   230     900     1534    1535    1635    1634    0.      0.
CQUAD4   231     900     1535    1536    1636    1635    0.      0.
CQUAD4   232     900     1536    1537    1637    1636    0.      0.
CQUAD4   233     900     1537    1538    1638    1637    0.      0.
CQUAD4   234     900     1538    1539    1639    1638    0.      0.
CQUAD4   235     900     1539    1540    1640    1639    0.      0.
CQUAD4   236     900     1540    1541    1641    1640    0.      0.
CQUAD4   237     900     1541    1542    1642    1641    0.      0.
CQUAD4   238     900     1542    1543    1643    1642    0.      0.
CQUAD4   239     900     1543    1544    1644    1643    0.      0.
CQUAD4   240     900     1544    1545    1645    1644    0.      0.
CQUAD4   241     900     1545    1546    1646    1645    0.      0.
CQUAD4   242     900     1546    1547    1647    1646    0.      0.
CQUAD4   243     900     1547    1548    1648    1647    0.      0.
CQUAD4   244     900     1548    1549    1649    1648    0.      0.
CQUAD4   245     900     1549    1550    1650    1649    0.      0.
CQUAD4   246     900     1601    1602    1702    1701    0.      0.
CQUAD4   247     900     1602    1603    1703    1702    0.      0.
CQUAD4   248     900     1603    1604    1704    1703    0.      0.
CQUAD4   249     900     1604    1605    1705    1704    0.      0.
CQUAD4   250     900     1605    1606    1706    1705    0.      0.
CQUAD4   251     900     1606    1607    1707    1706    0.      0.
CQUAD4   252     900     1607    1608    1708    1707    0.      0.
CQUAD4   253     900     1608    1609    1709    1708    0.      0.
CQUAD4   254     900     1609    1610    1710    1709    0.      0.
CQUAD4   255     900     1610    1611    1711    1710    0.      0.
CQUAD4   256     900     1611    1612    1712    1711    0.      0.
CQUAD4   257     900     1612    1613    1713    1712    0.      0.
CQUAD4   258     900     1613    1614    1714    1713    0.      0.
CQUAD4   259     900     1614    1615    1715    1714    0.      0.
CQUAD4   260     900     1615    1616    1716    1715    0.      0.
```

```
CQUAD4   261     900     1616    1617    1717    1716    0.      0.
CQUAD4   262     900     1617    1618    1718    1717    0.      0.
CQUAD4   263     900     1618    1619    1719    1718    0.      0.
CQUAD4   264     900     1619    1620    1720    1719    0.      0.
CQUAD4   265     900     1620    1621    1721    1720    0.      0.
CQUAD4   266     900     1621    1622    1722    1721    0.      0.
CQUAD4   267     900     1622    1623    1723    1722    0.      0.
CQUAD4   268     900     1623    1624    1724    1723    0.      0.
CQUAD4   269     900     1624    1625    1725    1724    0.      0.
CQUAD4   270     900     1625    1626    1726    1725    0.      0.
CQUAD4   271     900     1626    1627    1727    1726    0.      0.
CQUAD4   272     900     1627    1628    1728    1727    0.      0.
CQUAD4   273     900     1628    1629    1729    1728    0.      0.
CQUAD4   274     900     1629    1630    1730    1729    0.      0.
CQUAD4   275     900     1630    1631    1731    1730    0.      0.
CQUAD4   276     900     1631    1632    1732    1731    0.      0.
CQUAD4   277     900     1632    1633    1733    1732    0.      0.
CQUAD4   278     900     1633    1634    1734    1733    0.      0.
CQUAD4   279     900     1634    1635    1735    1734    0.      0.
CQUAD4   280     900     1635    1636    1736    1735    0.      0.
CQUAD4   281     900     1636    1637    1737    1736    0.      0.
CQUAD4   282     900     1637    1638    1738    1737    0.      0.
CQUAD4   283     900     1638    1639    1739    1738    0.      0.
CQUAD4   284     900     1639    1640    1740    1739    0.      0.
CQUAD4   285     900     1640    1641    1741    1740    0.      0.
CQUAD4   286     900     1641    1642    1742    1741    0.      0.
CQUAD4   287     900     1642    1643    1743    1742    0.      0.
CQUAD4   288     900     1643    1644    1744    1743    0.      0.
CQUAD4   289     900     1644    1645    1745    1744    0.      0.
CQUAD4   290     900     1645    1646    1746    1745    0.      0.
CQUAD4   291     900     1646    1647    1747    1746    0.      0.
CQUAD4   292     900     1647    1648    1748    1747    0.      0.
CQUAD4   293     900     1648    1649    1749    1748    0.      0.
CQUAD4   294     900     1649    1650    1750    1749    0.      0.
CQUAD4   295     900     1701    1702    1802    1801    0.      0.
CQUAD4   296     900     1702    1703    1803    1802    0.      0.
CQUAD4   297     900     1703    1704    1804    1803    0.      0.
CQUAD4   298     900     1704    1705    1805    1804    0.      0.
CQUAD4   299     900     1705    1706    1806    1805    0.      0.
CQUAD4   300     900     1706    1707    1807    1806    0.      0.
CQUAD4   301     900     1707    1708    1808    1807    0.      0.
CQUAD4   302     900     1708    1709    1809    1808    0.      0.
CQUAD4   303     900     1709    1710    1810    1809    0.      0.
CQUAD4   304     900     1710    1711    1811    1810    0.      0.
CQUAD4   305     900     1711    1712    1812    1811    0.      0.
CQUAD4   306     900     1712    1713    1813    1812    0.      0.
CQUAD4   307     900     1713    1714    1814    1813    0.      0.
CQUAD4   308     900     1714    1715    1815    1814    0.      0.
CQUAD4   309     900     1715    1716    1816    1815    0.      0.
CQUAD4   310     900     1716    1717    1817    1816    0.      0.
CQUAD4   311     900     1717    1718    1818    1817    0.      0.
CQUAD4   312     900     1718    1719    1819    1818    0.      0.
CQUAD4   313     900     1719    1720    1820    1819    0.      0.
CQUAD4   314     900     1720    1721    1821    1820    0.      0.
CQUAD4   315     900     1721    1722    1822    1821    0.      0.
CQUAD4   316     900     1722    1723    1823    1822    0.      0.
CQUAD4   317     900     1723    1724    1824    1823    0.      0.
CQUAD4   318     900     1724    1725    1825    1824    0.      0.
CQUAD4   319     900     1725    1726    1826    1825    0.      0.
CQUAD4   320     900     1726    1727    1827    1826    0.      0.
CQUAD4   321     900     1727    1728    1828    1827    0.      0.
CQUAD4   322     900     1728    1729    1829    1828    0.      0.
CQUAD4   323     900     1729    1730    1830    1829    0.      0.
```

```
CQUAD4   324     900     1730    1731    1831    1830    0.      0.
CQUAD4   325     900     1731    1732    1832    1831    0.      0.
CQUAD4   326     900     1732    1733    1833    1832    0.      0.
CQUAD4   327     900     1733    1734    1834    1833    0.      0.
CQUAD4   328     900     1734    1735    1835    1834    0.      0.
CQUAD4   329     900     1735    1736    1836    1835    0.      0.
CQUAD4   330     900     1736    1737    1837    1836    0.      0.
CQUAD4   331     900     1737    1738    1838    1837    0.      0.
CQUAD4   332     900     1738    1739    1839    1838    0.      0.
CQUAD4   333     900     1739    1740    1840    1839    0.      0.
CQUAD4   334     900     1740    1741    1841    1840    0.      0.
CQUAD4   335     900     1741    1742    1842    1841    0.      0.
CQUAD4   336     900     1742    1743    1843    1842    0.      0.
CQUAD4   337     900     1743    1744    1844    1843    0.      0.
CQUAD4   338     900     1744    1745    1845    1844    0.      0.
CQUAD4   339     900     1745    1746    1846    1845    0.      0.
CQUAD4   340     900     1746    1747    1847    1846    0.      0.
CQUAD4   341     900     1747    1748    1848    1847    0.      0.
CQUAD4   342     900     1748    1749    1849    1848    0.      0.
CQUAD4   343     900     1749    1750    1850    1849    0.      0.
CQUAD4   344     900     1801    1802    1902    1901    0.      0.
CQUAD4   345     900     1802    1803    1903    1902    0.      0.
CQUAD4   346     900     1803    1804    1904    1903    0.      0.
CQUAD4   347     900     1804    1805    1905    1904    0.      0.
CQUAD4   348     900     1805    1806    1906    1905    0.      0.
CQUAD4   349     900     1806    1807    1907    1906    0.      0.
CQUAD4   350     900     1807    1808    1908    1907    0.      0.
CQUAD4   351     900     1808    1809    1909    1908    0.      0.
CQUAD4   352     900     1809    1810    1910    1909    0.      0.
CQUAD4   353     900     1810    1811    1911    1910    0.      0.
CQUAD4   354     900     1811    1812    1912    1911    0.      0.
CQUAD4   355     900     1812    1813    1913    1912    0.      0.
CQUAD4   356     900     1813    1814    1914    1913    0.      0.
CQUAD4   357     900     1814    1815    1915    1914    0.      0.
CQUAD4   358     900     1815    1816    1916    1915    0.      0.
CQUAD4   359     900     1816    1817    1917    1916    0.      0.
CQUAD4   360     900     1817    1818    1918    1917    0.      0.
CQUAD4   361     900     1818    1819    1919    1918    0.      0.
CQUAD4   362     900     1819    1820    1920    1919    0.      0.
CQUAD4   363     900     1820    1821    1921    1920    0.      0.
CQUAD4   364     900     1821    1822    1922    1921    0.      0.
CQUAD4   365     900     1822    1823    1923    1922    0.      0.
CQUAD4   366     900     1823    1824    1924    1923    0.      0.
CQUAD4   367     900     1824    1825    1925    1924    0.      0.
CQUAD4   368     900     1825    1826    1926    1925    0.      0.
CQUAD4   369     900     1826    1827    1927    1926    0.      0.
CQUAD4   370     900     1827    1828    1928    1927    0.      0.
CQUAD4   371     900     1828    1829    1929    1928    0.      0.
CQUAD4   372     900     1829    1830    1930    1929    0.      0.
CQUAD4   373     900     1830    1831    1931    1930    0.      0.
CQUAD4   374     900     1831    1832    1932    1931    0.      0.
CQUAD4   375     900     1832    1833    1933    1932    0.      0.
CQUAD4   376     900     1833    1834    1934    1933    0.      0.
CQUAD4   377     900     1834    1835    1935    1934    0.      0.
CQUAD4   378     900     1835    1836    1936    1935    0.      0.
CQUAD4   379     900     1836    1837    1937    1936    0.      0.
CQUAD4   380     900     1837    1838    1938    1937    0.      0.
CQUAD4   381     900     1838    1839    1939    1938    0.      0.
CQUAD4   382     900     1839    1840    1940    1939    0.      0.
CQUAD4   383     900     1840    1841    1941    1940    0.      0.
CQUAD4   384     900     1841    1842    1942    1941    0.      0.
CQUAD4   385     900     1842    1843    1943    1942    0.      0.
CQUAD4   386     900     1843    1844    1944    1943    0.      0.
```

```
CQUAD4   387     900     1844    1845    1945    1944    0.      0.
CQUAD4   388     900     1845    1846    1946    1945    0.      0.
CQUAD4   389     900     1846    1847    1947    1946    0.      0.
CQUAD4   390     900     1847    1848    1948    1947    0.      0.
CQUAD4   391     900     1848    1849    1949    1948    0.      0.
CQUAD4   392     900     1849    1850    1950    1949    0.      0.
$ Referenced Material Records
$ Material Record : mat1.800
$ Description of Material :
$       2#      3#      4#      5#      6#      7#      8#
$MAT1*    800             6.89+10         2.618+10        .316            *       A
$*      A 2594.
$ Nodes of the Entire Model
GRID     1101            0.      -.00635  .0254
GRID     1102            .02073 -.00635  .0254
GRID     1103            .04147 -.00635  .0254
GRID     1104            .0622  -.00635  .0254
GRID     1105            .08294 -.00635  .0254
GRID     1106            .10367 -.00635  .0254
GRID     1107            .12441 -.00635  .0254
GRID     1108            .14514 -.00635  .0254
GRID     1109            .16588 -.00635  .0254
GRID     1110            .18661 -.00635  .0254
GRID     1111            .20735 -.00635  .0254
GRID     1112            .22808 -.00635  .0254
GRID     1113            .24882 -.00635  .0254
GRID     1114            .26955 -.00635  .0254
GRID     1115            .29029 -.00635  .0254
GRID     1116            .31102 -.00635  .0254
GRID     1117            .33176 -.00635  .0254
GRID     1118            .35249 -.00635  .0254
GRID     1119            .37322 -.00635  .0254
GRID     1120            .39396 -.00635  .0254
GRID     1121            .41469 -.00635  .0254
GRID     1122            .43543 -.00635  .0254
GRID     1123            .45616 -.00635  .0254
GRID     1124            .4769  -.00635  .0254
GRID     1125            .49763 -.00635  .0254
GRID     1126            .51837 -.00635  .0254
GRID     1127            .5391  -.00635  .0254
GRID     1128            .55984 -.00635  .0254
GRID     1129            .58057 -.00635  .0254
GRID     1130            .60131 -.00635  .0254
GRID     1131            .62204 -.00635  .0254
GRID     1132            .64278 -.00635  .0254
GRID     1133            .66351 -.00635  .0254
GRID     1134            .68424 -.00635  .0254
GRID     1135            .70498 -.00635  .0254
GRID     1136            .72571 -.00635  .0254
GRID     1137            .74645 -.00635  .0254
GRID     1138            .76718 -.00635  .0254
GRID     1139            .78792 -.00635  .0254
GRID     1140            .80865 -.00635  .0254
GRID     1141            .82939 -.00635  .0254
GRID     1142            .85012 -.00635  .0254
GRID     1143            .87086 -.00635  .0254
GRID     1144            .89159 -.00635  .0254
GRID     1145            .91233 -.00635  .0254
GRID     1146            .93306 -.00635  .0254
GRID     1147            .9538  -.00635  .0254
GRID     1148            .97453 -.00635  .0254
GRID     1149            .99527 -.00635  .0254
GRID     1150            1.016  -.00635  .0254
```

```
GRID     1201           0.     -.00635  .01693
GRID     1202           .02073 -.00635  .01693
GRID     1203           .04147 -.00635  .01693
GRID     1204           .0622  -.00635  .01693
GRID     1205           .08294 -.00635  .01693
GRID     1206           .10367 -.00635  .01693
GRID     1207           .12441 -.00635  .01693
GRID     1208           .14514 -.00635  .01693
GRID     1209           .16588 -.00635  .01693
GRID     1210           .18661 -.00635  .01693
GRID     1211           .20735 -.00635  .01693
GRID     1212           .22808 -.00635  .01693
GRID     1213           .24882 -.00635  .01693
GRID     1214           .26955 -.00635  .01693
GRID     1215           .29029 -.00635  .01693
GRID     1216           .31102 -.00635  .01693
GRID     1217           .33176 -.00635  .01693
GRID     1218           .35249 -.00635  .01693
GRID     1219           .37322 -.00635  .01693
GRID     1220           .39396 -.00635  .01693
GRID     1221           .41469 -.00635  .01693
GRID     1222           .43543 -.00635  .01693
GRID     1223           .45616 -.00635  .01693
GRID     1224           .4769  -.00635  .01693
GRID     1225           .49763 -.00635  .01693
GRID     1226           .51837 -.00635  .01693
GRID     1227           .5391  -.00635  .01693
GRID     1228           .55984 -.00635  .01693
GRID     1229           .58057 -.00635  .01693
GRID     1230           .60131 -.00635  .01693
GRID     1231           .62204 -.00635  .01693
GRID     1232           .64278 -.00635  .01693
GRID     1233           .66351 -.00635  .01693
GRID     1234           .68424 -.00635  .01693
GRID     1235           .70498 -.00635  .01693
GRID     1236           .72571 -.00635  .01693
GRID     1237           .74645 -.00635  .01693
GRID     1238           .76718 -.00635  .01693
GRID     1239           .78792 -.00635  .01693
GRID     1240           .80865 -.00635  .01693
GRID     1241           .82939 -.00635  .01693
GRID     1242           .85012 -.00635  .01693
GRID     1243           .87086 -.00635  .01693
GRID     1244           .89159 -.00635  .01693
GRID     1245           .91233 -.00635  .01693
GRID     1246           .93306 -.00635  .01693
GRID     1247           .9538  -.00635  .01693
GRID     1248           .97453 -.00635  .01693
GRID     1249           .99527 -.00635  .01693
GRID     1250           1.016  -.00635  .01693
GRID     1301           0.     -.00635  .00847
GRID     1302           .02073 -.00635  .00847
GRID     1303           .04147 -.00635  .00847
GRID     1304           .0622  -.00635  .00847
GRID     1305           .08294 -.00635  .00847
GRID     1306           .10367 -.00635  .00847
GRID     1307           .12441 -.00635  .00847
GRID     1308           .14514 -.00635  .00847
GRID     1309           .16588 -.00635  .00847
GRID     1310           .18661 -.00635  .00847
GRID     1311           .20735 -.00635  .00847
GRID     1312           .22808 -.00635  .00847
GRID     1313           .24882 -.00635  .00847
```

```
GRID     1314            .26955 -.00635  .00847
GRID     1315            .29029 -.00635  .00847
GRID     1316            .31102 -.00635  .00847
GRID     1317            .33176 -.00635  .00847
GRID     1318            .35249 -.00635  .00847
GRID     1319            .37322 -.00635  .00847
GRID     1320            .39396 -.00635  .00847
GRID     1321            .41469 -.00635  .00847
GRID     1322            .43543 -.00635  .00847
GRID     1323            .45616 -.00635  .00847
GRID     1324            .4769  -.00635  .00847
GRID     1325            .49763 -.00635  .00847
GRID     1326            .51837 -.00635  .00847
GRID     1327            .5391  -.00635  .00847
GRID     1328            .55984 -.00635  .00847
GRID     1329            .58057 -.00635  .00847
GRID     1330            .60131 -.00635  .00847
GRID     1331            .62204 -.00635  .00847
GRID     1332            .64278 -.00635  .00847
GRID     1333            .66351 -.00635  .00847
GRID     1334            .68424 -.00635  .00847
GRID     1335            .70498 -.00635  .00847
GRID     1336            .72571 -.00635  .00847
GRID     1337            .74645 -.00635  .00847
GRID     1338            .76718 -.00635  .00847
GRID     1339            .78792 -.00635  .00847
GRID     1340            .80865 -.00635  .00847
GRID     1341            .82939 -.00635  .00847
GRID     1342            .85012 -.00635  .00847
GRID     1343            .87086 -.00635  .00847
GRID     1344            .89159 -.00635  .00847
GRID     1345            .91233 -.00635  .00847
GRID     1346            .93306 -.00635  .00847
GRID     1347            .9538  -.00635  .00847
GRID     1348            .97453 -.00635  .00847
GRID     1349            .99527 -.00635  .00847
GRID     1350            1.016  -.00635  .00847
GRID     1401            0.     -.00635  0.
GRID     1402            .02073 -.00635  0.
GRID     1403            .04147 -.00635  0.
GRID     1404            .0622  -.00635  0.
GRID     1405            .08294 -.00635  0.
GRID     1406            .10367 -.00635  0.
GRID     1407            .12441 -.00635  0.
GRID     1408            .14514 -.00635  0.
GRID     1409            .16588 -.00635  0.
GRID     1410            .18661 -.00635  0.
GRID     1411            .20735 -.00635  0.
GRID     1412            .22808 -.00635  0.
GRID     1413            .24882 -.00635  0.
GRID     1414            .26955 -.00635  0.
GRID     1415            .29029 -.00635  0.
GRID     1416            .31102 -.00635  0.
GRID     1417            .33176 -.00635  0.
GRID     1418            .35249 -.00635  0.
GRID     1419            .37322 -.00635  0.
GRID     1420            .39396 -.00635  0.
GRID     1421            .41469 -.00635  0.
GRID     1422            .43543 -.00635  0.
GRID     1423            .45616 -.00635  0.
GRID     1424            .4769  -.00635  0.
GRID     1425            .49763 -.00635  0.
GRID     1426            .51837 -.00635  0.
```

```
GRID     1427           .5391  -.00635  0.
GRID     1428           .55984 -.00635  0.
GRID     1429           .58057 -.00635  0.
GRID     1430           .60131 -.00635  0.
GRID     1431           .62204 -.00635  0.
GRID     1432           .64278 -.00635  0.
GRID     1433           .66351 -.00635  0.
GRID     1434           .68424 -.00635  0.
GRID     1435           .70498 -.00635  0.
GRID     1436           .72571 -.00635  0.
GRID     1437           .74645 -.00635  0.
GRID     1438           .76718 -.00635  0.
GRID     1439           .78792 -.00635  0.
GRID     1440           .80865 -.00635  0.
GRID     1441           .82939 -.00635  0.
GRID     1442           .85012 -.00635  0.
GRID     1443           .87086 -.00635  0.
GRID     1444           .89159 -.00635  0.
GRID     1445           .91233 -.00635  0.
GRID     1446           .93306 -.00635  0.
GRID     1447           .9538  -.00635  0.
GRID     1448           .97453 -.00635  0.
GRID     1449           .99527 -.00635  0.
GRID     1450           1.016  -.00635  0.
GRID     1501           0.      0.      0.
GRID     1502           .02073  0.      0.
GRID     1503           .04147  0.      0.
GRID     1504           .0622   0.      0.
GRID     1505           .08294  0.      0.
GRID     1506           .10367  0.      0.
GRID     1507           .12441  0.      0.
GRID     1508           .14514  0.      0.
GRID     1509           .16588  0.      0.
GRID     1510           .18661  0.      0.
GRID     1511           .20735  0.      0.
GRID     1512           .22808  0.      0.
GRID     1513           .24882  0.      0.
GRID     1514           .26955  0.      0.
GRID     1515           .29029  0.      0.
GRID     1516           .31102  0.      0.
GRID     1517           .33176  0.      0.
GRID     1518           .35249  0.      0.
GRID     1519           .37322  0.      0.
GRID     1520           .39396  0.      0.
GRID     1521           .41469  0.      0.
GRID     1522           .43543  0.      0.
GRID     1523           .45616  0.      0.
GRID     1524           .4769   0.      0.
GRID     1525           .49763  0.      0.
GRID     1526           .51837  0.      0.
GRID     1527           .5391   0.      0.
GRID     1528           .55984  0.      0.
GRID     1529           .58057  0.      0.
GRID     1530           .60131  0.      0.
GRID     1531           .62204  0.      0.
GRID     1532           .64278  0.      0.
GRID     1533           .66351  0.      0.
GRID     1534           .68424  0.      0.
GRID     1535           .70498  0.      0.
GRID     1536           .72571  0.      0.
GRID     1537           .74645  0.      0.
GRID     1538           .76718  0.      0.
GRID     1539           .78792  0.      0.
```

```
GRID     1540            .80865  0.      0.
GRID     1541            .82939  0.      0.
GRID     1542            .85012  0.      0.
GRID     1543            .87086  0.      0.
GRID     1544            .89159  0.      0.
GRID     1545            .91233  0.      0.
GRID     1546            .93306  0.      0.
GRID     1547            .9538   0.      0.
GRID     1548            .97453  0.      0.
GRID     1549            .99527  0.      0.
GRID     1550            1.016   0.      0.
GRID     1601            0.      .00635  0.
GRID     1602            .02073  .00635  0.
GRID     1603            .04147  .00635  0.
GRID     1604            .0622   .00635  0.
GRID     1605            .08294  .00635  0.
GRID     1606            .10367  .00635  0.
GRID     1607            .12441  .00635  0.
GRID     1608            .14514  .00635  0.
GRID     1609            .16588  .00635  0.
GRID     1610            .18661  .00635  0.
GRID     1611            .20735  .00635  0.
GRID     1612            .22808  .00635  0.
GRID     1613            .24882  .00635  0.
GRID     1614            .26955  .00635  0.
GRID     1615            .29029  .00635  0.
GRID     1616            .31102  .00635  0.
GRID     1617            .33176  .00635  0.
GRID     1618            .35249  .00635  0.
GRID     1619            .37322  .00635  0.
GRID     1620            .39396  .00635  0.
GRID     1621            .41469  .00635  0.
GRID     1622            .43543  .00635  0.
GRID     1623            .45616  .00635  0.
GRID     1624            .4769   .00635  0.
GRID     1625            .49763  .00635  0.
GRID     1626            .51837  .00635  0.
GRID     1627            .5391   .00635  0.
GRID     1628            .55984  .00635  0.
GRID     1629            .58057  .00635  0.
GRID     1630            .60131  .00635  0.
GRID     1631            .62204  .00635  0.
GRID     1632            .64278  .00635  0.
GRID     1633            .66351  .00635  0.
GRID     1634            .68424  .00635  0.
GRID     1635            .70498  .00635  0.
GRID     1636            .72571  .00635  0.
GRID     1637            .74645  .00635  0.
GRID     1638            .76718  .00635  0.
GRID     1639            .78792  .00635  0.
GRID     1640            .80865  .00635  0.
GRID     1641            .82939  .00635  0.
GRID     1642            .85012  .00635  0.
GRID     1643            .87086  .00635  0.
GRID     1644            .89159  .00635  0.
GRID     1645            .91233  .00635  0.
GRID     1646            .93306  .00635  0.
GRID     1647            .9538   .00635  0.
GRID     1648            .97453  .00635  0.
GRID     1649            .99527  .00635  0.
GRID     1650            1.016   .00635  0.
GRID     1701            0.      .00635  .00847
GRID     1702            .02073  .00635  .00847
```

```
GRID     1703            .04147  .00635  .00847
GRID     1704            .0622   .00635  .00847
GRID     1705            .08294  .00635  .00847
GRID     1706            .10367  .00635  .00847
GRID     1707            .12441  .00635  .00847
GRID     1708            .14514  .00635  .00847
GRID     1709            .16588  .00635  .00847
GRID     1710            .18661  .00635  .00847
GRID     1711            .20735  .00635  .00847
GRID     1712            .22808  .00635  .00847
GRID     1713            .24882  .00635  .00847
GRID     1714            .26955  .00635  .00847
GRID     1715            .29029  .00635  .00847
GRID     1716            .31102  .00635  .00847
GRID     1717            .33176  .00635  .00847
GRID     1718            .35249  .00635  .00847
GRID     1719            .37322  .00635  .00847
GRID     1720            .39396  .00635  .00847
GRID     1721            .41469  .00635  .00847
GRID     1722            .43543  .00635  .00847
GRID     1723            .45616  .00635  .00847
GRID     1724            .4769   .00635  .00847
GRID     1725            .49763  .00635  .00847
GRID     1726            .51837  .00635  .00847
GRID     1727            .5391   .00635  .00847
GRID     1728            .55984  .00635  .00847
GRID     1729            .58057  .00635  .00847
GRID     1730            .60131  .00635  .00847
GRID     1731            .62204  .00635  .00847
GRID     1732            .64278  .00635  .00847
GRID     1733            .66351  .00635  .00847
GRID     1734            .68424  .00635  .00847
GRID     1735            .70498  .00635  .00847
GRID     1736            .72571  .00635  .00847
GRID     1737            .74645  .00635  .00847
GRID     1738            .76718  .00635  .00847
GRID     1739            .78792  .00635  .00847
GRID     1740            .80865  .00635  .00847
GRID     1741            .82939  .00635  .00847
GRID     1742            .85012  .00635  .00847
GRID     1743            .87086  .00635  .00847
GRID     1744            .89159  .00635  .00847
GRID     1745            .91233  .00635  .00847
GRID     1746            .93306  .00635  .00847
GRID     1747            .9538   .00635  .00847
GRID     1748            .97453  .00635  .00847
GRID     1749            .99527  .00635  .00847
GRID     1750            1.016   .00635  .00847
GRID     1801            0.      .00635  .01693
GRID     1802            .02073  .00635  .01693
GRID     1803            .04147  .00635  .01693
GRID     1804            .0622   .00635  .01693
GRID     1805            .08294  .00635  .01693
GRID     1806            .10367  .00635  .01693
GRID     1807            .12441  .00635  .01693
GRID     1808            .14514  .00635  .01693
GRID     1809            .16588  .00635  .01693
GRID     1810            .18661  .00635  .01693
GRID     1811            .20735  .00635  .01693
GRID     1812            .22808  .00635  .01693
GRID     1813            .24882  .00635  .01693
GRID     1814            .26955  .00635  .01693
GRID     1815            .29029  .00635  .01693
```

```
GRID     1816           .31102  .00635  .01693
GRID     1817           .33176  .00635  .01693
GRID     1818           .35249  .00635  .01693
GRID     1819           .37322  .00635  .01693
GRID     1820           .39396  .00635  .01693
GRID     1821           .41469  .00635  .01693
GRID     1822           .43543  .00635  .01693
GRID     1823           .45616  .00635  .01693
GRID     1824           .4769   .00635  .01693
GRID     1825           .49763  .00635  .01693
GRID     1826           .51837  .00635  .01693
GRID     1827           .5391   .00635  .01693
GRID     1828           .55984  .00635  .01693
GRID     1829           .58057  .00635  .01693
GRID     1830           .60131  .00635  .01693
GRID     1831           .62204  .00635  .01693
GRID     1832           .64278  .00635  .01693
GRID     1833           .66351  .00635  .01693
GRID     1834           .68424  .00635  .01693
GRID     1835           .70498  .00635  .01693
GRID     1836           .72571  .00635  .01693
GRID     1837           .74645  .00635  .01693
GRID     1838           .76718  .00635  .01693
GRID     1839           .78792  .00635  .01693
GRID     1840           .80865  .00635  .01693
GRID     1841           .82939  .00635  .01693
GRID     1842           .85012  .00635  .01693
GRID     1843           .87086  .00635  .01693
GRID     1844           .89159  .00635  .01693
GRID     1845           .91233  .00635  .01693
GRID     1846           .93306  .00635  .01693
GRID     1847           .9538   .00635  .01693
GRID     1848           .97453  .00635  .01693
GRID     1849           .99527  .00635  .01693
GRID     1850           1.016   .00635  .01693
GRID     1901           0.      .00635  .0254
GRID     1902           .02073  .00635  .0254
GRID     1903           .04147  .00635  .0254
GRID     1904           .0622   .00635  .0254
GRID     1905           .08294  .00635  .0254
GRID     1906           .10367  .00635  .0254
GRID     1907           .12441  .00635  .0254
GRID     1908           .14514  .00635  .0254
GRID     1909           .16588  .00635  .0254
GRID     1910           .18661  .00635  .0254
GRID     1911           .20735  .00635  .0254
GRID     1912           .22808  .00635  .0254
GRID     1913           .24882  .00635  .0254
GRID     1914           .26955  .00635  .0254
GRID     1915           .29029  .00635  .0254
GRID     1916           .31102  .00635  .0254
GRID     1917           .33176  .00635  .0254
GRID     1918           .35249  .00635  .0254
GRID     1919           .37322  .00635  .0254
GRID     1920           .39396  .00635  .0254
GRID     1921           .41469  .00635  .0254
GRID     1922           .43543  .00635  .0254
GRID     1923           .45616  .00635  .0254
GRID     1924           .4769   .00635  .0254
GRID     1925           .49763  .00635  .0254
GRID     1926           .51837  .00635  .0254
GRID     1927           .5391   .00635  .0254
GRID     1928           .55984  .00635  .0254
```

```
GRID     1929            .58057  .00635  .0254
GRID     1930            .60131  .00635  .0254
GRID     1931            .62204  .00635  .0254
GRID     1932            .64278  .00635  .0254
GRID     1933            .66351  .00635  .0254
GRID     1934            .68424  .00635  .0254
GRID     1935            .70498  .00635  .0254
GRID     1936            .72571  .00635  .0254
GRID     1937            .74645  .00635  .0254
GRID     1938            .76718  .00635  .0254
GRID     1939            .78792  .00635  .0254
GRID     1940            .80865  .00635  .0254
GRID     1941            .82939  .00635  .0254
GRID     1942            .85012  .00635  .0254
GRID     1943            .87086  .00635  .0254
GRID     1944            .89159  .00635  .0254
GRID     1945            .91233  .00635  .0254
GRID     1946            .93306  .00635  .0254
GRID     1947            .9538   .00635  .0254
GRID     1948            .97453  .00635  .0254
GRID     1949            .99527  .00635  .0254
GRID     1950            1.016   .00635  .0254
$ Loads for Load Case : Default
$SPCADD   2       1
$ Displacement Constraints of Load Set : bc1
$       2#      3#      4#      5#      6#      7#      8#  9#
SPC1    1       123456  1101    1201    1301    1401    1501    1601
       1701    1801    1901
$ Referenced Coordinate Frames
ENDDATA
```

Vita

Yong Yook Kim

Yong Yook Kim was born on April 14, 1971 in Chonjusi, Cholabukdo, South Korea. He graduated from Southern Illinois University at Carbondale with Bachelor or Science degree in Mechanical Engineering in 1996. He entered the Master of Science program in Aerospace Engineering at Virginia Polytechnic Institute and State University in 1997.